Novel methods for evaluation of osseointegration, bone regeneration and oral flap management

PhD thesis

Dr. Sándor Farkasdi

Doctoral School of Clinical Medicine
Semmelweis University

Supervisor: Gábor Varga, D.Sc

Official reviewers:
Kinga Laczkóné Turzó, Ph.D
József Tímár, MD, D.Sc

Head of the Final Examination Committee:
Tibor Fábián, DMD, Ph.D

Members of the Final Examination Committee:
Senior Zoltán Rakonczay, D.Sc
Árpád Joób-Fancsaly, DMD, Ph.D

Budapest, 2019

TABLE OF CONTENTS

LIST OF ABBREVIATIONS

ALP – alkaline phosphatase

ANOVA – analysis of variance

ASTM – American Society for Testing and Materials

BD – bony defect

BD OSSI – rat tail based experimental model for bone regeneration evaluation

BIC– bone to implant contact

BV/TV – bone volume/tissue volume

CBCT – cone-beam computed tomography

CSD – critical size bone defect

cPTi – commercially pure titanium

D – density

DALY – disability-adjusted life year

Direct OSSI - rat tail based experimental model for evaluation direct ossteogenesis

Gap OSSI - rat tail based experimental model for evaluation distant osteogenesis around implants

GBR – guided bone regeneration

GDP – gross domestic product

HU – Hounsfield units

IF – Immunofluorescence

i.m. – intramuscular

i.p. – intraperitoneal

IT – insertion torque

i.S/TS – intersection surface/tissue surface

ISQ – implant stability quotient

Micro–CT – microcomputer tomography

mPa – millipascal

N – Newton

n – number

Ncm – Newton centimeter

OSSI – osseointegration experimental model

p – probability value

PTS - Pammer torque system

PUF – polyurethane blocks

RFA – resonance frequency analysis

ROI – region of interest

RP – retromolar pad

RPM – revolutions per minute

Runx2 – Runt-related transcription factor 2

Ti – titanium

TV – tissue volume

SD – standard deviation

SEM – standard error of mean

V – version

WHO – World Health Organisation

1. INTRODUCTION

The function of lost tissues can be restored by three fundamentally different methods: **reparation**, **replacement**, **regeneration**. This PhD thesis addresses the open questions of tooth replacement with **intraosseous implants** and **bone regeneration** at the preclinical level.

Nowadays, in practical healthcare, the regeneration of simple tissues by methods such as transplantation is more and more feasible. But the engineering of complex organs consisting of multiple tissues is still restricted in most medical professions, including dentistry and oral and maxillofacial surgery.

In oral and maxillofacial medicine and dentistry, tooth disorders occur the most frequently. **Tooth loss** is the most frequent disease which affects a considerable rate of the population of the world (Kassebaum et al., 2017). The disorder which the most frequently affects the erupted part of the tooth is **dental caries**, which is primarily an infectious disease. Caries is a mechanical and chemical breakdown of teeth due to acids and bacteria (Silk, 2014). Its complications can include the inflammation process of the tooth and the periodontal tissue, tooth loss, or even abscess formation (Laudenbach et al., 2014). At the end of the twentieth century, the incidence and prevalence of caries showed a decreasing tendency in countries with high gross domestic product (GDP). According to World Health Organisation (WHO) data, this tendency was a consequence of governmental regulations regarding caries in these countries but the incidence is still very high (Kassebaum et al., 2017). The biggest side effect of tooth extraction/tooth loss is that it has a significant impact on functionality, aesthetic, and social status of people affecting the quality of their lives (Batista et al., 2014; Gerritsen et al., 2010). According to recently published data, tooth loss is responsible for 7.6 million disability-adjusted life years (DALY) (Kassebaum et al., 2017).

The incidence and prevalence of **periodontal diseases** are also very high. Accordingly, half of the US population over the age of 30 has periodontitis based on data published by the "Center for Disease Control and Prevention" (Eke et al., 2015). Neglected oral hygiene, inadequate nutrition, smoking and stressful lifestyle are important triggers for the development of periodontal disease (Albandar, 2014; Kinane et al., 2017; Kwon et al., 2014; Larsen et al., 2017). During the development of periodontal

disease, inflammation causes massive, irreversible tissue destruction in the alveolar bone, in the periodontal ligament and in the cement tissue and even in the gum (Kinane et al., 2017). The pathological cascades can lead to tooth loss in untreated cases. Despite the improvements in the quality of dental healthcare, policies to expand public health insurance coverage, increasing accessibility to dental clinics and advanced treatments, the rate of tooth extractions are continuously increasing due to periodontal disease (Lee et al., 2017). Periodontitis itself causes serious aesthetic and functional problems, and may also be associated with systemic diseases such as diabetes (Demmer et al., 2010), cardiovascular disorders (through the stimulation of the development of atherosclerosis) (Lockhart et al., 2012) (Humphrey et al., 2008; Iniesta et al., 2012), with adverse pregnancy (Chambrone et al., 2011) and immunosuppressive conditions (stress, HIV infection) (Kinane et al., 2001). Beside the socio-economic impact, numerous pieces of evidence demonstrate that chronic periodontitis can be a risk factor for cancer as well (Fan et al., 2016; Michaud et al., 2013; Michaud et al., 2007; Michaud et al., 2016; Michaud et al., 2008; Ogrendik, 2017).

As a result of both dental caries and periodontal inflammation, both **soft and hard tissue loss** will most probably appear. One of the greatest challenges of modern dental and craniofacial research is to restore the function of lost tissues.

1.1 Intraosseous implants for tooth replacement and their regulation

There is a strong need for the **replacement of missing teeth**. Unfortunately, it is not possible with regeneration yet. Not even the regeneration of separate parts/tissues of the tooth (such as the enamel or dentine) is available for standard clinical practice. The **intraosseous implant** is the gold standard for the replacement of the extracted tooth. Its application is the major example for reparative medical technology besides fillings and crowns. The clinical success of using artificial intraosseous implants for the rehabilitation of the human body is based on **osseointegration** (see part 1.3).

Intraosseous implants, which are used in dental practice, are called dental implants. A dental implant is the root part of the artificial tooth, which is in the bone. The superstructure, which is directly connected to the top of a dental implant, has two parts. One is the crown and the other is an abutment which connects the crown to the dental

implant. These structures can be replaced. But the dental implant of the artificial tooth should remain in the person's body during the whole of his life (Hof et al., 2014; Korfage et al., 2018).

The **clinical efficiency** of various dental implants is different (De Angelis et al., 2017; Jimbo et al., 2015; Marcello-Machado et al., 2018; Moraschini et al., 2015). This can be due to the different patient background (patient's general and local status, habits, additional treatments) (Baig et al., 2007; Candel-Marti et al., 2011; Gelazius et al., 2018; Javed et al., 2010), surgical protocol (Chrcanovic et al., 2015; Pjetursson et al., 2008; Tan et al., 2008) and loading protocol (Al-Sawai et al., 2016). Also, a significant impact on osseointegration is made by different surface treatments of the dental implants (Calvo-Guirado et al., 2015; Le Guehennec et al., 2007). In term of success and survival rates of implants the surface modifications plays one of the mayor role (Jimbo et al., 2015).

The majority of intraosseous implants are classified as **medical devices**. In clinical practice, the rules for new medical devices, instruments and methods have been becoming more and more rigorous during the last 100 years. Mostly, new **regulations** limit the access to new devices on the market based on new findings in clinical experience. In the European Union, the Medical Devices Directive 93/42/EEC regulates the market for medical devices (EuropeanParliament, 1993). This directives continuously change according to technical innovations and research developments. However, it is still relatively easy to introduce a new medical device into the market. For instance, implant manufacturers still have the possibility to launch new implant products on the market easily by avoiding important preclinical and clinical evaluations. The manufacturer of a dental implant can apply for a declaration of conformity, CE marking and, after successful registration, put the device on the market (based on Directive 93/42/EEC Annex III, module B) (EuropeanParliament, 1993). The actual regulation for the assessment of a medical device does not fully take into account the biological reaction in response to the transplantation of the newly developed product. This is because the current regulation is safety-centered and basically does not put too much emphasis on demonstrating efficiency. Therefore, there is a strong need for a standard evaluation of an upcoming medical device in experimental circumstances.

From the spring of 2020, a more rigorous guideline will come into effect regarding the regulation of new medical devices on the EU market. At present, this new law is in a

transitional period. According to Directive 93/42/EEC, the regulations of the medical device industry in Europe, which have been relatively unchanged since the 1990s, will be modified considerably. Incidents at the beginning of the 21st century, including the breast implant crisis (Heneghan, 2012) and the hip replacement problems (Cohen, 2012; Howard, 2016), have provoked urgent reforms in the regulation of medical devices (French-Mowat et al., 2012; Heneghan, 2012). Accordingly, the post-marketing activities and midterm onsite controls of manufacturing should be significantly improved. Based on the above-mentioned problems, the European Commission have come up with proposals for the regulation of medical devices (EU MDR) (EuropeanParliament, 2017). The recent problems with breast implants (Poly Implant Prothese (Greco, 2015)) and hip implants (metal on metal hip implants) reflected only a small part of the whole "iceberg" of necessary recalls from the medical market (Heneghan, 2012; Heneghan et al., 2012).

The purpose of the new regulations is to create better evidence-based control than before. It is worth noting that a really big difference between the current and next regulations will be that the manufacturer will not only have to prove the safety of his/her own medical device but also its efficacy. This will bring the regulation of medical devices closer to drug regulations. This target can be achieved if scientifically proved checklists of preclinical evaluations have been introduced. Scientific authorisation can be done for certain medical devices only if the particular device has been validated with well-described and standardly reproducible experimental models, experimental work to ensure repeatability. To prove the efficacy and compare it with similar medical devices, **standardised screening experimental models** will be needed. Moreover, often there is no clinical evidence of which commercially available implant and which surface modification of implant is better. For that, **preclinical, commercially independent evaluations** will be needed. This is also important for a financially more predictable social insurance support in case of treatments for possible complications.

1.2 Bone healing and regeneration

One of the thoroughly investigated tissues for regeneration is the **bone** (both in general medicine and dentistry). Firstly, this is because bone **regeneration** is a physiological process that leads to bone union (Tsiridis et al., 2007). It can be part of the repair process

after a trauma (such as a fracture or bone grafting) or the process of skeletal development, as well as continuous bone **remodelling** throughout human life. Secondly, bone regeneration is the second most frequent tissue transplantation in clinical practice after blood transfusion (Campana et al., 2014). Thirdly, the bone has become the most frequent hosting tissue for reconstructive intraosseous implants. Natural bone regeneration (after fracture) and man-made bone regeneration (after bone-grafting procedures and intraosseous implant placement) are among the few processes in the human body which can heal without the formation of a fibrous scar tissue (Marsell et al., 2011). But errors may happen during this process that can generate a delay in healing, and even develop pseudo-joints or non-unions (Marsell et al., 2010).

The process of normal **bone-healing** after a trauma, fracture, intraosseous implant placement and grafting procedure usually tends to repeat the process of bone formation (Caplan, 1987; Marzona et al., 2009; Shah et al., 2019; Shapiro, 2008; Vortkamp et al., 1998). Bone-healing in the damaged site involves the cooperation of inflammatory cells, stem cells, osteoblasts, chondrocytes, osteoclasts, and endothelial cells with surrounding pericytes, cytokines and growth factors (Frost, 1989a, 1989b; Marsell et al., 2011). As a result of the reunion of bone after fracture (Marsell et al., 2011) and even after bone regeneration, osteon formation takes place (Fernandez et al., 2014; Makihara et al., 2018). The fundamental unit of bone is the osteon (Haversian systems). Bone remodelling goes parallel to the streamline of the osteon system. When the bone equilibrium is breached, bone-healing starts immediately. Irrespective of the cause of the breach, the immune response starts with angiogenesis and recruitment of progenitor cells. One of the key elements for successful bone-healing is continuous blood supply (Carano et al., 2003).

Regarding the mechanism, bone-healing can follow two pathways (Marsell et al., 2011; Ono et al., 2017). The most common among fractures is **indirect bone-healing** or secondary bone-healing (Marsell et al., 2011). Indirect or secondary healing happens, when there is a gap and an insufficient stability of the fractured edges (Marsell et al., 2011). During indirect healing mostly endochondral ossification takes place (Marsell et al., 2011). There are three phases of secondary bone-healing (Sfeir C, 2005). The first one is the inflammatory phase, which ends up in granulation tissue formation (Schell et al., 2017; Sfeir C, 2005). The second phase is the reparative phase when first fibrocartilage callus and then bony callus develops (Marsell et al., 2011; Sfeir C, 2005).

During this process the hyaline cartilage and the woven bone is replaced by lamellar bone (Marsell et al., 2011; Sfeir C, 2005). The third step is bone remodelling and addition of compact bone to the mechanical stressors. Finally, the fractured site is totally remodelled by the balanced work of osteoclasts and osteoblasts into a new shape, which almost repeat the original shape and strength (Marsell et al., 2011; Sfeir C, 2005).

The second type of bone-healing after bone integrity impair is referred to as **direct bone-healing** (Marsell et al., 2011; Ono et al., 2017). Direct healing happens when there is no gap between the fractured edges at all (Marsell et al., 2011) or when the rigid fixation of the fractured fragments is done (Marsell et al., 2011) or in case of alveolar bone-healing after tooth extraction (Vieira et al., 2015), implant placement and bone-grafting (Colnot et al., 2007; Shah et al., 2019). During the direct healing of the bone intramembranous ossification takes place (Marsell et al., 2011). Bone fragments are joined by continuous ossification avoiding woven bone or cartilaginous bone formation, and the remodelling of the newly-formed bone happens to a tiny extent (Shapiro, 2008).

Blood clots play an important role in the initial phase of bone-healing (Schell et al., 2017). Further on, sufficient **blood supply** and a gradual increase in mechanical stability are needed for an uncompromised remodelling phase (Einhorn et al., 2015; Marsell et al., 2011; Runyan et al., 2017). Accordingly, the angiogenesis goes parallel with all phases of fracture healing. At the end of the bone healing, the Haversian system is re-established by the creation of remodelling units called «cutting cones» (McKibbin, 1978).

The difference between fracture-healing and bone-healing after tooth extraction is that in case of fracture-healing (closed fracture) the endochondral ossification happens in sterile conditions (Vieira et al., 2015). In case of alveolar healing intramembranous ossification happens with constant microbial challenge from the oral cavity (Vieira et al., 2015). The same microbial challenge influences the osseointegration of dental implants after implantation. There are differences between intramembranous ossification and new bone formation after tooth extraction and implantation (Shah et al., 2019). They are due to the presence of titanium, a foreign body between the "fractured" edges of the bone. By implant insertion the fractured gap is considerably reduced (Shah et al., 2019). Accordingly, the area needed for regeneration decreases. The titanium surface modifies local cell response in the site of the fracture (Schwarz et al., 2007; Shanbhag et al., 2015).

The **titanium** and titanium alloys are unique, because when they are exposed to air or water, a spontaneous formation of native titanium oxide (TiO_2) layer (5-10 nm) occurs (Shah et al., 2019; Wang et al., 2016). This TiO_2 layer prevents the release of metallic ions from the implant surface (Okazaki et al., 2005) and also prevents adverse reactions of the body (Tengvall et al., 1992; Wang et al., 2016). Accordingly, the TiO_2 layer is needed for successful osseointegration and becomes a biologically inert metal (Wang et al., 2016). We know that changing the properties of **titanium oxide** surface leads to biocompatibility having an effect on the titanium intraosseous implant (Wang et al., 2016). As a result of osteotomy, haemostasis and blood clot formation happen in the presence of bone debris (Shanbhag et al., 2015). After osteotomy, local hypoxia starts due to the disruption of the local vasculature (Potier et al., 2007; Shanbhag et al., 2015). After surgical placement of the implant oxidization continues and the hypoxic environment can be enhanced. The hypoxic environment induces angiogenesis. Osteogenesis starts simultaneously with angiogenesis (Mamalis et al., 2013). The complete understanding of osseointegration remain unclear (Shah et al., 2019). For a clear analysis of the effect of the different surface modifications, standardised experimental models are needed, which allow the evaluation of pure biological integration without any additional influence of the geometrical design (threads, holes, self-tapping).

The **mechanical strain** and the **distance between** the two fractured edges of the bone are the two crucial factors, which affect the quality of healing after the initial trauma (Claes et al., 1998; Ghiasi et al., 2017). In case of an intraosseous implant, the mechanical strain can lead to micromotion. If **micromotion** is more than 100-200 μm, fibro-osseointegration occurs, which means the failure for the placed implant (Brunski, 1999; Szmukler-Moncler et al., 1998). The increase in the size of the bone defect directly correlates with a delay in the healing process (Claes et al., 1998). The minimum size of bone defect, which is large enough not to be able to heal spontaneously, is called "critical size bone defect" (CSD) (Agarwal et al., 2015). The size of CSDs is different depending on the location and live specimen (Harris et al., 2013).

After severe bone traumas, complicated tooth extractions can lead to CSD formation; the method for bone reunion can be **guided bone regeneration** (GBR). The GBR procedure is considered to be one of the most widespread dental surgical procedures for rebuilding the width and the height of the alveolar ridges before implant placement

(Elgali et al., 2017; Khojasteh et al., 2017; Windisch et al., 2017). GBR is characterized by using barrier membranes with or without particulated bone grafts or/and bone substitutes (Elgali et al., 2017; Liu et al., 2014). The membrane is mainly applied for eliminating the penetration of non-osteogenic tissues into the grafted area and for space maintenance (Elgali et al., 2017; Liu et al., 2014). Particulated bone-grafting materials are used as scaffolds to facilitate bone formation. These grafts are biodegradable, have no antigen-antibody reaction, and serve as a mineral reservoir (Kumar et al., 2013; Thrivikraman et al., 2017). Bone-grafting materials are usually classified according to their origin. They are called autografts when harvested from the same individual as the one receiving the graft; allografts when harvested from the same species (i.e. from other humans); xenografts when harvested from a species other than a human; synthetic when produced in laboratory conditions and finally the combination of grafting materials, which are listed above (Campana et al., 2014; S. Titsinides, 2018).
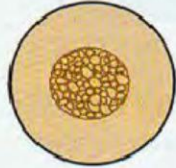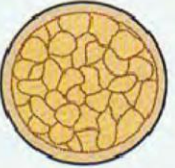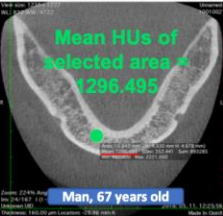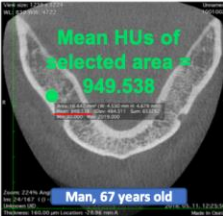
1.3 Osseointegration

The incorporation of titanium implants into the living bone utilises direct bone-healing; this process is called osseointegration. **Osseointegration** is defined as the development of a direct structural and functional contact between the artificial implant surface and the living bone tissue (Branemark, 1983). Furthermore, the term also refers to the process of forming this direct fixation which has a high dependency on the preceding surgical procedure and preoperative circumstances (Trisi et al., 2009). The process of osseointegration is defined as bone growth or bone bonding from the broken ends of the drilled site to the artificial implant surface without any intermediate fibrous tissue formation. The osseointegration of implants has further key steps: inflammatory phase, proliferative phase and maturation phase. After the osseointegration, bone remodelling happens lifetime. The initial tissue response around the inserted implant is the inflammatory response involving the release of growth factors and cytokines (Bielemann et al., 2018; Kuzyk et al., 2011), which lasts for the first three days (Bielemann et al., 2018; Kuzyk et al., 2011). As a result of the initial tissue response, extracellular matrix and haematoma are formed (Davies, 2003). Then the process of adhesion and aggregation leads to a fibrin matrix formation (Davies, 2003; Kuzyk et al., 2011). During the

osseointegration process the implant surface acts as biomimetic scaffold (Davies, 2003). This scaffold promotes migration, proliferation and differentiation of cells (Davies, 2003; Kuzyk et al., 2011). Then angiogenesis around the implant starts in the next four days (Kuzyk et al., 2011). In the meantime, mesenchymal progenitor cell differentiation results in osteoblast formation until the end of the second week (Biguetti et al., 2018). Within this period, osteoblasts form calcified collagen fibers and early mineralisation begins at the bone-implant interface (Biguetti et al., 2018; Kuzyk et al., 2011). As a result, a woven bone is formed (Kuzyk et al., 2011). Finally, the woven bone is transformed to a lamellar bone (Biguetti et al., 2018; Davies, 2003).

Bone-bonding to the implant can be considered to be completed when there is no motion between the bone and the implant at all. After healing, that connection can be loaded (Cochran et al., 1998; Ledermann et al., 1998). Bone healing/regeneration and bone-bonding to the implant surface are somewhat different in various bone types. Bones are classified into three main types which are complementary to each other (Chugh et al., 2013) (***Figure 1***).

It is essential for dentists to recognize bone types during their clinical practice. Classification of bones according to density and their typical locations in the jaws are presented in ***Figure 1***.

A.	Homogenous cortical bone / oak or maple wood.	Thick cortical bone with marrow cavity / spruce or white pine wood.	Thin Cortical bone with dense trabecular bone of good strength / Balsa wood.	Very thin cortical bone with low density trabecular bone of poor strength / Styrofoam.	Cortical bone is absent around the trabecular bone.
B.	> 1250 HU	850 to 1250 HU	350 to 850 HU	150 to 350 HU	< 150 HU.
C.	Anterior mandible, buccal shelf and midpalatal region.	Posterior mandible, Anterior Maxilla, the midpalatal region.	Anterior Maxilla, Posterior maxilla.	Posterior Maxilla in the tuberosity region.	Posterior Maxilla in the tuberosity region.
D.	Type 1.	Type 2.	Type 3.	Type 4.	Type 5.
E.	D1	D2	D3	D4	D5
F.	Mean HUs of selected area = 1296.495 Man, 67 years old	Mean HUs of selected area = 949.538 Man, 67 years old	Mean HUs of selected area = 694.594 Man, 67 years old	Mean HUs of selected area = 256.373 Man, 67 years old	Mean HUs of selected area = 116.705 Man, 67 years old

Figure 1.

Description of bone densities based on Lekholm&Zarb, Misch classifications. Visual comparison of different bone densities: **A.** Description by Lekholm and Zarb based on conventional radiographs and histological components / by Misch based on descriptive morphology combined with clinician's tactile sensation (Anitua et al., 2015; Blazsek, 2008; Misch, 1989, 1990; Zarb et al., 1985). **B.** Hounsfield units (HU) (Shapurian et al., 2006; Schreiber et al., 2011; Turkyilmaz et al., 2008). Different bone densities of edentulous jaws can be assigned to different Hounsfield units (HU) (Shapurian et al., 2006; Turkyilmaz et al., 2008) *C.* Most frequent localisations in adults. **D.** Bone quality classification and visualisation according to Lekholm & Zarb (1985) based on conventional radiographs. **E.** Bone quality classification and visualisation by Misch (1988) based on macroscopic cortical and trabecular bone characteristics divided into four types. **F.** Screenshots from CBCT viewer program (Osirix, Pixmeo SARL) of horizontal cross-sections of the human mandible and maxilla showing the Hounsfield units (from the left to the right: inter-foraminal region of the mandible, lateral zone of the mandible, frontal area of the maxilla, lateral area of the maxilla, tuberosity area of the maxilla).

Osseointegration comprises two parallel processes: **contact** and **distance osteogenesis**, which lead to new bone formation around the titanium implants (Davies, 2003; Mavrogenis et al., 2009). Contact osteogenesis is the new bone formation on the implant surface, which is to be colonized by bone cells before bone matrix formation (Davies, 2003; Mavrogenis et al., 2009). Contact osteogenesis is also called "de novo bone formation" (Davies, 2003). Distance osteogenesis is the process of new bone formation on the surface of the old hosting bone (Davies, 2003; Mavrogenis et al., 2009). Both types of osteogenesis result in a direct bone to implant contact (Sivolella et al., 2012). The process of osseointegration starts when the primary stability of the implant is achieved by mechanical fixation (Berglundh et al., 2003). Then bone regeneration and remodelling proceed continuously, which finally **leads to a rigid and stable fixation of the implant** into the surrounding bone tissue. After the initial bone-healing around titanium implants, bone remodelling is practically lifelong (Haga et al., 2009). In spite of continuous efforts, the course of osseointegration, bone remodelling and regeneration around the implants have not yet been fully understood (Pearce et al., 2007; Yin et al., 2016). To more extensively investigate this complex process, there is a need for developing reliable and reproducible preclinical and clinical methods.

On the whole, bone regeneration and implant integration depend on many factors. The main factors are the location of the defect, its extent, the mobility of edges, the presence or absence of infection, general diseases of the patient and the types of used reconstructive materials.

1.4 Dental implantology

Dental implant placement is one of the most common procedures in oral healthcare. At present, there are only a few absolute **contraindications** for implantation. They include intravenous bisphosphonate treatment during cancer therapy (for instance radiotherapy protocols in the head or neck region); patients who are unable to comprehend dental treatment logically; immunosuppressed conditions (when the total white blood count falls below 1500–3000 cells/mm3); acute bleeding (a loss of 500 mL of blood); one month after repair of cardiac or vascular defects, and less than one year since myocardial infarction or a cerebrovascular accident (Gomez-de Diego et al., 2014; Hwang et al.,

15

2006). Indeed, oral bisphosphonate intake seems to be an important contraindication for treatment with dental implants (Gomez-de Diego et al., 2014). Also, relative contraindications for dental implantations are adolescence, ageing, osteoporosis, smoking, diabetes, human immunodeficiency virus, cardiovascular disease, hypothyroidism and interleukin-1 genotype (Hwang et al., 2007).

The crucial element for intraosseous implant placement is its integration into the living tissues, which is osseointegration. Since PI Branemark introduced **osseointegration** as a rigid fixation of an implant in bone tissue more than half-century ago (Branemark et al., 1969), numerous in vitro, *in vivo* preclinical and clinical studies have been carried out to investigate this process.

The **proper planning** of implant placement procedure is a key factor for the success of the procedure. There are different **bone diagnostic** approaches for planning the surgical procedure of implantation, such as palpation bone sounding, x-ray evaluation, planning the positioning of the implant digitally or conventionally (Anwandter et al., 2016; Greenberg, 2015; Katsoulis et al., 2009). Based on x-ray diagnostics, the clinician can first choose the most appropriate position of the implant surgically and prosthetically (Karami et al., 2017; Katsoulis et al., 2009). Second, the dentist can modify the time needed for osseointegration by considering the fact that the higher the primary stability, the faster the secondary stability is achieved (Anitua et al., 2015; Javed et al., 2013). But one always has to keep in mind that primary stability has to be sufficient to avoid micromotion (Javed et al., 2013) but not large enough to prevent bone resorption of the hosting bone (Wang et al., 2017). Beside knowing the parameters of the implant site, the surgeon should know the difference in the behavior of different implant geometries in various **bone conditions**.

The major bone condition, which directly influences implant stability is **bone density** (Merheb et al., 2016). Based on this, recommendations exist for which density which implant should be inserted. As it was described above, there are three main bone density classifications (Lekholm U, 1985; Misch, 1990; Schreiber et al., 2011; Shapurian et al., 2006). The classification of density is relative because in humans there are variations of densities even within one region of interest (*Figure 1.F*).

Clinically there is a need to choose the proper **implant geometry** for the planned, specific implant site. Only sufficient primary stability guarantees a high resistance of the

implant in response to external micro-movements. The local milieu of the hosting implant is the **bone bed/implant site**. The bone bed is one of the most influencing factors for primary stability (Alsaadi et al., 2007). Primary stability is the mechanical retention of the implant in the bone bed without mobility after implantation (Sennerby et al., 1998). Primary implant stability during the implant placement is documented as peak **insertion torque** (IT) (Alsaadi et al., 2007; Meredith, 1998). Sufficient insertion torque prevents the appearance of micromotion (Trisi et al., 2009). Micromotion, which is more than 100-200 μm, can lead to fibro-osseointegration, which is actually a failure of the placed implant (Brunski, 1999; Szmukler-Moncler et al., 1998). The peak insertion torque is influenced by **macro-, as well micro-designs** (Dos Santos et al., 2011). Macro-design includes implant body shape, thread intensity (pitch) and thread geometry (Gehrke et al., 2015). Surface modifications are considered to be the **micro-design** variations of implants. There is a generally accepted rule that the insertion torque predicts the outcome of implantation and determine submerged healing time (Walker et al., 2011). There are factors, which influence the longitudinal success rate of implants. Endogenous factors include bone density, cortical bone thickness and osseointegration. Exogenous factors include thread pitch, thread depth, the diameter of implant neck and body size (Cheng et al., 2015).

Nowadays the number of **implant factories** is higher than 200 worldwide (Yakir). Each implant factory has a couple of implant systems. As a result, there are thousands of clinically available implant systems. The majority of dental intraosseous implants share the characteristics that they have threads to reach primary mechanical retention.

Modern radiological pre-surgical diagnostic methods such as cone-beam computed tomography (CBCT), provide three-dimensional morphologic analysis of the cortical and trabecular alveolar bone of the hosting side of dental implants (Salimov et al., 2014). Based on well-described **clinical protocols**, a proper prognosis of **primary implant stability** can be estimated before surgery (Cortes et al., 2015; Dorogoy et al., 2017; Salimov et al., 2014; Wada et al., 2016). By receiving all data from x-ray analyses, the proper implant geometry, drilling protocol can be planned. The images provided by CBCT give very precise data (Anderson et al., 2014). Based on these precise images, the exact copy of the clinical reality to prepare surgery can be printed in 3D (Huang et al., 2016; Shui et al., 2017). Having a 3D model before surgery, the surgical procedure can

be improved in accuracy, time and predictability. Recently published data on intra-operatory bone density measurement system allow to measure the density with a special probe connected with a surgical/implant motor (Di Stefano et al., 2015; Iezzi et al., 2015). This bone density system can be applied using the 3D printed copies of the planned surgical site. For this, the surgeon can receive all the relevant information before surgery and plan the procedure properly. The motor is capable of measuring instantaneous torque. This torque is a function of the friction exerted by the bone walls of the implant bed. The average torque along implant bed significantly correlates with the bone density of the surrounding bone wall (Di Stefano et al., 2015; Iezzi et al., 2015).

Apart from primary stability, the **success of the osseointegration** process depends on a number of factors (*Figure 2*). It is strongly influenced by the performed medical procedure and the selected implant. The important factors here are the applied implant surface modifications (Campana et al., 2014), the type of implant placement immediately after tooth extraction or later, conventionally (Pal et al., 2011) and bone debris (Bosshardt et al., 2011). Osseointegration can be influenced by growth hormone supplementation (Abduljabbar et al., 2017), smoking (Ekfeldt et al., 2001) and the patient's medical conditions. For example, AIDS, uncontrolled diabetes mellitus, osteoporosis, corticosteroids, bisphosphonate therapy, collagen disorders and other adverse conditions can strongly influence the initial healing process of the bone (Sakka et al., 2012). The list of important factors affecting primary and secondary implant stabilities are shown in *Figure 2*.
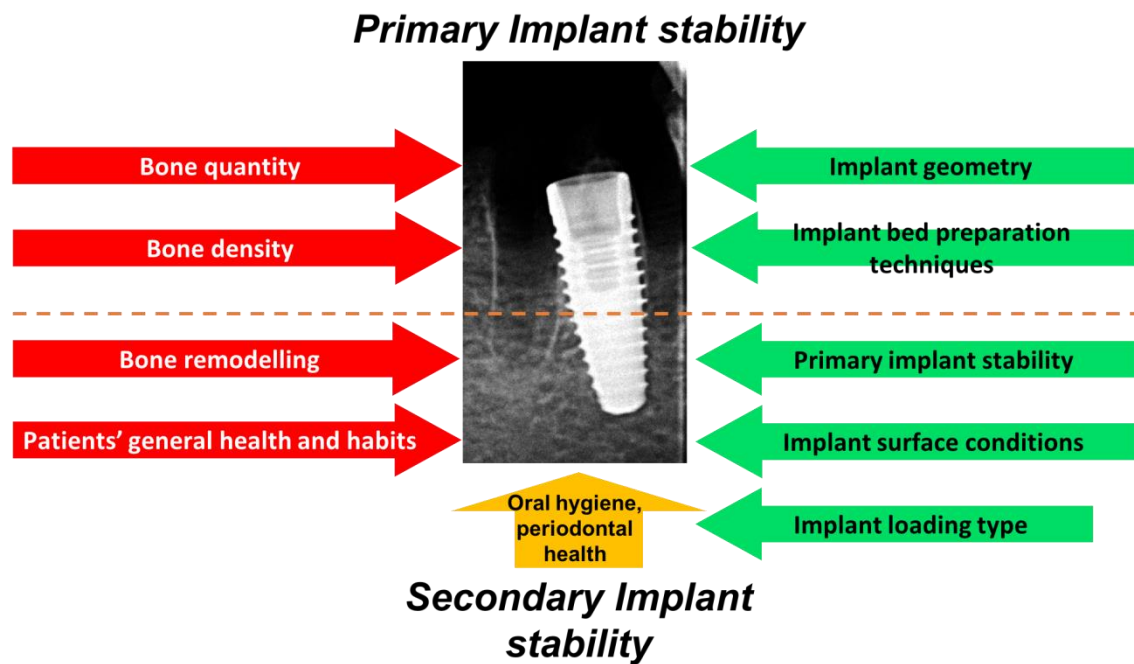
Figure 2.

Parameters influencing primary stability of implants.
Factors in this figure are categorized based on whether the clinician can influence them or not. Factors which are painted with red cannot be controlled by the expert and those with green should be controlled by the surgeon. Factors which are labeled with orange depend on the patient as well as on the surgeon.

Implant stability is an important indicator of the level of osseointegration. Osseointegration can be assessed by invasive and non-invasive ways. The invasivity in this classification is distinguished based on the destruction of the bone to implant connection during the analysis or saving it for further analysis. **Non-invasive methods** include radiological analysis/diagnostics (Atsumi et al., 2007), resonance frequency analysis (RFA) (Huwiler et al., 2007), "damping characteristics" (Cranin et al., 1998) and also the perception of the surgeon (Swami et al., 2016). Radiological analysis is considered to be one of the first and oldest methods for determining implant stability (Atsumi et al., 2007). The main disadvantage of x-ray diagnostics for osseointegration analysis is the metal artifact (Ritter et al., 2014). The 3D x-ray diagnostics with high resolution (such as micro-CT) can eliminate artifacts and provide a more precise morphological picture of the surroundings of the implant (Kang et al., 2015). The most widely available and most investigated methods are RFA and "damping characteristics" (performed with a "Periotest" device, among others) validations.

RFA is an easy-to-use and standardly reproducible method. RFA is considered to determine the stability of implants and the time of their **loadability**. Damping characteristics are not as reliable for the assessment of implant stability (Zix et al., 2008). Accordingly, this method is not the most suitable approach for analyzing osseointegration. Meanwhile, there are new approaches on the horizon, which are at a developing stage. These methods do not induce the implant with electromagnetic waves, but with an electrically-controlled rod that punctures the implant similarly to "Periotest". On the dental market this device is called "Implomates" (Biotech One Inc., San Chung, Taiwan). Another representative of the new methodologies for non-invasive testing of implant stability is based on quantitative ultrasound (Mathieu et al., 2011a, 2011b). This device generates a broadband ultrasonic pulse through the transductor (6-14 MHz) (Zanetti et al., 2018). The perception of surgeons is very subjective and not reproducible. Thus, implant stability evaluation should not rely on this methodology.

Invasive techniques include pull-out/push-in tests (Blazsek et al., 2009; Brunski et al., 2000; Swami et al., 2016), reverse/removal torque measurement (Carvalho et al., 2010), cutting torque resistance (Friberg et al., 1999), tensional or micromotion test (Chang et al., 2010; Trisi et al., 2011) and histology/histomorphometry (Bernhardt et al., 2012; Bissinger et al., 2017; ISO/TS_22911:2016, 2016). Invasive methods are not applicable for clinical monitoring and diagnostic procedures. Therefore, the refinement of non-invasive methods is of great significance for human application (Davies, 2007; Rodrigo et al., 2010).

The pull-out test is the most reliable biomechanical test for implant stability evaluation (Bell et al., 2014; Sivolella et al., 2015). This is because the main loading on implants arrives vertically. Accordingly, using pull-out tests with non-threaded implants, we can precisely evaluate the bone anchorage strength to the implant surface (Bell et al., 2014). In studies on the use of non-threaded implants (Nonhoff et al., 2015; Seong et al., 2013; Stubinger et al., 2016) it was shown that the pull-out test is a very reliable method for the follow-up of osseointegration. Reverse torque evaluation is the process of unscrewing the implant from the bone when we can detect the minimally needed level of torque for destroying bone implant contact (BIC) (Atsumi et al., 2007). This method evaluates osseointegration indirectly (Atsumi et al., 2007). The assessment of reverse torque can serve as control for osseointegration at the level of loading the implant. It is

suggested that trying to unscrew the implant with 30 Ncm can be an acceptable force for evaluating osseointegration (Simeone et al., 2016). Reverse torque assessments can be done only with threaded implants. Even getting the peak value for destroying the BIC during reverse torque is difficult to translate to any mechanical property. The cutting torque resistance analysis describes the energy needed by a surgical motor for cutting off one unit of bone during implant bed preparation (Atsumi et al., 2007). Consequently, this method allows the analysis of bone density in the hosting area of the implant. The disadvantage of this method is that it strongly depends on the operator and it cannot describe implant stability precisely (Friberg et al., 1995). With tensional tests or micromotion testing we can evaluate the lateral resistance of bone to implant connection (Branemark et al., 1998; Chang et al., 2010). It is also difficult to translate these results to any mechanical property (Chang et al., 2010). Histomorphology is the gold standard and the most descriptive method for bone to implant contact. This method is required in guidelines for morphological assessments (ISO/TS_22911:2016, 2016). For preclinical testing, the combination of both non-invasive and invasive methods could offer good outcome providing a safe basis for clinical application. Accordingly, **in the studies of this thesis** we have chose **RFA** and micro-CT **x-ray diagnostics** from **non-invasive methods** being the most thoroughly described, reliable non-invasive methods. From **invasive methodology**, the **pull-out test** was chosen to be the most appropriate for validating bone to implant contact biomechanically. Finally, **histomorphometry** was selected, which is the gold standard in the evaluation of osseointegration (ISO/TS_22911:2016, 2016).

The RFA non-invasive approach has already been used in daily clinical practice for more than a decade as the main tool for the clinical decision concerning loading time (Stanley et al., 2017). RFA has been introduced in practical healthcare as a non-invasive method to assess implant stability. There was a huge need to have a simple and reliable evaluation approach for evaluating the stability of implants (Kuchler et al., 2016; Sadeghi et al., 2015). Osstell Ltd. (Osstell AB, Gothenburg, Sweden) introduced this measuring device into the clinical market at the end of the 20th century.

Animal models are indispensable tools to develop better devices for medical application (Spicer et al., 2012; van Griensven, 2015). The currently available methods still need to be improved by reducing the number of experimental animals and increasing

reliability (Hartung, 2010; Renaud et al., 2015). Although various animal models have been developed to study osseointegration, there is still a lack of a well-reproducible, relatively inexpensive and reliable model (Pearce et al., 2007; Schmitz et al., 1986). Particularly, even the currently available **ISO guideline** (ISO/TS_22911:2016, 2016) for performing a preclinical evaluation of dental implant systems suffers from a lack of biomechanical tests. The present guideline requires only morphological, radiographical and histopathological assessments but does not include any functional investigations of osseointegration (ISO/TS_22911:2016, 2016). This deficiency is clearly due to the lack of reliable, well-developed biomechanical tests for experimental animals.

Most animal models for investigating osseointegration were developed **without considering the similarity of bone microstructure of animal and human jaw bones**. Consequently, the thereby achieved biomechanical characteristics may be inappropriate since there are remarkable differences between animal and human bones (Martiniakova et al., 2006). To approach this problem, we searched for a massive, cortical and cancellous bone compartment in rats, suitable for supporting titanium implants. We found that caudal tail vertebrae were constituted by abundant spongiosa, which presented an alveolar structure similar to that of the human mandible. Furthermore, the bone marrow parenchyma is also absent in tail vertebrae, thus having greater similarity to human jaw bone than haematopoietic femur of rats, a commonly used experimental model site (Blazsek et al., 2009). Based on these findings, in our department Blazsek et al. (Blazsek et al., 2009) developed **a novel experimental model for the evaluation of osseointegration and bone remodelling around** longitudinally placed **titanium implants** in tail vertebrae and proposed to name it "OSSI" (OSSeoIntegration) model (*Figure 3*). The original methodology for osseointegration analysis using rat tail vertebrae applied only rough evaluation procedures, which were not very sensitive. Thus, it was important to further develop the OSSI model for the quantitative and qualitative characterization of osseointegration. During further developments of the "OSSI" model we analysed the available implant stability evaluation methods. Accordingly, the most reliable four methods were chosen: RFA, micro-CT, histology and pull-out test. We expected that this would allow us to assess the biological integration of titanium implants with multiple, clinically proven analyses, in contrast with existing experimental setups, where one or two variations are evaluated usually. It is important to use multiple

evaluation methods and combining clinically reliable methodology with experimental approaches **to improve the reproducibility of experiments**.

1.5 Preclinical studies to provide a basis for human bone regeneration and osseointegration

In the field of regeneration and replacement a huge variety of animal models have been used. The preclinical experimental setups have to have to be **reasonable** and have **evidence** from human clinical practice. **Pre-clinical evaluations** would be required before the clinical use of any **medical devices** (Wancket, 2015). Experimental setup selection includes many factors: costs of acquiring, care for animals, availability, acceptability for the society, tolerance to captivity and ease of housing. Also, there are factors which should be considered during model selection. The first factor is the matching of a model site and human bone according to macro (anatomically) and microstructure (histologically). The second parameter is blood supply. Blood supply is often affected by the macroscopic structure of the bone (in spongiosa vascularisation is higher than in the cortical bone) (Zoetis et al., 2003). The third parameter is the possibility of recruiting control groups for treatments. It is obvious that self-control is much more valuable than using other specimens as controls. The fourth parameter is nutrition and general condition of animals. Nutrition and general condition should be close to human reality, in which we would like to use the medical device further on. The fifth parameter is the age of experimental animals (Meyer et al., 2001). The younger the animals, the faster the healing process (Meyer et al., 2001). The sixth parameter is the extent of intra- and inter-animal differences.
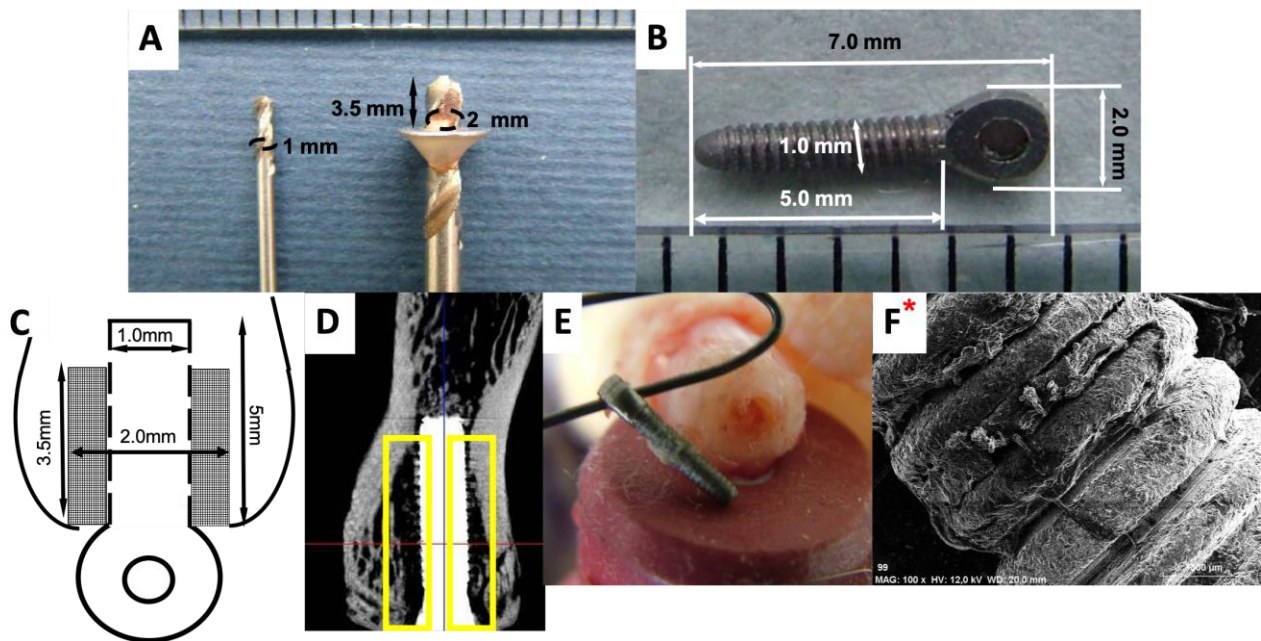
Figure 3.

Photographic documentation and schematic illustration of rat tail based experimental setup developed by József Blazsek (permitted to be used by József Blazsek) and the image taken by the PhD candidate of the present thesis * (Blazsek et al., 2009).

A. Drills for bone preparation in the classical "OSSI" experimental model. **B.** The titanium implant with threads used for the classical "OSSI" experimental model. **C.** Schematic illustration of the longitudinal section of the rat tail vertebra with an inserted titanium implant. An empty space created for bone neogenesis **D.** The radiological image from micro-CT analysis showing the empty space around the implant (highlighted with yellow rectangles). The yellow rectangles showed the region of interest for the evaluation of new bone formation. **E.** The result of the pull-out test (tensional test machine Tenzi TE 18.1; TENZI Ltd., Hungary) was used to detect the absolute force needed for vertical removal of the threaded implant from the bony bed. **F.** After pull-out test the bone-implant interface was destroyed due to threaded implant geometry. The scanning electron microscopy image represents threaded titanium implant with fractured bone tissue between the threads after pull-out test for integrated implant.

Unfortunately, it is difficult to use the human implant size during preclinical evaluation using small animals. But the importance of improving medical devices is essential for **screening evaluations**. Accordingly, downscaling of the implant size should be done. The main outcomes (biological relevance, bifunctionality and biocompatibility/safety) will also be achieved during the insertion of downscaled intraosseous implants into the small mammals. Also, the use of small animal models will involve much smaller financial investment for primary *in vivo* evaluation and will provide

a reliable basis for further *in vivo* evaluations when using bigger animal models. The methods for the evaluation of the integration process should assess the biological parameters of integration more closely to clinical reality.

Many mammalians (such as sheep, goats, dogs, pigs or rabbits) are suitable for testing bone regenerative materials, materials for intraosseous implants and their modifications (Pasupuleti et al., 2016; Pearce et al., 2007; Stricker et al., 2014; Wancket, 2015). Non-human primates are sometimes also used despite their costs (Jerome et al., 2001). Rodents such as mice (Biguetti et al., 2018; Li et al., 2017; Li et al., 2015b), rats (Back et al., 2012; Jariwala et al., 2017) and hamsters (Lee et al., 2013) have been widely used for osseointegration and bone regeneration research because of specific advantages such as small size, low cost, known age and genetic background, controllable microflora, and ease of handling and housing (Boix et al., 2006). Rat models are suitable for the assessment of histological bone regeneration providing sufficient statistical significance achieved by using numerous animals and for providing pre-clinical relevance (Bhardwaj A, 2012). Different rat models have been developed based on reproducible defects in different bone locations (Bhardwaj A, 2012; Stavropoulos et al., 2015). Calvaria, tibial, femoral and critical size of mandibular bone defects in rats have been used in various studies to investigate the effectiveness of bone regenerative agents such as growth factors, biomaterials, cell or tissue implantation, or any combination of these (Ebina et al., 2009; Espitalier et al., 2009; Kummari et al., 2009; Morad et al., 2013). Unfortunately, none of these models combine minimal morbidity to the experimental animal, easy reproducibility, similarity to the human jaws (histologically and anatomically) and multifactorial analysis of healing according to the clinical loading of implants. The assessment of biological relevance, biofunctionality and biocompatibility/safety (assessment of physiological, biomechanical and hormonal functions of the bone) of intraosseous implants and bone-grafting materials should be done using smaller animal models first (Wancket, 2015).

The pioneer research targeting the solution of the above described open questions was primarily initiated by József Blazsek. Blazsek et al. first described the rat tail vertebrae as a potential hosting tissue for neo-ossification and osseointegration (Blazsek et al., 2009). Blazsek and his colleagues used the 4th caudal (C4) rat vertebrae for implant placement. The implant used in this work had threads. The bone cavity preparation for

implant insertion had a special shape. The apical part of the implant had a direct contact with the bone for primary anchorage of the implant. The implant was screwed into this 1 mm bone cavity at the apical part. The remaining two thirds of the implant body were surrounded by a space between the implant surface and the bone. The space between the implant body and the hosting bone tissue provided possibility for local application of bio-materials and/or selected cell populations to be tested. It also allowed us to measure the effect on neo-ossification and the biomechanical properties of the implants. In his PhD thesis Blazsek called this experimental model an "OSSI model" (Blazsek, 2008). *Figure 3* schematically illustrates the main principles of the "OSSI model" described by József Blazsek. From the PhD thesis of József Blazsek we know the dynamical developments of the secondary stability of titanium implants in the rat tail (*Figure 4*). Based on the dynamics of osseointegration growth we could separate three main levels. The first level was from the first week to the fourth week, the second level was from the fifth week to the twelfth week and the third period was from the thirteenth week to infinity. We can assume that the three main steps represent different levels of new bone formation around the implant. It can be assumed that the first period represents the inflammatory phase, the second – proliferative phase and the third – maturation phase, which is followed by bone remodelling lifelong. Accordingly, the end points of these three evaluations could provide useful data for the evaluation of osseointegration in further studies.
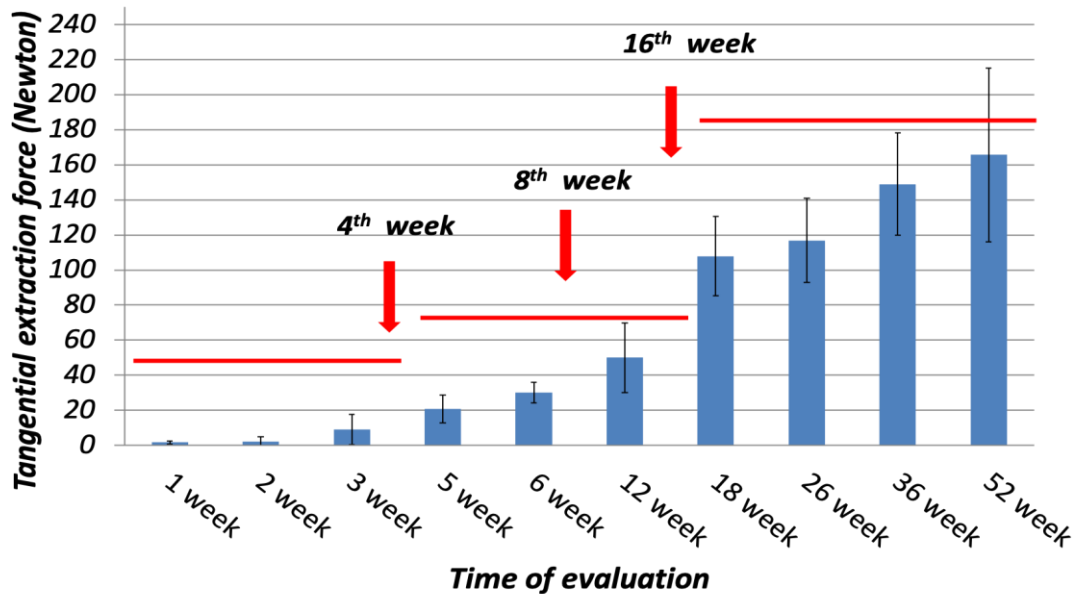
Figure 4.

The time-dependent changes in extraction force, expressed in Newton (N), following implantation evaluated by the specially developed Tenzi TE 18.1 (TENZI Ltd. Hungary) machine, using healthy adult Wistar rats ("OSSI model"). The base of the graph is taken from the PhD thesis of József Blazsek with his permit (Blazsek, 2008).

1.6 Surgical wound closure in humans

In modern clinical practice implant placement in the edentulous areas has become a standard of care. Their loading, as it was described above, is determined by primary implant stability. Low implant stability values (less than 20 Ncm or 60 ISQs) and simultaneous bone-grafting accompany conventional loading (from 2 months after implantation) (Gallucci et al., 2014). If there is a bone defect of jaws (horizontal or/and vertical), which cannot heal spontaneously during lifetime, it is called critical bone defect, that is CSD (Bosch et al., 1998). **Guided bone regeneration** (GBR) is the gold standard for recovering the bone volume vertically and horizontally. The success rate of GBR is determined by the experience of the surgeon, habits of the patients, morphology of the defect, applied regenerative materials, preparation of the cortical bone, graft stability, flap closure above the grafted area (Cesar-Neto et al., 2005; Saldanha et al., 2004; Machtei, 2001; Majzoub et al., 1999; Palmer et al., 1994; Simion et al., 1994a; Simion et al., 1994b;

Vanden Bogaerde, 2004; Zitzmann et al., 1997). The experience of clinicians can be improved dynamically by trainings. Habits of patients can be adjusted by personal education and follow ups. There is a huge variety of regenerative materials of different origin, which yield good standard results for integration and regeneration. The most essential elements for successful regeneration of all parameters are **flap design, flap release, flap closure**. In order to properly achieve primary closure to minimise the occurrence of complications and maximise long-term regenerative outcomes, adequate flap release of both the buccal and the lingual flap is required (Simion et al., 2007; Urban et al., 2017). In recent years, **different flap management techniques** for bone augmentation in the posterior mandible have been proposed in the literature. However, the level of evidence is limited to technical descriptions and case series studies (Pikos, 2005; Ronda et al., 2011). Additionally, these "classic" techniques present limitations associated to complete (Pikos, 2005) or partial (Ronda et al., 2011) detachment of the mandibular insertion of the mylohyoid muscle, which can lead to serious **postoperative complications**.

Successful and predictable management of complex clinical scenarios to facilitate prosthetic-driven implant placement via vertical bone augmentation in severely resorbed edentulous ridges require profound anatomical knowledge, understanding essential biological principles and refined surgical skills. Understanding the implications of local anatomical structures respective to the planned surgical technique and the possible challenges and complications that may arise, both intra- and post-operatively, is fundamental (Greenstein et al., 2008).

Vertical ridge augmentation is considered as a type of GBR. Vertical ridge augmentation in the posterior mandible remains a technique-sensitive procedure associated with an increased risk of damaging key anatomical structures, such as the lingual nerve, the sublingual artery and Wharton's duct (Simion et al., 1994c; Tinti et al., 1998; Urban et al., 2014; Urban et al., 2016). It is important to **determine the effectiveness of different flap designs** for oral and periodontal surgeries for the extent of lingual flap release, for the augmentation of the vertical ridge **in the posterior mandible**.

2. OBJECTIVES

1. The primary aim of the present work was to **refine the original**, previously developed preclinical *in vivo* rat tail implant model to make it **suitable for quantitative** and **qualitative monitoring of osseointegration** of implants by combination of biomechanical and structural evaluations:

> **1.a**: to **adapt** the **resonance frequency analysis**, originally developed for humans, **to the rat tail** model for more precise evaluation of osseointegration
>
> **1.b**: to develop an **implant design** that will later be suitable for the investigation of the effect of surface modifications on osseointegration excluding the influence of macro-design on the bone bonding strength to the implant surface
>
> **1.c**: to develop a **complex biomechanical evaluation** by the combination of resonance frequency analysis and pull-out techniques
>
> **1.d**: to **combine the biomechanical evaluations with structural tests** in order to reliably monitor the osseointegration process in a small animal model that is suitable for preclinical screening
>
> **1.e**: to **improve surgical conditions** and postsurgical care.

2. We also aimed to develop an **experimental model** for **monitoring** of **bone** defect **regeneration**, and **integration** of **multiple implants** placed simultaneously in a perpendicular direction into the tail by modifying the original rat tail model.

3. Finally, we attempted to **determine** the **effectiveness** of two different flap designs for oral and periodontal surgeries for the improvement of lingual flap release, applying fresh human cadaver heads. We compared the outcomes of the **"non-detaching" and "detaching" techniques for the mylohyoid muscle**.

3. MATERIALS AND METHODS

3.1 The refinement of original *in vivo* rat tail implant model for quantitative and qualitative monitoring of osseointegration

In his pioneering work J. Blazsek et al. (Blazsek et al., 2009) developed a novel experimental model for osseointegration and bone remodelling around longitudinally placed titanium implants in tail vertebrae, the classical "OSSI" model. Although the original model was fundamentally new and innovative, it did not allow quantitative evaluations of implant osseointegration (Blazsek et al., 2009). Thus, it was necessary to further elaborate the surgical procedure, the implant design, the postsurgical care, and also the complex detection of the integration process. Therefore, in the present study, we aimed to refine our original model to develop a quantitative preclinical screening model for osseointegration of implants with special emphasis on biomechanical evaluations. We assumed that in the rat tail vertebrae, osseointegration of titanium implants could be quantitatively monitored by a combination of biomechanical resonance-frequency analysis and pull-out test, and by the structural micro-CT and histomorphometry methods. To do this, we first adapted the resonance-frequency analysis technique, which was previously available only for humans, to the rat tail vertebra dimensions. Afterwards, we developed a new implant design, then we tested its integration using a complex evaluation system under strict experimental conditions.

3.1.1 Development of an implant design that is suitable for the investigation of the effect of surface modifications to osseointegration

Here the task was to develop an appropriate implant design which fits into the bone volume of rat caudal vertebrae and allows to perform the non-invasive RFA followed by the invasive pull-out test, using the same implant.

For RFA, the direct connection should be made between an implant and a specific SmartPeg type. SmartPeg is a magnetic transducer of modern Osstell devices – ISQ, IDX and Beacon (Osstell AB, Gothenburg, Sweden) (*Figure 5*). The aim during the fabrication of the head of the implant was to create a proper connection between the

implant and the SmartPeg, which would allow a reproducible evaluation of implant stability.
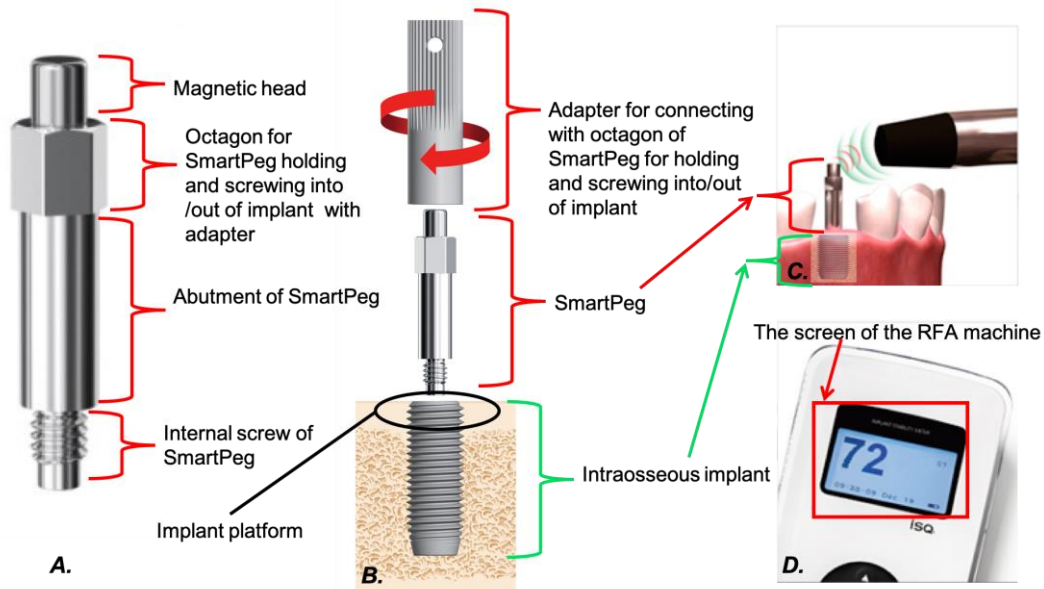
Figure 5.
Schematic illustration of SmartPeg, its installation and application for measuring implant stability non-invasively during resonance frequency analysis (RFA).
A. Parts of SmartPeg. ***B.*** Steps of SmartPeg installation into the implant before measurements (RFA). ***C.*** The RFA of the intraosseous implant using SmartPeg transductor. The magnetic impulses are generated from the pin of the RFA machine. The magnetic head of SmartPeg absorbs and refracts some of them back to the pin. The difference between the absorbed and refracted impulses: the machine calculates implant stability quotient (ISQ). The ISQ can range from 1 to 100, which indicates that the higher the value the higher the stability. ***D.*** On the screen of the RFA machine, the individual ISQ value of the measured implant is presented.

Resonance frequency, determining implant stability, can be measured by modern Osstell devices through a magnetic transducer (SmartPeg), which, by screwing, is directly connected to the implant. The transducer is stimulated by the electromagnetic waves of the probe (created by the coil in the probe) of the Osstell device. By sending a magnetic impulse from the probe, the apparatus switches automatically to a mode for detection of resonance frequencies from the SmartPeg (***Figure 5.C***). The frequency and amplitude are directly proportional to the vibrations of the implant. Based on the levels of resonance, the Osstell device produces an implant stability quotient (ISQ) between values 1 and 100

(referring to a resonance frequency range from 3500 to 8500 Hz) (*Figure 5.D*). Larger ISQ values indicate higher stability. Clinically, RFA is usually performed from multiple directions. This is important because the stability of the implant is strongly dependent on the surrounding bone configuration (Chatvaratthana et al., 2017). To find the lowest stability, the manufacturer recommends measurements at least from two different directions (Chatvaratthana et al., 2017; OsstellAB). Clinically, the lowest stability is found in the buccal-lingual direction, while the highest stability - in the mesial-distal direction (Chatvaratthana et al., 2017). In our further studies, we placed the implants directly into the middle of the rat tail vertebrae. Rat tail vertebrae have cylindrical shape. It means that the implant surrounding bone configuration can be different in four different directions. Accordingly, we planned to perform RFA standardly: from four different directions during all resonance frequency measurements. Between the steps of development, we performed calibration measurements using a calibration block provided by the manufacturing company, Osstell AB.

After describing our aims to Osstell company, they advised us (personally by Anders Peterssen, Chief Operating Officer (COO) of Osstell in 2012) to try and work with a couple of different SmartPeg types. All developments of the implant head were controlled and approved by Anders Peterson, who was the main theoretical inventor of RFA measurements.

The Osstell company produces a vast variety of SmartPegs which are suitable for the majority of implant systems present on the market. The main differences between their individual types are in the lower part of the abutment of the SmartPeg (shape) and the internal screw of the SmartPeg (length, threaded part location, width) (*Figures 5.A, 5.B*). Variations among implants at the platform level are based on the differences in the diameter of abutment-implant connection. The recommended SmartPegs have the thinnest internal screw parts. After receiving various SmartPeg types from Osstell, the technical implant developments and their adaptation to the implants were done by collaboration with Full-Tech Ltd. (Hungary). We conducted a series of evaluations based on our developments.

Finally we selected SmartPeg type 62, which had the narrowest internal screw part (Ø1.4 mm). This was essential for producing the narrowest implant head because we had size limitations from the caudal rat vertebrae. The boundaries of our developments were

limited by bone structure volume of rat tail vertebrae. The limits were determined by the height/length of the vertebrae (approximately 9.8 mm) and the width (approximately 3.8 mm) of caudal vertebrae of the adult Wistar rats (from 380 to 500 grams). Based on that, we developed different shapes of implants with varying parts of heads, which were pre-determined by the sizes of SmartPeg type 62. Unlike the strong limitations of the implant head size, the body of the implant was able to vary significantly. The only restriction for the size of the implant body was the residual bone volume around the implant after insertion.

Altogether, there were three major different macro designs developed considering rat caudal vertebrae sizes: fully-threaded, half-threaded and non-threaded (***Figure 6***). For all of them, the implants' core was cylindrically shaped with a diameter of 1.3 mm at the body part and 2.9 mm at the neck part. The total length of the implant was 9.5 mm, and only 7.5 mm were planned to be placed into the bone, and 2.0 mm - above the bone. Altogether, the head part of the implant was 3.0 mm long. By submerging the half height of the implant head into the vertebra, we could provide tension-free wound closure above the implant. That was an essential aspect for reducing the possible rate of soft tissue complications during healing. The head part of the implant was the connecting point to the SmartPeg with the implant.

Figure 6.
The schematic illustration of three main implant geometries suitable for RFAs and pull-out tests. The green line labels the level to which the surface treatment was done. The first red box highlights the head part of the implant and the second yellow box shows the implant body.
A. Fully-threaded implant. **B.** Half-threaded implant. **C.** Non-threaded implant.
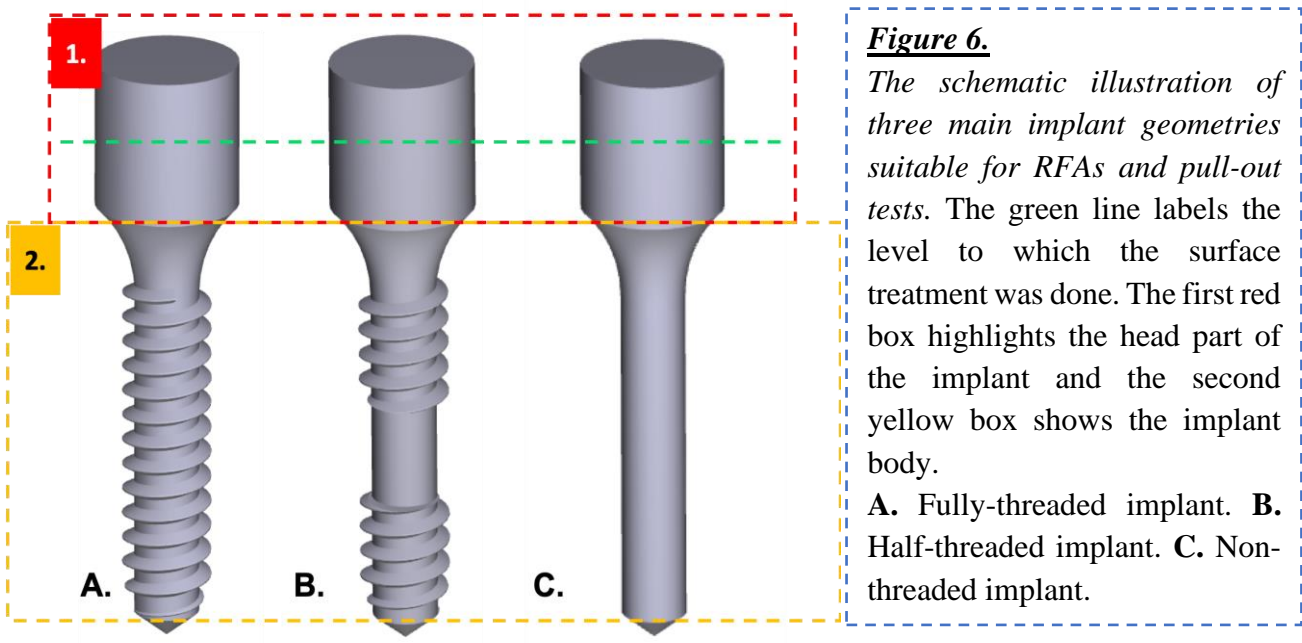
The implants were made of biocompatible Grade 4 commercially pure titanium (cPTi). The titanium rods were machined to the needed shapes by CNC lathe instruments (EMCO Turn 325, Siemens Ltd., Germany) based on the 3D plans. The implant sizes for manufacturing were based on the bone volume of rat caudal vertebra. Accordingly, the intrabony part of the implant could not be longer than 9.0 mm and wider than 3.0 mm. The remaining bone was needed to maintain the vertebrae volume after implantation. The intrabony part of all titanium implants (7.5 mm) was uniformly modified by sand-blasting (Korox® 250, Bego, Germany) and subsequently by chemically-etching with 43% orthophosphoric acid. This surface treatment was needed for distinguishing the intrabony and extrabony parts.

3.1.2 Development of complex biomechanical evaluation by the combination of resonance frequency analysis and pull-out techniques

The head geometry of our customized implants was specially designed and fabricated to allow a direct fixation of SmartPeg type 62 into the implant head by screwing. We had followed a similar strategy for developing the SmartPeg connection to our custom implants for the RFA method as described in a previous publication (Nienkemper et al., 2013). The implant head was fabricated with inner threads. The thread design inside the head allowed direct screwing into and out of any other components such as a hook for further biomechanical evaluations (for instance for pull-out test) (***Figures 7.C, 7.D***).

3.1.2.1 Validation of the individually developed connection between SmartPeg and customized implant using RFA

The validation of the newly formed connection between SmartPeg and implant was done on implants after fixing them into the plaster. The implants were submerged until the surface treated part of the implant. The plaster was let to be fully set for 15 minutes. After plaster fixation, the stability of each implant was recorded in 4 perpendicular directions, five times per direction. For each implant, twenty ISQ values were averaged to describe the stability of the particular implant. Altogether, 20 fully threaded implants were analyzed.

In a second set of evaluating the newly formed connection, implants were inserted into amputated rat tail vertebrae. Before implant insertion, the implant bed preparation protocol was developed *ex vivo*. We worked with specially-selected and fabricated drills (Full-Tech Ltd., Hungary). The drills for implant bed preparation were also carefully tested. Consequently, the subsequent drilling protocol was established: primarily a pilot drill, secondly a twist drill and finally a neck drill (***Figure 9.A***). With the pilot drill, we perforated the cortical layer with a diameter of 0.5-1 mm using 1500 revolutions per minute (rpm). Then, a twist drill with a diameter of 1.3 mm was used to create the 7.5 mm deep cavity using 1000 rpm. The preparation depth, using a twist drill, was controlled with an individually developed adjustable stopper, which was fixed to the twist drill by screwing. Finally, a neck drill was used to prepare the space for the implant neck using 200 rpm in 2.5 mm depth. The described drilling protocol was further used for in vitro and *in vivo* implant placements. During the first two steps of the described drilling protocol, a specially developed surgical guide assisted in standardized implant bed creation (***Figure 9.B***). The surgical guide was jointly developed in collaboration with Full-Tech Ltd. (Hungary) for positioning the drills in the middle of the vertebrae irrespective of the exact diameter of the tail. The mechanism of the surgical guide resembles the mechanism of a camera diaphragm shutter *(**Figure 9.B***). The implants were installed up to the surface-treated part. Altogether, 5 fully-threaded implants were installed into 5 different vertebrae *ex vivo*.

Each step of drilling was performed with surgical handpieces and physio-dispenser, similar to human surgical procedures. Throughout all the steps of implant bed cooling, preparation was done by the irrigation of sterile water from a syringe. After cavity preparation, implants were placed using an implant driver into the prepared cavity. The vertebrae with implants were dipped into plaster in order to avoid any external influence and standardizing the RFA. During installing the samples into the plaster, it was important to position the vertebra's surface (which had the implant head externally) at the same level as the plaster (***Figures 7.F, 7.G***). Consequently, only non-treated implant head parts towered. The time for plaster fixation was the same as before. Afterwards, the SmartPeg type 62 was screwed gently into the inner thread of the implant neck until reaching resistance (***Figures 7.A, 7.B***). Then RFA measurement was performed 20 times for each implant.

Figure 7.

Technical development steps of implants (for insertion into the rat vertebrae) and supplementary parts for RFA.
A. The cross section of SmartPeg and implant head. **B.** Magnified (2x) cross-section of SmartPeg and implant head. The pin part of the SmartPeg is highlighted with green interrupted line. **C.** The screwed hook for implant extraction. **D.** The fully-threaded implant with a hook. **E.** Stoned models with caudal vertebrae and inserted implants with SmartPeg. **F.** RFA analysis. **G.** Setup for the pull-out test: a stainless steel cable (Ø1.5 mm) was pulled through the hook to provide an appropriate grip for the measuring device. **H.** The pull-out force measurements. **I**. The extracted fully threaded implant. **J.** The registered maximum pull-out strength needed to remove the fully threaded implant from the rat tail vertebrae.

3.1.2.2 Evaluation of implant-hook connection during pull-out tests

The evaluation of pull-out testing was performed with fully-threaded implants after their RFA in the vertebrae. A special hook was screwed into the fully-threaded implant head to register the axial extraction force for the evaluation of biomechanical implant stability. Through a hook, a very thin stainless-steel cable (Ø 1.5 mm) was pulled, and the end of that cable was attached to the sensor of the pull-out machine. Thus, it was possible to measure the peak force needed for the destruction of the implant connection to the surrounding tissues. For the pull-out testing, we used a much more sensitive device than the previously used Tenzi TE 18.1 (TENZI Ltd., Hungary). That could be done because of a collaboration with the Department of Materials Science and Engineering, Budapest

University of Technology and Economics, Budapest, Hungary (personally with Dávid Pammer). Besides the peak force detection, the new methodology allowed us to register the instant force as a function of the implant displacement in the axial direction, which can be detected using a tensional test machine Instron® 5965 (Instron®, USA). Altogether, 5 fully-threaded implants were analyzed using the pull-out test from the vertebrae.

Based on the efficient evaluation of RFA and pull-out test measuring methods, it was decided to evaluate the primary stability with the mentioned methods by using three different implant geometries. The three geometries were the non-threaded, half-threaded and fully-threaded ones.

3.1.2.3 Evaluation of three implant geometries with RFA

3.1.2.3.1 Artificial bone blocks

For in vitro implant stability evaluations polyurethane foam (PUFs) artificial bone blocks were used (Sawbones Ltd., USA) (model 1522–05; Pacific Research Laboratories, Vashon Island, WA). The standard D1, D2, D3, D4, D5 densities of these artificial blocks correspond to the human bone density classification, according to Misch (Misch, 1989) (Misch, 1990). We used all the five types of density of these PUF blocks. Polyurethane resins are available in all density classes that could simulate different bone densities. These five bone densities are the most frequent ones in mammals. The technical specifications of the PUF blocks are correlated with ASTM F1839 – 08 (2016) (American Society for Testing and Materials, Standard Specification for Rigid Polyurethane Foam for Use as a Standard Material for Testing Orthopedic Devices and Instruments) (ASTM, 2016).

3.1.2.3.2 Implant bed preparation and implant insertion

The location of each implant bed in PUF blocks was performed on standard distances to each other. The drilling sequence for all implants was the same as it was described above by using the pilot, twist and neck burs. During all the steps of PUF preparation, cooling was done by irrigation with tap water from a syringe so as to avoid the melting of PUF.

All needed implant beds were prepared ahead of implantations. For achieving primary stability, the three types of implants were simply inserted into the prepared implant bed up to the surface-treated head part. The fully-threaded and half-threaded implants were screwed. The non-threaded implants were press-fitted. Altogether, five implants from each implant geometry were placed in each artificial bone density.

3.1.2.3.3 Implant stability measurements using RFA

After implant insertions, the RFA measurements were performed. The algorithm of the measurements was in accordance with the already described parameters. For each implant, RFA was repeated 4 times.

3.1.3 Combination of biomechanical evaluations with structural tests for reliable and complex monitoring of the osseointegration process using "Direct OSSI" model

In these experiments we used the above-described non-threaded implant design, which seem to be entirely suitable for further *in vivo* osseointegration analyses.

3.1.3.1 Experimental animals for "Direct OSSI" model

A total of 63 male Wistar rats (Crl(Wi)Br, Charles River; 450-550 g) from the breeding colony of Semmelweis University were used. All international and national guidelines for the care and use of animals were followed. This investigation was carried out according to the EU Directive (2010/63/EU) and was approved by the animal ethics committee of the Hungarian National Food Chain Safety Office (PEI/001/2894-11/2014).

The animals were kept at a light-controlled, 23°C room temperature before and after the surgery. Rats were operated on under general anesthesia with sodium pentobarbital (Nembutal, CEVA, France, 40 mg/kg body weight, intraperitoneally (i.p.)).

Before surgery, the animals were kept together in large stainless-steel cages (5 rats in one cage), then held individually in stainless steel cages in the first two weeks after the interventions. The surgical procedure was carried out in the operating room.

3.1.3.2 Mini-implant design

For *in vivo* studies, we used non-threaded implants, based on the in vitro results. Those implants were cylindrical in shape without threads, and were made of biocompatible Grade 4 cPTi, fabricated using a CNC lathe machine (EMCO Turn 325, Siemens Ltd., Germany). Applying such a design, we aimed to develop a shape that is suitable for the unaltered evaluation of biological integration without any additional influence of the geometrical design (threads, holes, self-tapping). The cylindrical shape of the implants allowed us to measure the real strength of anchorage of the bone to the titanium and to exclude the influence of the form of the implant, thus, standardly monitoring the osseointegration by biomechanical and structural tests. As we previously reported, the size of the caudal vertebrae of 450-550 g rats was from 9.8 to 10.2 mm in length, and from 3.8 to 4.5 mm in diameter (Renaud et al., 2015). Accordingly, the implants were set at 2.9 mm in diameter at the level of the neck, and 1.3 mm at the body part. The length of the entire implant was 9.5 mm (***Figure 8.A***).

The implant head was constructed to have an inner thread, which first served to connect the SmartPeg for RFA measurements (***Figures 7.A, 7.B, 8.C***). Afterwards, the same threads allowed to connect the specially designed hook, which served as a stable connection between the pull-out device and the implant during extraction force measurement.
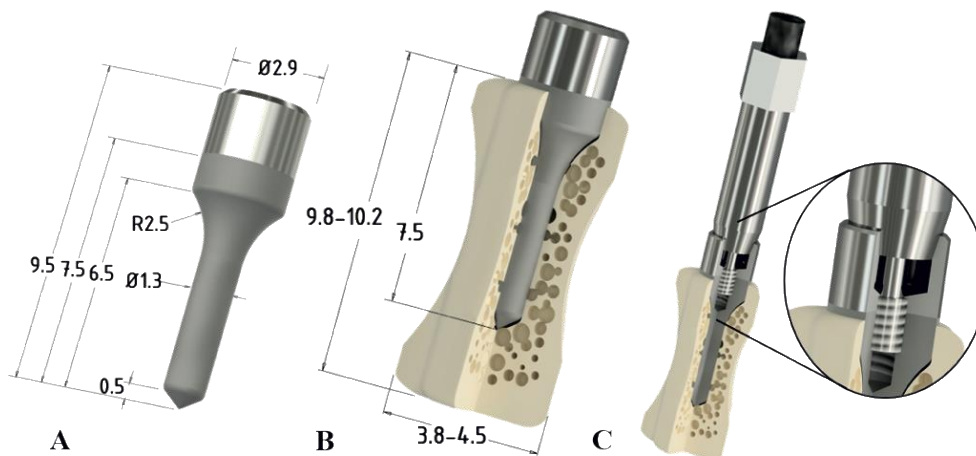
Figure 8.

Schematic illustration of the customized implant and its insertion in the hosting bone. **A.** The drawing of the implant. **B.** Schematic illustration of the implanted titanium device with the bone. **C.** Cross-section of connected SmartPeg type 62 with the customized implant.

3.1.3.3 Surgical procedure in "Direct OSSI" experimental model

The surgical procedure is based on our previously published model (Blazsek et al., 2009) with a number of important modifications. All the operative procedures were performed in sterile conditions using sterilized equipment, surgical hand pieces and physiodispenser, similar to human surgical procedures. The rats were operated on under general anesthesia with sodium pentobarbital (Nembutal, CEVA, France, 40 mg/kg body weight, i.p.). The animal was covered with a sterile tissue "barrier" (Mölnlycke®, Sweden), only the surgical field of the tail remained exposed. The weight of animals was registered before and after surgery. First, the tails were mechanically cleaned with warm water and a detergent, second, they were washed in three steps with a disinfectant solution (Softasept, B-Braun) for 3 minutes each. To control bleeding, double ligatures were positioned at the beginning of the tails. The skin surface of the entire tail was treated with 10% povidone-iodine (Betadine, Egis, Hungary). Three mm distally from the C4-C5 vertebrae joint, a circular incision was made and the skin was retracted. With a new blade, the distal part (after C4 vertebra) of the tail was amputated 3.0 mm proximal to the skin incision.

After the amputation of the distal part of the tail, an axial cavity was made in the opened surface of the C4 vertebra to host the implants using specially-selected and fabricated drills (pilot, twist drill and neck drill) (Full-Tech Ltd, Hungary) (**Figure 9.A**) and drilling protocols. The drilling protocol was the same as described above in section 3.1.2.1. The surgical guide was developed to fit the needs of rat tail vertebrae longitudinal preparation. By using the surgical guide, we were able to position the drills in the middle of the vertebrae irrespective of the exact diameter of the tail (**Figure 9.B**). After implant placement with the press fitting method, the soft tissues were repositioned and the wound was closed using standard non-resorbable 4.0 atraumatic sutures (Dafilon, B.Braun). Then skin was disinfected with 10% povidone-iodine and the amputated end of the tail was covered with tissue-adhesive strips (SteriStrip, 3M). Animals were kept at 37°C until awakening. No lethal complications happened during the surgery or afterwards.
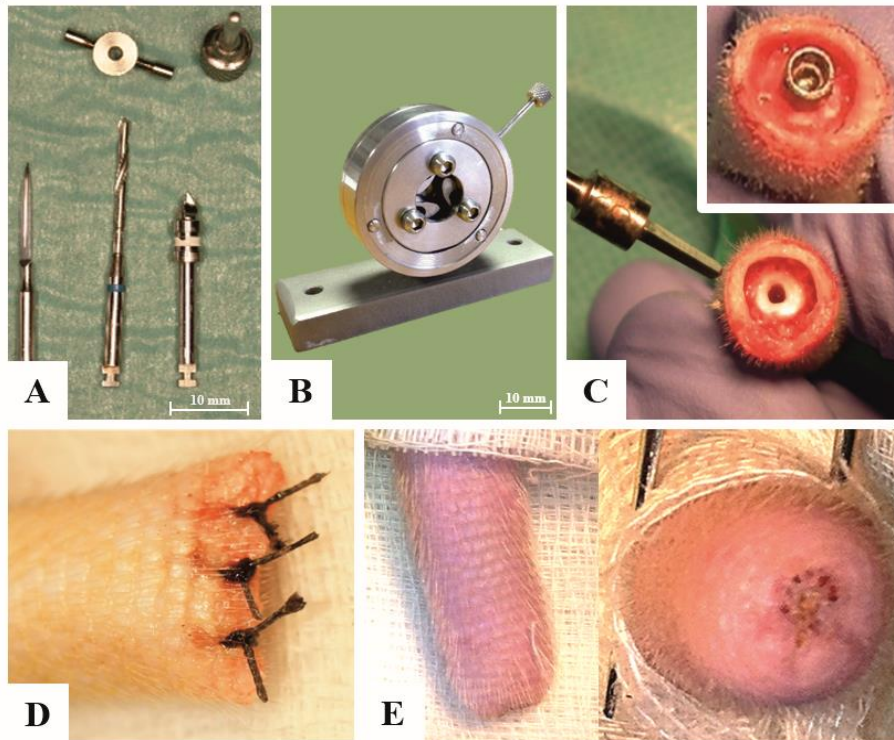
Figure 9.
Surgical and postoperative workflow of the preclinical screening model in the rat tail.
A. Surgical drilling kit for the preparation of the bone bed. **B.** Surgical guide for standard cavity preparation. **C.** Preparation of the hosting tissue and inserted titanium devices in the C4 rat vertebra. **D.** Wound closure of the amputated rat tail after implantation (the stump). **E.** The amputated tail after 8 weeks of healing, horizontal and vertical views.

3.1.3.4 Postsurgical treatment

Postsurgical care is as important as the surgery itself. This method included the application of tissue-adhesive strips (Steri-Strip™, 3M, USA) at the stump immediately at the end of the surgery. The applied bandage helped in the formation and stabilization of the blood clot. When the animals woke up after general anesthesia, the adhesive strip was removed by them very easily during the movements in the cage without any bleeding. Wound-healing was monitored every day during the first week and twice during the second week after surgery. Two types of antiseptic solutions were applied on the surface. Tails were disinfected using 3% hydrogen peroxide solution (Hyperol, Meditop Ltd., Hungary), then 10% povidone-iodine (Betadine, Egis, Hungary). Direct gentle palpation of the tail was done during handling of the animals for the detection of any inflammation

or other changes. A massage of the tail was performed during palpation to stimulate local blood circulation during the first three postoperative days.

3.1.3.5 Sample harvesting and evaluations for "Direct OSSI" experimental model

The animals were sacrificed under general anesthesia with sodium pentobarbital (Nembutal, 40 mg/kg body weight, i.p.). We sacrificed 21 animals after 4 weeks, 21 animals after 8 weeks, 7 animals after 12 weeks, 14 animals after 16 weeks. Since we did not have preceding data with the presently developed methodology, for sample size calculation we used the pull-out evaluation data at the 4th and 8th weeks' endpoints. At these endpoints we had 14 animals per group. Then we used the G*Power-free software (University of Dusseldorf, http://www.gpower.hhu.de/en.html). The α-error probe was 0.05, the power was 0.8, the allocation ratio N2/N1 was 1 and the effect size was counted as 2.87. Based on this calculation, we applied sample size n=7 in consecutive experiments.

The samples were used for either biomechanical (RFA and pull-out test) or for structural (micro-CT and histomorphometry) analysis. The tail was ligated at the bottom to control bleeding, then C3-C4 vertebrae were separated from the tails through surgical cutting the joint between C3-C2 vertebrae. The C3 vertebrae were used as healthy controls for C4 in histomorphometric and micro-CT analyses. For biomechanical evaluation, soft tissues were removed and the vertebrae were kept in 0.9% NaCl solution at 4°C until evaluations (from 12 to 48 hours). For structural analysis, the samples were fixed in a 10% buffered formaldehyde solution.

Based on the in vitro results, we set a complex evaluation protocol to analyze the interosseous implant anchorage in the bone tissue using combined biomechanical and structural methods. The biomechanical evaluation of osseointegration was performed applying RFA and pull-out tests, both on the same samples (*Figure 10*). The structural analysis was carried out by micro-CT and histomorphometry using the same samples.

3.1.3.5.1 Biomechanical evaluations

The two biomechanical tests were completed on the day of harvesting. We first performed RFA and then the pull-out test. 14-14 animals were tested at 4 and 8 weeks, while 7-7 animals were evaluated at 12 and 16 weeks.

3.1.3.5.1.1 RFA

A non-invasive (RFA) analysis was performed according to the previously described approach in the in vitro part. The RFA was recorded in 4 perpendicular directions, 5 times per direction (**Figure 10.A**). Then the average value of these 20 ISQ values was used to describe the stability of the particular implant.

3.1.3.5.1.2 Pull-out test

After the non-invasive evaluation by RFA, the axial extraction force was used to evaluate secondary implant stability. For the pull-out testing, we used a tensional test machine Instron® 5965 (Instron®, USA) in collaboration with the Department of Materials Science and Engineering, Budapest University of Technology and Economics, Budapest, Hungary (personally with Dávid Pammer).

Measurements were done according to the following steps: a) the hook was screwed into the head of the implant. Then a thin stainless-steel cable (Ø1.5 mm) was pulled through the hook-head to provide an appropriate grip for the measuring device; b) after that the PUF block was fixed with a metal bracket to the plate of the Instron® 5965 and the instrument was balanced, the implant was steadily pulled along the vertical axis until extraction (**Figure 10.B**). The maximal pull-out force (N) represents the strength of primary or secondary stability in the vertical axis. The pull-out test was applied in accordance with the ASTM F543 - 17 (American Society for Testing and Materials, Standard Specification and Test Methods for Metallic Medical Bone Screws) (ASTM, 2017). Its Annex A3 contains directives for the determination of pull-out test measurement parameters. Only one peak extraction value was detected for each implant.
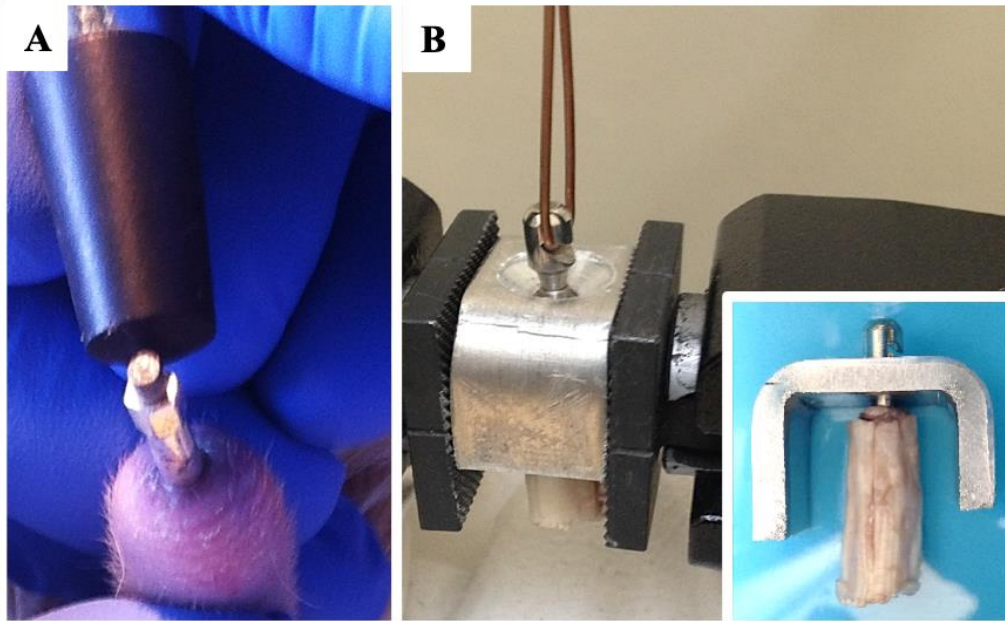
Figure 10.
Biomechanical evaluations of osseointegration of longitudinally placed implant into rat tail caudal vertebrae.
A. Evaluation of implant stability with resonance frequency analysis (RFA) using SmartPeg 62 transductor, which was screwed into the implant head directly. **B.** Axial extraction force measurement algorithm, with sample positioning.

3.1.3.5.2 Structural analyses

Twenty-one specimens (n=7 animals per group) were used for structural analysis such as micro-CT and histomorphometric analysis. The evaluation endpoints for structural analysis were at weeks 4, 8 and 16.

3.1.3.5.2.1 Micro-CT analysis

Before histological testing, we performed a 3D radiographic data acquisition to detect the structural basis of implant stability in the reconstructed 3D images (1172 SkyScan micro-CT, Bruker, USA). The device has an X-ray source from a sealed micro focus X-ray tube with a spot size of 8μm. In the present work an Al+Cu filter (Al 1.0 mm and Cu 0.05 mm) was used. The implant samples with bone were scanned at 360° rotation at 0.3 degree rotation step at 80kV, 124mA, 4598ms exposure time with an isometric voxel size of

12μm. For the reconstruction of raw images, a cone-beam volumetric algorithm was used with the NRecon V1.6.10.1 software (Bruker, USA). Measurements were performed within a certain region of interest (ROI) in the reconstructed images using the software CTAn V1.14.4.1+ (Bruker, USA) (Cha et al., 2009). The described protocol for scanning and reconstruction was specially designed and optimized to our experimental conditions in order to overcome the x-ray scattering on the metal surface.

The scanned samples were evaluated in 2D and 3D perspectives with task lists developed for this purpose in the CTAn software (*Figure 11.A*). The 2D analysis was done on slices from the 3D reconstructed sample. The calculated intersection surface/tissue surface ratio (i.S/TS) was used in the 2D analysis for characterizing the bone to implant contact. Based on the manufacturer's instruction (1172 SkyScan micro-CT, Bruker, USA) and our calibration process, we chose the 12 pixel-wide dilation length around the implant for determining the intersection surface value expressed in percentage. For bone volume assessment, a 38-voxel (0.461 μm) thick cylindrical volume of interest was selected around the titanium implant (Cha et al., 2009; Chang et al., 2013; Song et al., 2013). The manual global threshold method was used for the segmentation of new bone visualization. For determining the percentage of bone volume value, bone volume/tissue volume ratio was calculated (BV/TS). These studies were performed in collaboration with the Department of Oral Diagnostics of Semmelweis University.

3.1.3.5.2.2 Histology and histomorphometry

After micro-CT measurements, the samples were chemically fixed and embedded as previously reported (Liu et al., 2007). The sample processing was as follows: fixation in 10% buffered formalin; than the specimens were dehydrated in an ascending series of alcohol concentrations (50%–99%) and finally embedded in autopolymerizing methyl methacrylate resin (Wako Pure Chemical Industries Ltd., Osaka, Japan); afterwards the undecalcified tail vertebra specimens were cut using a diamond saw (SP 1600; Leica Microsystems, Wetzlar, Germany); then the received sections were adhered to the Teflon slides, and successively ground to a thickness of ~80 μm. The slices were then surface-stained with McNeal's Tetrachrome, basic Fuchsine and Toluidine Blue O (Schenk RK,

1984) for the histomorphometric analysis. The bone-implant contacts (BICs) were then analyzed under a light microscope with 4x and 10x magnification.

The bone to implant contact (BIC) evaluation was done using all the images. The BIC values of each sample were measured, and the average of the group was received. The BIC measurements were performed manually. On each histological slide the same ROI was chosen (*Figure 11.B*). The ROI for BIC assessments was considered to be the intrabony 1.3 mm wide implant body part with parallel walls. The perimeter of the total ROI was measured for each sample, which was the total area for possible BICs. Also, for each sample, the length of individually-formed direct bone contacts to the implant surface was measured. According to the two measurements, BIC ratio was calculated for each sample individually. For that purpose, the total BIC length was divided by a sum of the established BICs. Based on that, we received the BIC ratios. Then the percentage was calculated from the ratio. Consequently, the average data were calculated for each healing period.
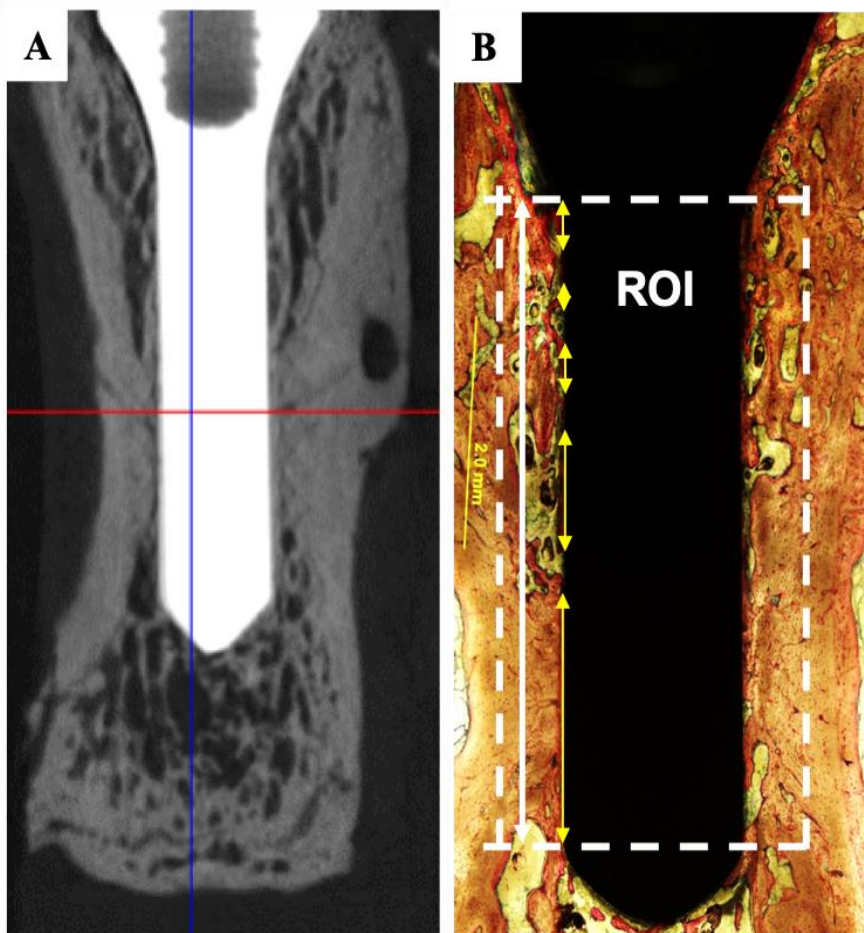
Figure 11.
Structural evaluations of longitudinally placed implant into rat tail caudal vertebrae.
A. Micro-CT capture of the implant within the bone. **B.** Histological undecalcified slide prepared for histomorphometric (4x magnification). The white broken lines represent the ROI. The vertical double-sided white arrow is showing the total length of the ROI. The double-sided yellow arrows shows the bone to implant contacts in the region of interest (ROI) (during the calculations of real samples the same calculations were done from both sides).

3.2 Development of a preclinical model for quantitative, qualitative monitoring of the regeneration of multiple bone defects and the integration of simultaneously-placed several implants perpendicular to the rat tail

Based on the principles, developed by Blazsek et al. (Blazsek et al., 2009) in the classical "OSSI" model, we further elaborated the original "OSSI" model to enable multiple placements of implants in positions perpendicular to the tail and to achieve multiple bone defects (Renaud et al., 2015) in collaboration with French colleagues in the frame of a joint Hungarian-French Science and Technology project. These studies were primarily done based on local Ethical committee of the Montpellier University permissions. In these studies the tails were not amputated. Instead, wounds for implantation and for the creation of bone defects were done transversally. This project was also started by setting the drilling sequence of the caudal bone transversally *ex vivo*. Then with our French partners, we first focused on the development of an experimental model based on rat tail vertebrae for monitoring quantitative and qualitative regeneration of bone defects. This model is called as "BD OSSI" model. Second, we worked to modify the original "OSSI" suitable for placements of multiple implants in a perpendicular direction of the tail. We call latter this model as "Gap OSSI" experimental model.

3.2.1 *Ex vivo* developments for rat caudal vertebrae bone drilling to create transversal defects

Knowing the skeletal limits of rat tail vertebrae, we started to test different drills provided by Full-Tech Ltd. for bony bed preparation transversally. Based on these preliminary experiments, five drills were chosen. The first drill was the pointer drill and was used for perforating the cortical layer of the bone in 2.0 mm depth (*Figure 12.C.a*). The second drill was the initial twist drill with 1.3 mm in diameter and 3.0 mm depth for drilling the vertebrae through one layer of cortical and the entire spongiosa layer (*Figure 12.C.b*). The third drill was also a twist drill, with parallel walls was used in the same depth and the diameter was 1.7 mm (*Figure 12.C.c*). The fourth drill was the countersink drill (*Figure 12.C.d*). The countersink drill gave a funnel shape to the cavity that allowed a softer preparation with less resistance of the bone tissue with the next drill. The fifth drill

was the main drill with 2.9 mm in diameter and was used also for 3 mm in depth (***Figure 12.C.e***). The location of the drilling was also calibrated. The middle of the vertebrae was not chosen because from the side to the middle of the vertebrae there was convexity, which reduced the diameter of the vertebrae (***Figure 12.A***). That is why the mesial part of the vertebra was selected for the creation of bone defects (***Figure 13***).
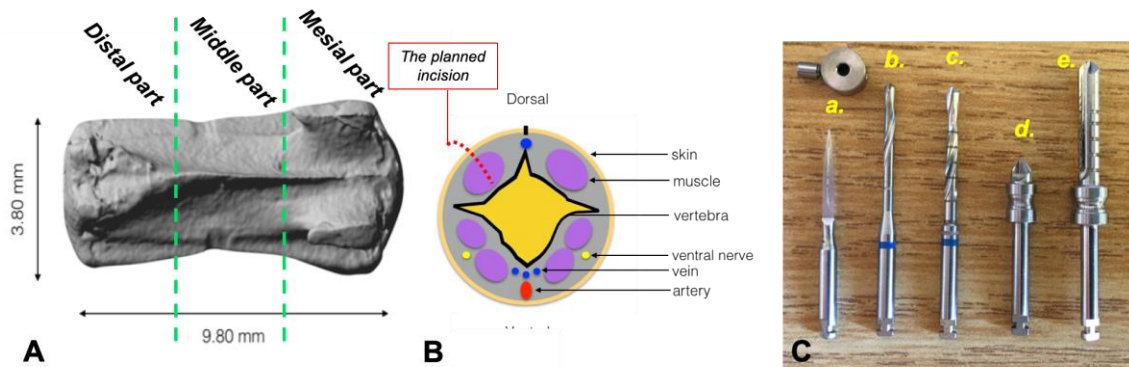
Figure 12.

Rat caudal vertebrae anatomy and adopted surgical drill set.
A. Dorsal view of micro-CT 3D reconstruction of C5. The caudal vertebrae is schematically divided in three different parts. The convexity of the middle part is highlighted. **B.** Schematic representation of muscle and vascular organization. Accordingly, the planned incision is positioned. **C.** The selected surgical drills for bone preparation transversally of the rat caudal vertebrae. **a.** pointer drill; **b.** 1.3 mm wide twist drill; **c.** 1.7 mm wide twist drill; **d.** countersink drill; **e.** main drill.

The anatomy of the rat tail was studied to avoid any damage to the mobility and blood supply during surgery. The surgical method was planned according to this (***Figure 12.B***).

3.2.2 Experimental animals for "BD OSSI" and "Gap OSSI" models

"BD OSSI" and "Gap OSSI" experimental work was performed at the Montpellier University, France. The "BD OSSI" experimental model focused on the evaluation of self-healing capacities of bone defects created in the bony structure of rat tail vertebrae. The "Gap OSSI" was developed to evaluate the osseointegration process of implants which were placed transversally to the axis of the tail. In both experimental setups male

Wistar rats were used ((Crl:(Wi)Br) from Charles River France) weighing 380 to 450 grams. That size of animals was selected to have an adequate size of vertebrae. All the animals were kept in light-controlled, air-conditioned rooms and fed ad libitum. Based on received ethical approval (from Montpellier University, referral number 1083 16/06/2014), we first evaluated the "BD OSSI" model and then the "Gap OSSI" model.

3.2.2.1 Experimental setup for "BD OSSI" model

In this experimental model, the animals were divided into two groups based on the healing time after bone defect creation. In the first group, healing was evaluated after 4 weeks and in the second group it was checked after 8 weeks. Three rats were used per group. For each animal four transversal defects were created from C2 to C5 rat tail vertebrae (*Figure 13*). In both groups, randomly two vertebrae were left empty after bone defect creation. In both groups, two vertebrae were used as controls (defect empty of materials), and two other vertebrae were used for xenograft (Bio-Oss® (Geistlich Pharma AG, Switzerland)) implantation. The treatments for the individual vertebrae were randomly selected.
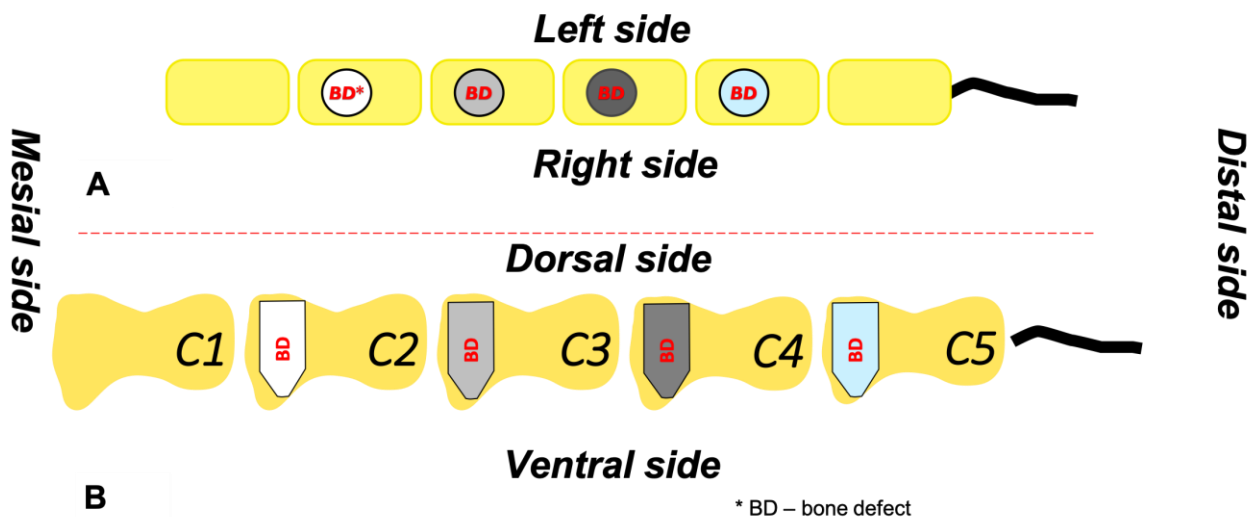
Figure 13.
Schematic illustration of bone defects localization in caudal vertebrae of a rat.
The size of one defect is 2.9x3.0 mm. *A.* Dorsal view of the tail. *B.* Lateral view of the tail.

3.2.2.2 Experimental setup for "Gap OSSI" model

In each caudal vertebra (from C2 to C5) customized titanium implants (Grade 4 commercially pure titanium (cPTi)) manufactured by Full-Tech Ltd. were press-fitted into the bony bed. The manufacturing of the implants was the same as it was described during the methodology of "Direct OSSI" model. Implant shape was designed to allow "distance osteogenesis" (new bone growth from the bone walls towards the implant body, *Figures 14.A, 14.B)*. The osseointegration was evaluated three months after implantation. Three rats were used for the osseointegration evaluation of the multiple transversally placed implants in rat tail vertebrae.
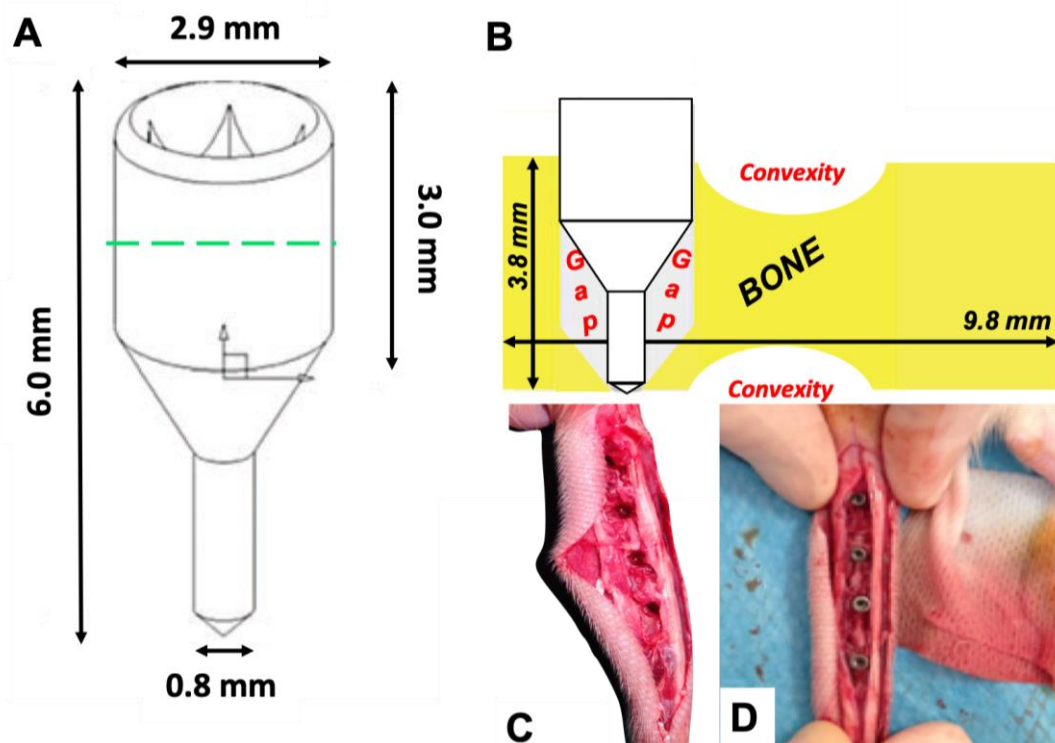
Figure 14.
Illustration of "Gap OSSI" model.
A. Drawing of the implant applied for "Gap OSSI". Under the green line the surface treatments of the implant take place. **B.** Schematic rat caudal vertebra with an implant inserted from the dorsal side. **C.** The prepared cavities in caudal vertebrae from C2 to C5. **D.** Visualization of implanted intraosseous implants from C2 to C5.

3.2.3 Surgical interventions

Presurgical preparations and soft tissue management were the same as described during the description of "Direct OSSI" model. During the bone preparation, the aim was to create the biggest possible bone defect in C2 to C5 vertebrae. During that, it was important to leave enough cortical tissue for the mechanical maintenance of the vertebrae. Accordingly, the defect size became 2.9x3.0 mm, cylindrically shaped from the longitudinal cross-section view (*Figure 13*). The artificially created defect of the bone can be grafted immediately after the bone preparation with different regenerative materials. The development of "BD OSSI" and "Gap OSSI" were done in collaboration with our partners from the University of Montpellier (Montpellier, France).

<u>3.2.3.1 Surgical procedure of the "BD OSSI"</u>

A dorsal incision was made approximately from C1 to C6 vertebrae. The skin and the muscles were retracted and irrigated by buffered saline solution (Otec®, Aguettant). As a result of retraction, the vertebrae were exposed. Then the hard tissue preparation happened in the exposed surface of the vertebrae. The sequence of the drilling was: the first drill – pointer drill, the second drill – initial twist drill with 1.3 mm in diameter and 3.0 mm depth (*Figure 12.C.b*), the third drill – a twist drill with 1.7 mm width (*Figure 12.C.c*), the fourth drill – the countersink drill (*Figure 12.C.d*), the fifth drill was the main drill with 2.9 mm in diameter and was also used for 3.0 mm in depth (*Figure 12.C.e*). Finally, 2.9x3.0 mm bone defects were created for xenograft (Bio-Oss®) implantation and the empty cavity control (*Figure 13*).

<u>3.2.3.2 Surgical procedure of the "Gap OSSI"</u>

The same steps of the soft and hard tissue preparation were done from C2 to C5 vertebrae as it was described in the surgical procedure of the "BD OSSI". After the soft tissue preparation, the bone was drilled with the previously described sequence of drills. Additionally, to the described bone drilling protocol, we also perforated the cortical layer of the vertebrae -using the twist drill - on the opposite side from the transversal bone

cavity in the rat tail vertebra. The additional cortical perforation was done for tip insertion of the implant, which provided extra implant stability. That kind of bone-drilling was performed for vertebrae C2 to C5. The specially developed implants were placed into each vertebra with a press-fitting method. Implants had two parts, the body, which was 0.8 mm in diameter, and the head 2.9 mm wide. The head part of the implant was the same as it was used for the "Direct OSSI" model (*Figure 14.A*). The difference was just in the body part. The implant body had a pin, which was reduced from 1.3 mm width to 0.8 mm width. The aim with this reduction was to create the distance between the bone tissue and the implant body. The 0.8 mm width of the body was also a technical limit for manufacturing. The head of the implant (with 2.9 mm width) stabilized the implant in the drilled cavity (*Figure 14.B*). The space between the body-part was left empty, or it could even be filled even with biomaterial (*Figure 14.B*). The created distance was aimed to model "distance osteogenesis" (Davies, 2003), which usually dominates when the surgeon performs immediate implant placement after a tooth extraction and a gap appears between the implant and the bone.

Soft tissue closure was performed in the same way in the "BD OSSI" and "Gap OSSI" setups. The muscles were repositioned over the defects and sutured together with resorbable sutures (Vicryl 4/0, Ethicon, USA). Then the skin was sutured with resorbable sutures too (Vicryl 3/0, Ethicon, USA) without high pressure.

The last step of the surgical intervention was skin disinfection with 10% povidone-iodine and the entire length of the tail and was covered with tissue-adhesive strips (Steri-Strip™, 3M, USA). Animals were kept at 37°C until awakening. No lethal complications happened during the surgery or afterwards in any experimental setups.

3.2.4 Postsurgical treatment

Rats were kept in individual cages and the wound-healing was controlled daily for the first week and twice per week during the following healing periods. Every second day, the tails were disinfected using povidone-iodine solution (Betadine®, Mundipharma, Paris, France). During handling the animals for the detection of any inflammation or other changes, direct gentle palpation with superficial massage movements (the first three times) of the tail were also done.

3.2.5 Sample harvesting and evaluations for "BD OSSI" and "Gap OSSI"

Rats were sacrificed by intraperitoneal injection of Pentothal® (Alcyon Pau, France) with a suitable dosage (200 mg/1.5 kg) at the end of the different long experimental periods. We sacrificed animals after four weeks and eight weeks from BDs formation. And the animals' sacrificing for the evaluation of osseointegration with "Gap OSSI" was done at the end of the 12th week from implantation. The tail was ligated at the bottom to control bleeding, then C2-C5 vertebrae were separated from the tails through surgical cutting of the joint between C1-C2 vertebrae. The soft tissues were removed, and the vertebrae were fixed in 5% formaldehyde solution at 4°C for 24 h. All the samples were used either for micro-CT or histomorphometry analysis.

3.2.5.1. Radiological visualization with micro-CT

For 3D radiographic, an X-ray micro-computed tomography (CT) instrument (SkyScan 1172, Kontich, Belgium) was used. The scanning parameters for the samples with an implant and without one were different. For implanted samples, further parameters were used: 360° rotation with 0.7° intervals and an Al+Cu filter (Al 1.0 mm and Cu 0.05 mm). For the nonimplanted samples, just 180° rotations with 0.5° intervals were applied with a peak voltage of 100 kV and 100 µA with an 0.5 mm aluminum filter.

The grayscale images were reconstructed from the software NRecon (SkyScan, Kontich, Belgium) and visualized with FIJI 1.5 software (NIH, USA). Then, these images were analyzed and aligned along the axis of the implant with DataViewer 1.5.2.4 software (SkyScan, Kontich, Belgium). The BIC analysis was performed with CTAn 1.15.4.0 software (SkyScan, Kontich, Belgium) and the visualization of the mesh with MeshLab 1.3.4 (INRC, Italy) and FIJI (NIH, USA) software. In the selected ROI, the tissue volume (TV) was analyzed on 3D reconstructed samples.

3.2.5.2 Histomorphological visualization

After micro-CT measurements, the rat tail samples with titanium implants were chemically fixed and embedded. The sample processing was as follows: the specimens,

fixed in 5% formaldehyde were dehydrated in an ascending series of alcohol concentrations (50%–95%) and finally embedded in epoxy resin (Epoxy embedding medium kit; Sigma-Aldrich, Lyon, France). Afterwards, the undecalcified tail vertebra specimens were cut in the centre of the implant using a precision diamond saw (Isomet 2000, Buehler, USA); then the received sections (with ~ 300 μm thickness) were successively ground to a thickness of ~ 150 μm with Escil 69680 grinding machine (Escil, Chassieu, France). The received sections were adhered to the slides. The slices were then surface-stained with Toluidine Blue for a histomorphometric analysis. The bone-growth around implants was then visualized under a light microscope.

3.3 Evaluation of the effectiveness of two oral different flap designs for the improvement of lingual flap release, applying fresh human cadaver heads

These studies were performed at the Institute of Anatomy of the Medical University of Vienna (Austria) according to local ethical approval. This was in accordance to our determination of the effectiveness of two different flap designs for oral and periodontal surgeries for the improvement of lingual flap mobility.

3.3.1 Sample and randomization

Twelve fresh human cadaver heads missing all posterior mandibular teeth bilaterally and with comparable extent of alveolar ridge resorption were selected. In this split-mouth study, the surgical technique corresponding to each side was randomly assigned with a coin toss. All surgical interventions were performed under the same environmental conditions and by the same surgeon, Dr. István Urbán, assisted by the PhD candidate of the present thesis, in order to control technical consistency.

3.3.2. Flap management technique

The control technique consisted of the mylohyoid muscle "detaching" release, as described elsewhere (Pikos, 2005; Ronda et al., 2011). The test side received the

mylohyoid preservation technique ("non-detaching" technique), which considers three key anatomical zones (***Figure 15***) and is sequentially described below:

A. *Tunnelling and lifting of the retromolar pad (RP) - Zone I*: Following a straight supracrestal incision within keratinized mucosa, the facial and lingual flaps are carefully elevated. A periosteal instrument is used to gently reflect the RP from the bone and then pull it up in a coronal direction. Since this tissue tends to be very elastic and resistant, it is relatively easy to perform this step. This allows the incorporation of the RP into the lingual flap, which contributes to the maximisation of flap release and reduces the risk of perforation when working on Zones II and III.

B. *Flap separation with mylohyoid muscle preservation - Zone II*: After visual identification of the mylohyoid muscle insertion, the soft tissue superior to the muscle is gently pushed with blunt instruments in the direction of the tongue. This way, the flap can be separated from the superior fibers of the muscle in a minimally invasive fashion, without detachment of the muscular insertion.

C. *Anterior, semi-blunt periosteal release - Zone III*: In the premolar region, where the mylohyoid muscle is attached deeply in the mandible, flap reflection should be no deeper than in zone II. A semi-blunt periosteal incision is performed with a N° 15C blade in a rotated perpendicular angle using a "sweeping" motion (Zone III) with the middle zone (Zone II). This manoeuvre provides flexibility to Zone III and helps to prevent postoperative wound dehiscence, which typically occurs if flap management is not adequate. If adequately performed, this technique typically allows for sufficient flap release to achieve passive primary closure.
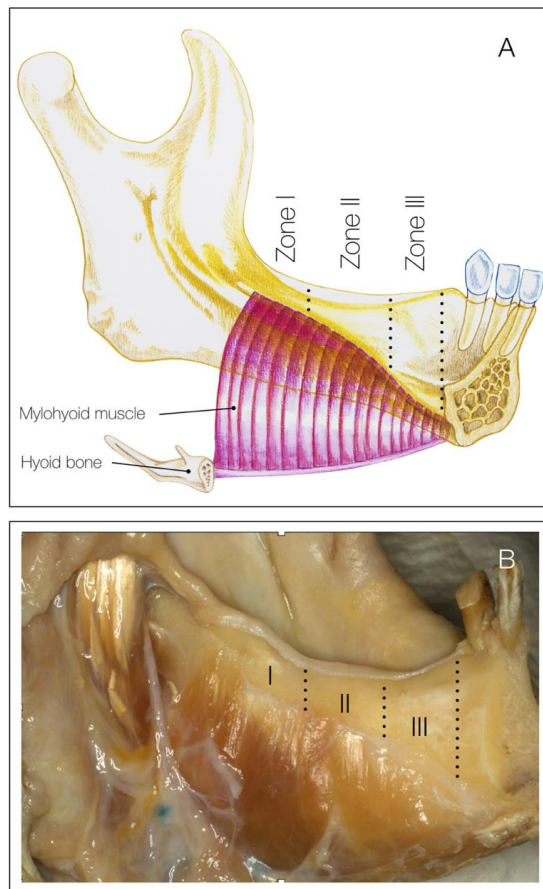
Figure 15. Drawing (A) and specimen photography (B) illustrating the anatomy of the typical insertion of the mylohyoid muscle on the internal aspect of the mandibular body and the location of Zones I, II and III.

3.3.3 Outcome measurements

The amount of vertical flap mobility was measured bilaterally in Zones I, II and III from the alveolar crest to the margin of the lingual flap at two different time points. The primary measurements served as baseline, after the initial flap elevation, but before flap improvement manoeuvres. And the secondary measurements were at the final step, after flap release was completed. At baseline, on both sides, the lingual flap was stretched until it reached its maximum passive stretch by using a high precision force gauge (Force Gauge SN-20 Series, Sundoo Instruments Co., Zhejiang, China) connected to straight mosquito forceps, as illustrated in *Figure 16*.

The forces were applied in a vertical direction, following a perpendicular vector respective to the floor of the mouth. The same "standard" forces were applied to stretch the flap after complete release. This standardization was achieved in order to maintain consistency between the baseline and final measurements for each surgical site. The

standard force ranged from 1 to 1.2 N, depending on the inherent elastic properties of each individual specimen. Two previously trained and calibrated examiners performed all the measurements in duplicate using a surgical probe scaled at intervals of 1-mm. When an agreement was not reached, independent measurements from both examiners were averaged and rounded up to the nearest millimeter. The mean value of all the duplicate measurements was used for statistical analyses.

Figure 16.
Force gauge connected to straight mosquito forceps to pull the released flap in a perpendicular direction respective to the floor of the mouth. Note that the applied force was approximately 1.1 N.

3.4 Statistical analysis of in vitro and *in vivo* evaluations

For all studies the data were given in the mean ± standard error of the mean (SEM) form. Each statistical test was performed using Statistica 12 software (TIBCO Software Inc., USA).

3.4.1 Statistical analysis for the refinement of original *in vivo* rat tail implant model

3.4.1.1 Statistical analysis of in vitro RFA stability results measured in PUF blocks

One-way analysis of variance (ANOVA) test and Tukey-Kramer Multiple Comparisons post-hoc test were applied to evaluate the statistical significance between bone densities using RFA of three different implant shapes.

3.4.1.2 Statistical analysis of biomechanical and structural evaluation of osseointegration in different endpoints using "Direct OSSI model"

One-way ANOVA and Tukey-Kramer Multiple Comparisons post-hoc tests were used to evaluate the statistical significance between different endpoints of healing using RFA, a pull-out test, micro-CT and histomorphometric analysis. Each data from each healing period were compared to each other. For the evaluation of correlations, Spearman's tests were performed to seek interrelationships between pull-out vs RFA biomechanical tests and also between micro-CT and histomorphometric structural analyses, respectively.

3.4.2 Analysis of self-regeneration of the bone in "BD OSSI" and osseointegration of customized implants in "Gap OSSI" model

Only the description of morphological healing results were performed after 1 and 2 months of bone regeneration in BD of rat caudal vertebrae. The osseointegration of implants, which had a gap around, was morphologically evaluated 3 months after healing. No statistical analyses between different healing periods and treatments were done.

3.4.3 Statistical analyses for the evaluation of the differences in flap mobility after two flap preparation techniques

The differences between measurements per zone, expressed in millimeters, as well as the percentage of change between baseline and final flap improvement between the two techniques were calculated. A Shapiro-Wilk normality test was performed to assess whether there was normality in the data set for both groups. Paired t-tests were performed to calculate flap release differences between the two surgical techniques per region, with the alpha value set to 0.05 for significance.

4. RESULTS

4.1 Quantitative and qualitative monitoring of osseointegration using "Direct OSSI" model to refine the original *in vivo* rat tail implant model

4.1.1 Validation measurements of an implant design suitable for the investigation of the effect of surface modifications to osseointegration in rat tail

First we tested the new implant design that is suitable for the adaptation of resonance frequency analysis measurements in the rat tail. The primary validation measurements of the newly formed connection between SmartPeg and fully-threaded implants were successful. The average ISQ of 20 implants stoned into the plaster was 58.82±1.59 ISQ. Thus, the results showed standardly repeatable measurements with very small deviations (***Figure 17***). This observation verified the applicability of the newly developed connection between the SmartPeg type 62 (***Figure 18.B***) and the customized implant. Finally, three implant geometries were fabricated with SmartPeg type 62 connection, fully-, half- and non-threaded implants for further in vitro evaluations (***Figures 18.C-E***). The fully-threaded one was designed to imitate the clinically used implant geometry. The half-threaded implant had a notch in the middle of the implant. The notch aimed to provide a surface for direct bone to implant connection without threads. The non-threaded implant was made for the evaluation of the strength of the real bonding of bone to the implant surface.
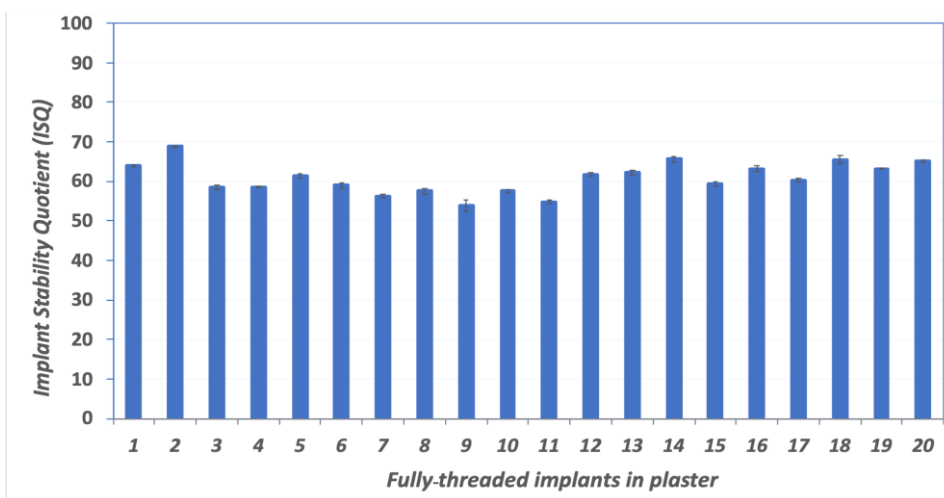
Figure 17.
Results of Resonance Frequency Analysis calibration. Each fully-threaded implant the SmartPeg was measured 20 times (mean ± SEM).
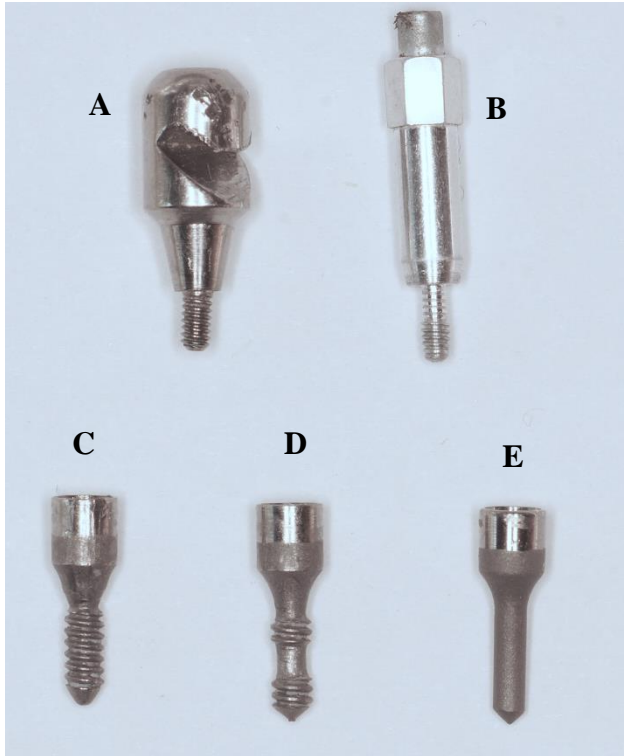
Figure 18.
*Photographic documentation of the three different implant geometries (**C** - fully-threaded, **D** - half-threaded, **E** - non-threaded) which can be inserted into the caudal vertebrae.* The stability can be measured with RFA using the SmartPeg (**B**) and the hook (**A**) to detect the maximal vertical extraction force.

4.1.2 Development of complex biomechanical evaluation by the combination of resonance frequency analysis and pull-out techniques

The secondary validation of the newly-developed connection between SmartPeg type 62 and the customized implant inserted into the amputated rat vertebrae showed reliable results again. The average primary stability of 5 fully-threaded implants was 33.81±4.17 ISQ. The evaluation of the pull-out testing from *ex vivo* vertebrae was also successful. We were able to extract all of the inserted implants. The average extraction force necessary for the removal of the implants from the bony bed was 89.60±6.05 N, showing uniform, repeatable outcomes.

RFA measurements, using artificial bone blocks, revealed significant differences only between D1 (48.00±1.37 ISQ) and D2 (40.58±1.86 ISQ), D1 and D4 (40.45±1.44 ISQ), D1 and D5 (15.00±3.21 ISQ), D2 and D5, D3 (42.45±0.59 ISQ) and D5, D4 and D5 PUF blocks by using fully-threaded implants without cementum. Between ISQ values

of half-threaded implants without cementum within different densities of blocks, RFA found the same differences as in case of fully-threaded implants. The ISQ value of half-threaded implants in D1 (46.70±1.97 ISQ) was significantly higher than in D2 (38.15±0.85 ISQ), D4 (36.40±0.48 ISQ) and D5 (15.90±2.08 ISQ). Also, ISQ values of D5 were significantly lower than in D2, D3 (39.55±2.01 ISQ), D4. There were no significant differences between fully-threaded and half-threaded implants within the same PUF bone block densities. Most importantly, the ISQ values linearly decreased in the case of non-threaded implants by the decrease in bone density (**Figure 19**). The ISQ values of non-threaded implants showed significant differences when compared to their respective PUF densities of the two types of threaded implants. Thus, ISQ values for the non-threaded implant showed a stepwise, continuous linear decrease, a feature that does not apply to fully-threaded and half-threaded implants. These data show that the non-threaded implants are the most suitable for the evaluation of the difference in PUF densities and the level of osseointegration.
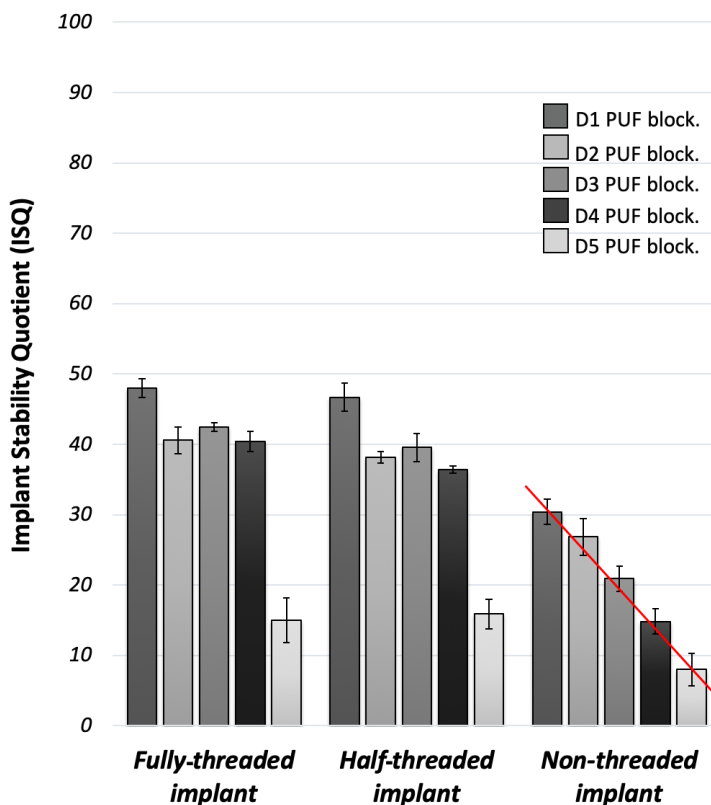
Figure 19.

Comparison of implant stabilities between fully-, half- and non-threaded implant using a non-invasive implant stability evaluation method based on resonance frequency analysis (RFA) by Osstell ISQ device (Osstell AB, Gothenburg, Sweden). The ISQ values linearly decreased in parallel with the reduction in the PUF artificial bone block densities. A regression line was juxtaposed on non-threaded implant data which illustrates the gradual change in their RFA results.

4.1.3 Complex monitoring of osseointegration with biomechanical and structural tests; assessment of improved surgical conditions and postsurgical care

4.1.3.1 Biomechanical evaluation of implant osseointegration

In our rat tail model, the ISQ values moderately changed in the initial healing time. A significant increase (1.6 folds) of ISQ values occurred from weeks 4 (32.84±8.86 ISQ) to week 16 (58.58±1.32 ISQ) (*Figure 20.A*). However, no significant difference was observed between values corresponding to healing periods at week 4 (32.84±8.86 ISQ), week 8 (34.67±2.08 ISQ) and week 12 (32.2±2.08 ISQ). The pull-out force significantly increased with time and reached a plateau at week 12 (171.75±15.12 N) postoperatively (*Figure 20.B*). The high sensitivity of this test was demonstrated by the fact that the pull-out force increased by approximately 500% between week 4 (26.54±2.54 N) and week 12 (171.75±15.12 N).

There was no further significant change in this parameter between weeks 12 and 16. Since no clear data were available about the meaning of ISQ unit of the Osstell ISQ device in any previous literature, we attempted to translate it to real physical force by correlating the ISQ values to the corresponding pull-out forces. The correlation analysis showed only a weak relationship (r=0.203) (*Figure 20.C*).
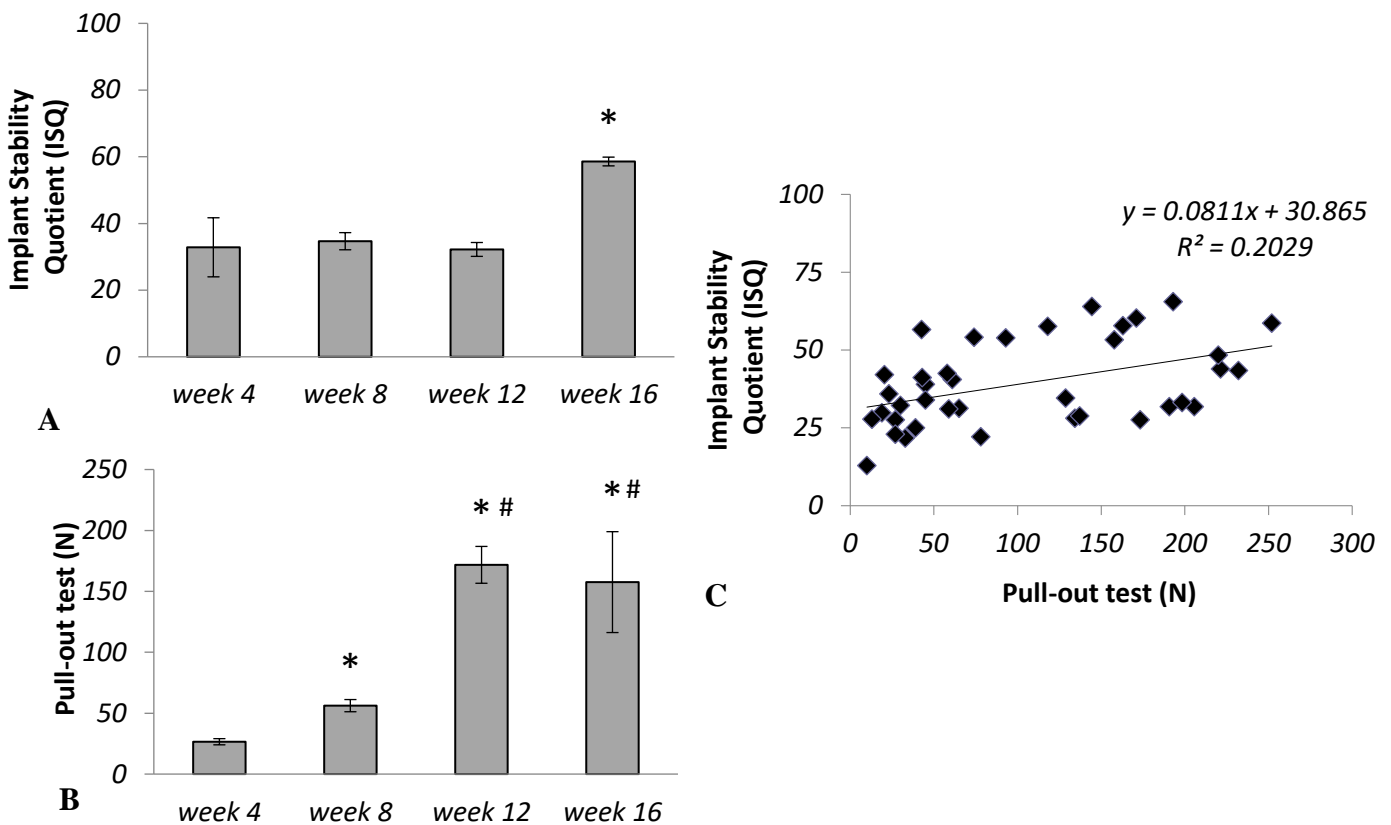
Figure 20.
Comparison of pull-out test and resonance frequency analysis as measures of osseointegration at different time-points during healing.
A. Evaluation of titanium devices stability using RFA on week 4, week 8 and week 16 after implantation in rat tail model. Mean ± SEM. * $p<0.05$ week 16 vs. week 4, 8 and 12 results. **B**. Evaluation of titanium devices stability using pull-out test on week 4, week 8 and week 16 after implantation in rat tail model. Mean ± SEM. * $p<0.05$ week 8 vs. week 4; # $p<0.05$ week 16 vs. week 8 results. **C**. Correlation analysis between non-invasive (RFA) and invasive evaluation (pull-out test) methods of the implant stabilities (r=0.202).

4.1.3.2 Structural evaluation of implant osseointegration

The 2D analysis results of micro-CT scans showed that the *i.S/TS* values were 52±5.78%, 47±4.62%, and 61±4.49% at weeks 4, 8 and 16, respectively. Statistically significant difference ($p<0.05$) was observed between weeks 8 and 16 (**Figure 22.A**). The unexpectedly high i.S/TS values obtained at week 4 after surgery were due to the high level of remaining debris between the implant body (labeled with a yellow star in **Figure 21.D**. As it appeared, the x-ray absorption of the debris was nearly the same as that of the

vertebral bone tissue. Indeed, individual images showed that at week 4, an approximately 200 μm thick homogenous debris layer covered almost the entire surface of the implant (***Figures 21.D, G***). At week 8, this coverage around implants was interrupted as the smear layer gradually disappeared (***Figures 21.E, H***). Finally, at week 16, no debris was seen on the images (***Figures 21.F, I***).

In the 3D evaluation, **BV/TV** values were 58±6.64%, 54±4.48% and 62±4.93% at weeks 4, 8 and 16, respectively **(*Figure 22.B*)**. No significant differences were found between the groups in ***BV/TV*** results. A positive correlation was found between BV/TV and i.S/TS data (r=0.544) on bone micromorphometric results **(*Figure 22.F*)**. This correlation indicated a relationship between the intersection surface coverage of the bone and BV/TV values in individual specimens.

At week 4, a low level of real ***BIC*** was detected corresponding to 29±3.54% coverage of the interface by histomorphometry (***Figure 22.C***). In comparison with week 4, BIC values (62±3.31%) increased significantly at week 8 (p<0.05) (***Figure 22.C*).** At week 16, BIC values further increased to 74±2.12% (***Figure 22.C***) (p<0.05 vs week 8). The bone around the implant was regularly a trabecular bone (***Figures 21.A-C***). These data indicated that BIC sensitively reflected the progress of osseointegration with time during a 16 weeks' experimental period.

There was no correlation between BV/TV and the histomorphometric BIC results (r=0.014) **(*Figure 22.E*)**. However, a very weak positive correlation was detected between i.S/TS and BIC (r=0.096) **(*Figure 22.D*)**.
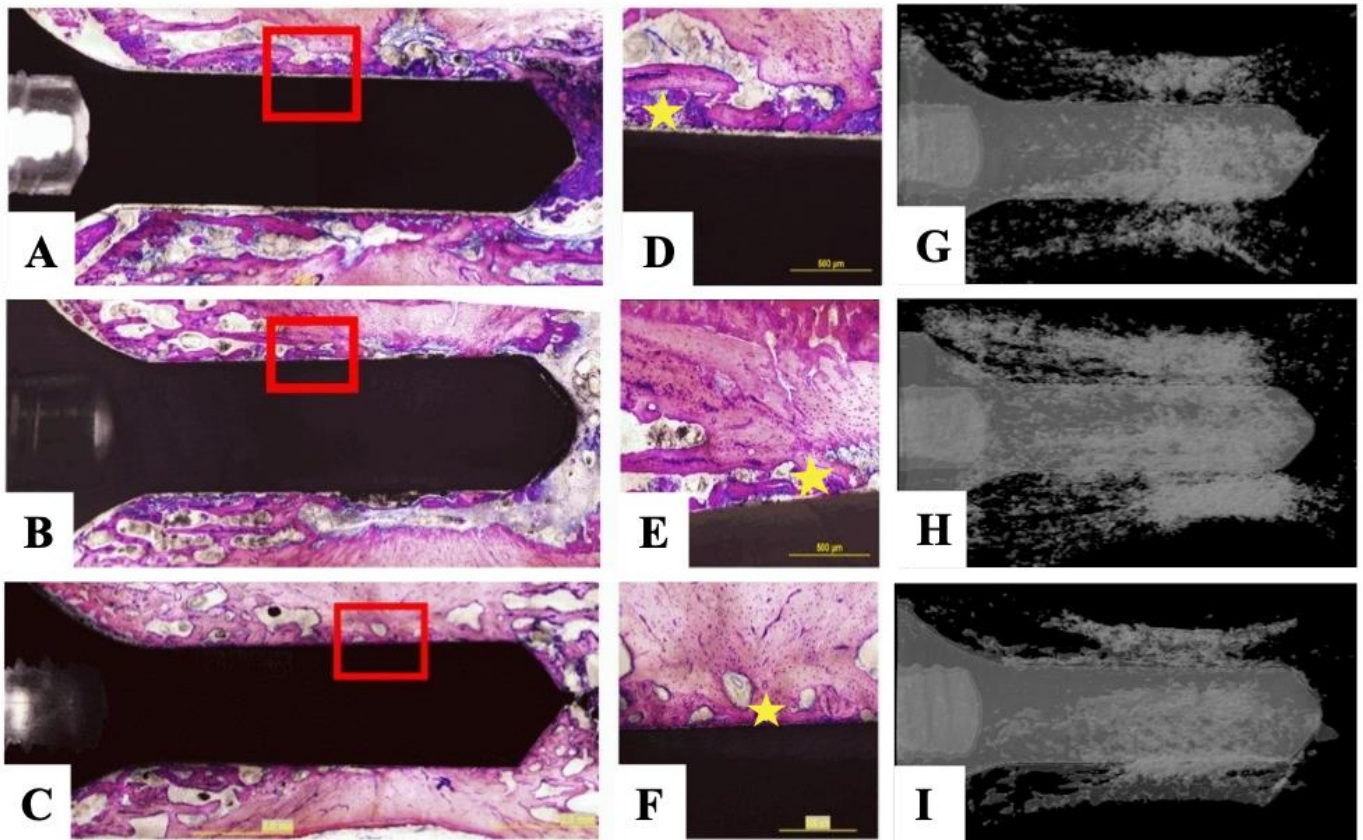
Figure 21.

Histological slices and 3D rendered images from different healing periods.

A. Histomorphometric slide of healing at week 4: active bone remodelling takes place (1.25x). **B.** Histomorphometric slide of healing at week 8: newly formed bone has a higher intensity of staining due to the lower mineralization rate of the bone compared to the mature one. Bone density is lower at week 4 compared to week 16 (1.25x). **C.** Histomorphometric slide of healing at week 16: bone regeneration around titanium surface reached biological equilibrium. We did not detect any higher intensity of staining due to the stabilized remodelling process (1.25x). **D.** High percentage of smear layer is presented 200 µm around the implant at week 4 (10x). **E.** A lower rate of debris is found at week 8 suggesting the progress of new bone formation (10x). **F.** Well-formed direct bone to implant contacts are present. The biological equilibrium is reached at week 16 (10x). **G.** In the micro-CT image of healing from week 4 the implant is surrounded by a smear layer of approximately 200 µm thickness. **H.** Micro-CT image of healing after week 8 shows newly formed bone at the same localization as observed in the histological slide. Bone density is lower than the corresponding values at week 4 and week 16. **I.** Micro-CT images of healing at week 16 show that bone regeneration around titanium surface reached biological equilibrium.
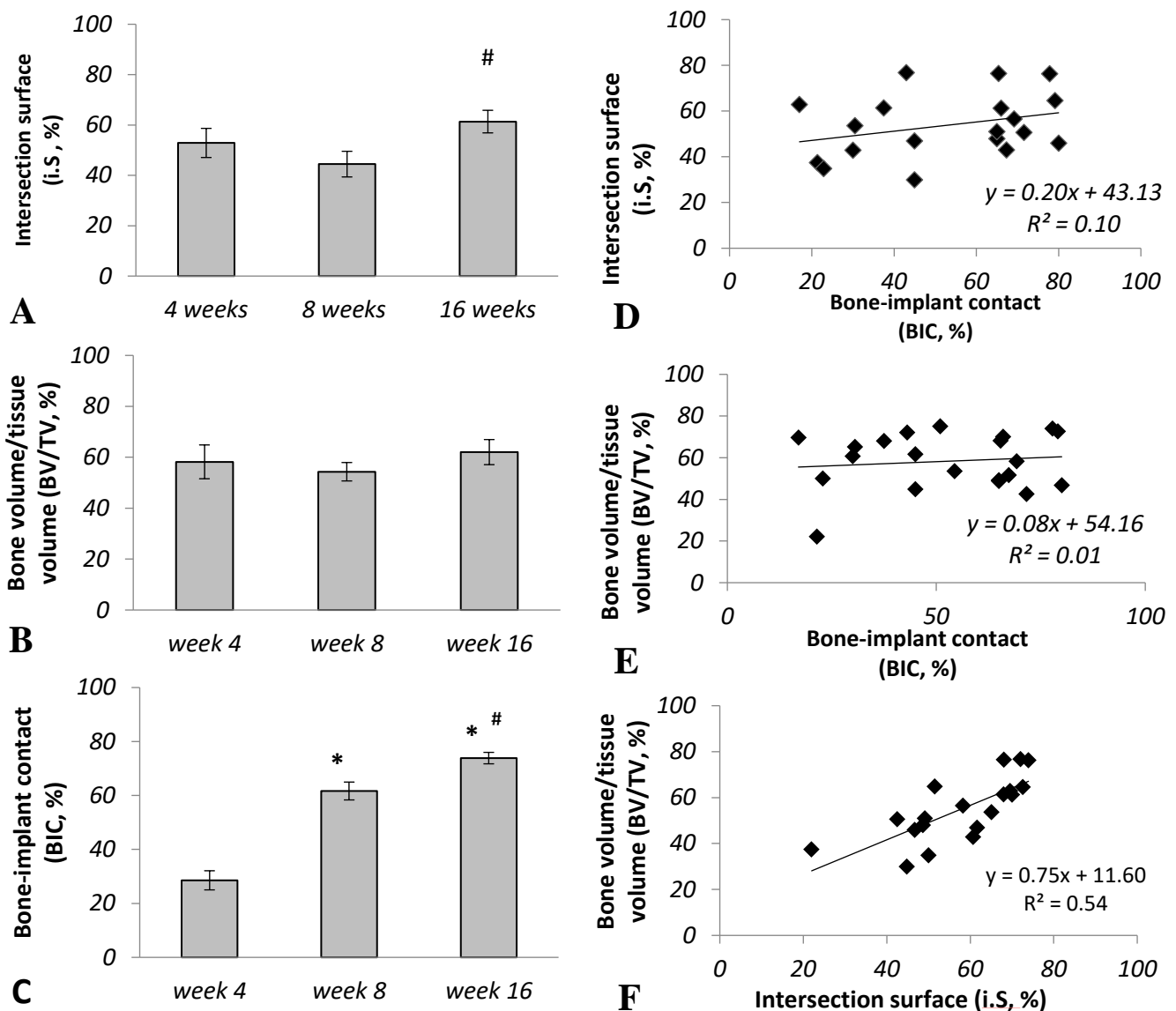
Figure 22.

Comparison of histomorphometry and micro-CT analysis as measures of osseointegration at different time-points during healing:

A. Evaluation of implant stabilities using 2D analysis of the micro-CT data presented in i.S/TS (intersection surface) at weeks 4, 8 and 16 after implantation in rat tail model. Mean ± SEM. # $p<0.05$ at week 8 vs week 16. **B.** Evaluation of bone volume around titanium implants using 3D analysis of the micro-CT data presented in BV/TV at weeks 4, 8 and 16 after implantation in the rat tail model. Mean ± SEM. **C.** Evaluation of the stability of titanium devices using histomorphometric analysis, measuring the BIC ratio at weeks 4, 8 and 16 after implantation in the rat tail model. Mean ± SEM. * $p<0.05$ at week 4 vs week 8, 16; # $p<0.05$ week 8 vs week 16 . **D.** Weak correlation was observed between BIC values measured by histomorphometry and intersection surface evaluated by micro-CT. **E.** No correlation was found between of BV/TV and histologically evaluated BICs. **F** A positive correlation was observed between intersection surfaces evaluated by micro-CT and BV/TV.

4.2 Development of "BD OSSI" and "Gap OSSI" experimental models

We successfully established two novel surgical procedures: 1) to form multiple bone defects ("BD OSSI"), 2) to achieve simultaneous implantation of multiple mini-implants transversal to the rat tail vertebrae. During these experiments, no infection in the operative site was observed. The behaviour of rats did not change during the experiments or the post-surgical care period.

The selected healing time of the grafted area was different in the "BD OSSI" model from the healing period of the implants in the "Gap OSSI" model. For the "BD OSSI" model the healing was evaluated at weeks 4 and 8. In the "Gap OSSI" model healing lasted 12 weeks. This time point was selected because earlier Dr. József Blazsek found that that the significant osseointegration level of titanium implant in the caudal vertebrae of rats starts at the 12th week of healing (J. Blazsek, personal communication, and *Figure 4 on page 27*).

In case of the "BD OSSI" model, the morphological results gained from micro-CT analyses did not show bone formation when the defect (2.9x3 mm) was left empty after either weeks 4 (*Figure 23.A*) or 8 (*Figure 23.C*). When we used a xenograft bone-grafting biomaterial to fill the defect, we obtained a good stability of the material in the defect after weeks 4 (*Figure 23.B*) and 8 (*Figure 23.D*).
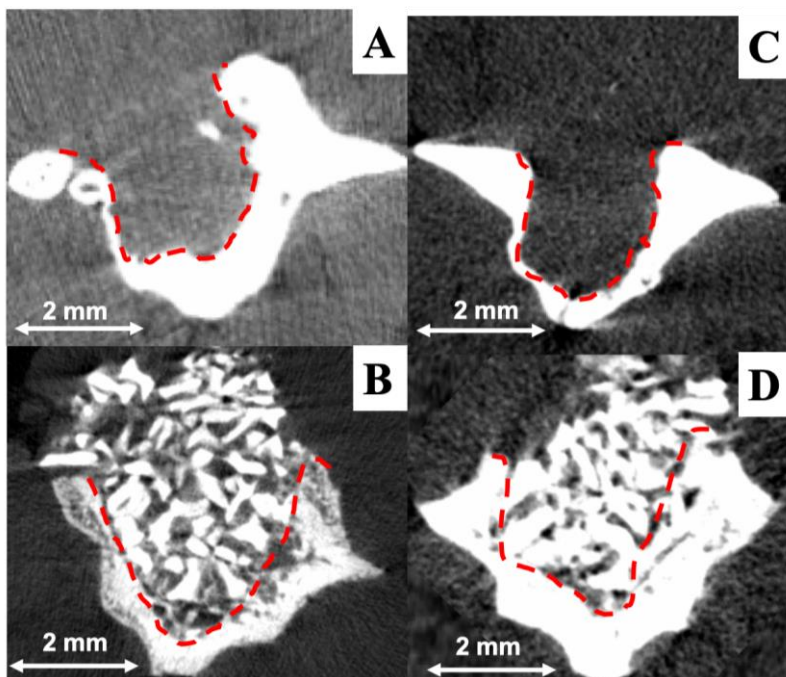
Figure 23.
Transversal view of bone defects in rat caudal vertebra the ("BD OSSI") after different healing periods based on reconstructed micro-CT images. The areas of defects are labelled with red broken lines. **A.** Micro-CT image of week 4 after the defect creation shows the absence of new bone formation. **B.** Micro-CT image of week 4, after the defect was augmented with xenograft, shows the stability of the grafted area. **C.** Micro-CT image of week 8 after the defect creation also shows the absence of new bone formation. **D.** Micro-CT image of week 8 after the defect was augmented with xenograft.

In the "Gap OSSI" model, *Figure 24* demonstrates the implant position through the vertebra after implantation. This titanium implant was specifically designed to be press-fitted into the cavity. Because of the special narrowing shape of the implant and the bed preparation of the wider implant, we could preserve an empty space between bony walls and implant in its apical part (*Figure 14*). This space created the conditions for distance osteogenesis, which actually happened successfully (*Figures 24.A-C*).

After the insertion of the individually developed implant at week 12, micro-CT scanning showed the implant position through the vertebra (*Figure 24.B*). The histological analysis showed a successful new bone growth from the bone walls towards the implant body ("distance osteogenesis"), which led to the osseointegration of multiply-installed implant in one rat tail. The newly formed bone around implant is highlighted in *Figure 24.C* 12 weeks after healing.
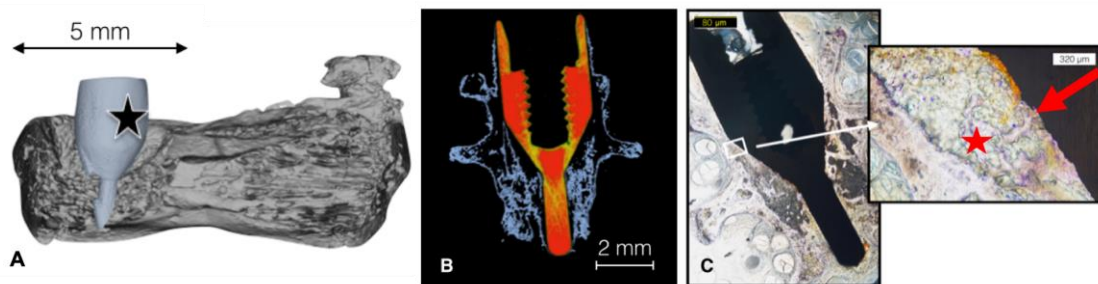
Figure 24.

Implant placement in the of "Gap OSSI" experimental model.
A. 3D reconstructed micro-CT image of rat caudal vertebra. Internal view of a metal implant (*) inserted into the mesial part of the vertebra. **B.** Transversal reconstruction of micro-CT images of a rat caudal vertebra with an inserted implant 12 weeks after healing. **C.** Histological slices showing implant osseointegration 12 weeks after healing. The red arrow shows the bone implant contact, while the red star shows the new trabecular bone.

4.3 *Ex vivo* evaluation of oral-surgical flaps mobility following "non-detaching" and "detaching" techniques for the mylohyoid muscle

All measurement results passed the normality test (Shaphiro-Wilk) (p>0.05) (**Table 1**). Only one of the measurement results was not included into the analysis, because in this case (specimen 3) the sample suffered a flap tear on the control side at the time of establishing the baseline standard force, which prevented a fair comparison with the test

side. Therefore, the data from this specimen were excluded from the analysis, resulting in a final sample of 11 heads and 22 surgical sites (i.e. 11 test and 11 control).

Table 1. Shapiro-Wilk normality test of the data.

	ZONE I		ZONE II		ZONE III	
	CONTROL	**TEST**	**CONTROL**	**TEST**	**CONTROL**	**TEST**
Number of values	11	11	11	11	11	11
W	0.8634	0.8969	0.9400	0.9342	0.8755	0.9203
P value	0.0637	0.1694	0.5200	0.4552	0.0911	0.3209
Passed	Yes	Yes	Yes	Yes	Yes	Yes
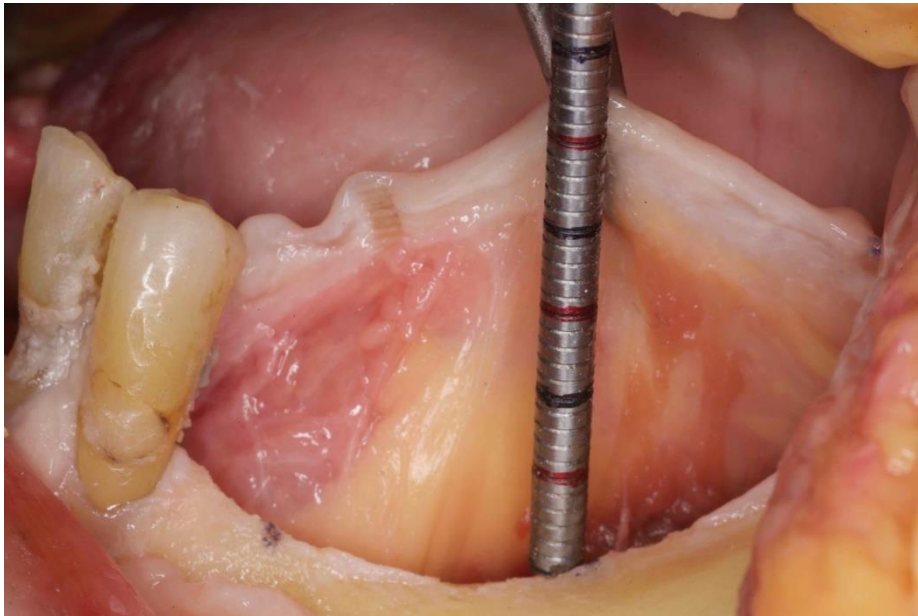
Figure 25.
Release of the lingual flap using the novel "non-detaching" technique. Flap release was reached by using two different flap preparation techniques. The difference in flap mobility was measured in by using a calibrated probe.

The difference between the test (***Figure 25***) and control groups in Zone I (retromolar pad area), Zone II (middle area) and Zone III (premolar area) was 8.3 mm (SEM=0.54), 10.1 mm (SEM=0.89) and 10.3 mm (SEM=0.89), respectively, reaching very strong statistical significance ($p < 0.0001$) in each of them (***Figure 26***). In

proportional terms, relative to the control, the test technique allowed for 8.2, 2.5 and 5.3 times more flap release in Zones I, II and III, respectively.
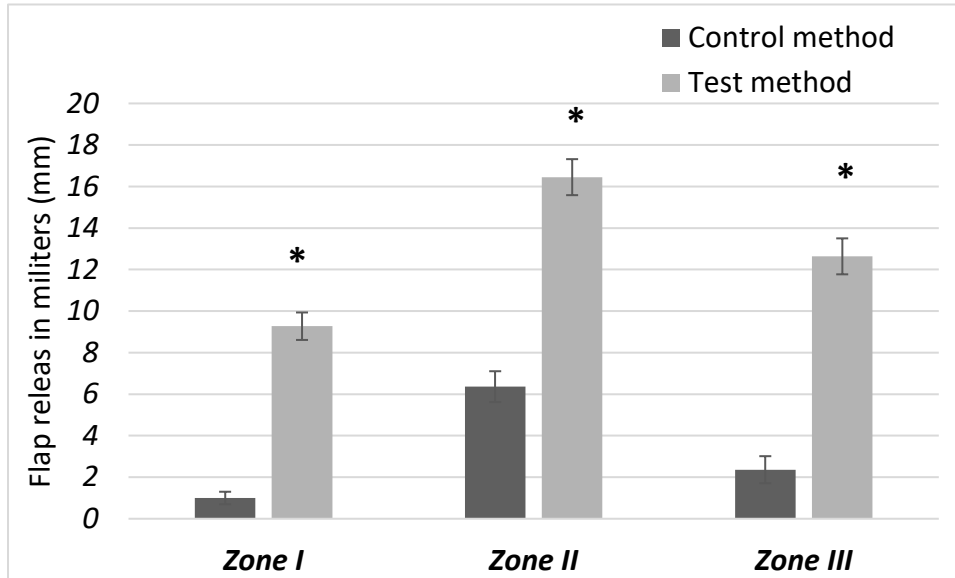
Figure 26.

Comparison of flap mobility in different anatomical zones after applying two different flap preparation techniques the "non-detaching" technique and the classic 'muscle-detaching' technique. In each zone, the levels of flap immobilization were significantly higher after using the tested (novel method) flap preparation technique in comparison with the classic mylohyoid muscle release (* $p < 0.05$ "muscle-detaching" technique vs. "non-detaching" technique, paired Student's t-test, n=11, mean ± SEM).

5. DISCUSSION

5.1 Quantitative and qualitative monitoring of osseointegration using the "Direct OSSI" rat tail implant model

In order to further develop our preclinical osseointegration model, first we had to adapt the resonance frequency analysis technique, originally developed for human studies, to application for rats. The new implant design had to allow us to perform RFA and pull-out tests after its insertion into the rat caudal vertebrae. At C4-C5 levels, caudal vertebrae have a cylindrical body shape with 9.8 mm length and 3.8 mm width (Renaud et al., 2015). We designed the implants to fit this size. It was also important to create a special implant connection for SmartPeg that is necessary for RFA measurements. We found the best outcome when our customized implants were prepared to house the SmartPeg type 62 based on validation in experiments using plaster and amputated vertebrae. These results proved to be reliable and repeatable with small standard errors. The standard error values measured in vertebrae were higher than those measured in plaster as the various vertebrae used represent some level of variations in mechanical properties of the bone, even within the same area (Banse et al., 1996) and bone quality of the implant-hosting area is one of the main influencing factors of primary stability (da Cunha et al., 2015; Javed et al., 2013; Merheb et al., 2016). Our adaptation is similar to others' who also successfully adapted the resonance frequency analysis method to non-human situations, namely in pigs (Nienkemper et al., 2013).

Further on, we used the internal threads of the developed implant head to connect a specially designed and fabricated hook to the implant to perform the pull-out testing in amputated vertebrae. In various vertebrae, the pull-out test showed uniform stability levels in different specimens. The pull-out test is one of the oldest methods for the biomechanical analysis of implant stability. It is most commonly used for primary stability evaluations. Different research groups successfully evaluated implant stability after external design changes in vitro (Mazzo et al., 2012; Valente et al., 2016; Yashwant et al., 2017). The disadvantage of the pull-out test is that it destroys the formed bone to implant connection. However, it can provide valuable data even after the biological integration of implants (Javed et al., 2013; Schwarz et al., 2009). Therefore, the pull-out

test can specify new findings for further developments in medical device construction (van Arkel et al., 2018) or in surgical techniques (Shukla et al., 2014).

Next we studied the sensitivity of RFA measurements to detect the stability of threaded, half-threaded and non-threaded implants using various, D1-D4 PUF artificial bone blocks. We found that the ISQ values linearly decreased in the case of non-threaded implants by the decrease of bone density, showing a stepwise manner. On the contrary, RFA values did not show high sensitivity in the threaded implants, obviously, no linear relationship existed between ISQ values and bone density decrease. Moreover, the reduction of half of the threads from the implant surface did not make any implant stability difference between fully- and half-threaded implants in the PUF blocks. Accordingly, the RFA implant stability evaluation method is significantly influenced by threads of the implant. Our data showed an outcome similar to what was previously published, which demonstrates a linear relationship between peri-implant bone quality and RFA (Turkyilmaz et al., 2011; Wada et al., 2015). Other studies also detected a significant difference in the artificial bone-implant stiffness comparing the same implant shapes in different densities using RFA (Barikani et al., 2013; Bayarchimeg et al., 2013; Huang et al., 2016; Lozano-Carrascal et al., 2016).

On the whole, our data suggest that we can evaluate the bone-bonding strength to titanium at different healing endpoints, irrespective of threading, by using non-threaded implants during the *in vivo* studies applying the newly adapted resonance frequency analysis in the rat tail.

There were no studies which used RFA as an evaluation method for detecting different implant thread numbers and different bone densities. The RFA was accepted in the majority of studies as an implant stability evaluation method with high sensitivity (Nedir et al., 2004; Zix et al., 2008) for detecting implant integration level (Acil et al., 2017; Scarano et al., 2006). Nevertheless, clinically it was also shown that the RFA cannot be a reliable method for predicting early implant failure (Monje et al., 2014).

For further *in vivo* osseointegration analysis we chose a non-threaded implant with the appropriate implant bed preparation based on in vitro evaluation results. For the planned *in vivo* analysis, it was essential for us to have an implant design which can be inserted into rat tail vertebrae.

Moreover, it was very important to use a reliable structural technique. For that, the application of micro-CT and histology are most suitable. During the X-ray analysis of samples, where metal is involved, metal artifacts may strongly affect the quality of radiological evaluation (Ernstberger et al., 2007; Kataoka et al., 2010). The causes of metal artifacts are multifactorial (Ernstberger et al., 2007; Kataoka et al., 2010). The main factor by which we could decrease the artifacts was to minimise the geometric complexity of the implant. We achieved this by using cylindrical, non-threaded implants. Additionally, by having the above sort of implants, we provided a very standard base for further histomorphology and radiological analyses of bone to implant contact.

Functional tooth replacement and bone regeneration are parts of the daily practice of modern dentistry, but a well-reproducible and relatively inexpensive preclinical functional test system is still missing. In the present work, we aimed to refine our original rat tail implantation model of Blazsek et al (Blazsek et al., 2009) to develop a quantitative preclinical screening model for osseointegration of implants with special emphasis on biomechanical evaluations during contact and distant osteogenesis. We hypothesized that in the rat tail vertebrae, osseointegration of titanium implants could be biomechanically monitored by the combination of RFA and pull-out tests, and by structural analyses, such as micro-CT and histomorphometric methods. We found that all of these test systems were applicable to evaluate the implant osseointegration process. The new evaluation algorithm provides a highly reliable and reproducible outcome using a limited number of small experimental animals.

Accordingly, in the rat tail vertebrae, we can monitor the osseointegration of titanium implants quantitatively by the combination of RFA, bio-mechanical pull-out tests, micro-CT and histomorphometric methods (Farkasdi et al., 2018). We observed that these test systems are individually applicable to evaluate the implant osseointegration process. But the simultaneous application of these methods and a combined evaluation are much more advantageous for the screening process to provide highly reliable and reproducible outcome using a limited number of experimental animals. The present ISO guideline for preclinical evaluation of dental implants suffers from a complete lack of biomechanical testing (ISO/TS_22911:2016, 2016). Accordingly, it is essential to set up and standardize such methods.

The refined "Direct OSSI" model offers a considerable upgrade over our

previously published data (Blazsek et al., 2009) which had already introduced longitudinal implant placement into the vertebral axis. The high variability of the previous results was primarily caused by the fact that the cylindrical cavities for implantation were 1 mm wider in diameter than the size of the implants creating a space around the implant. Only the very tips of the implants were connected directly to the bone (Blazsek et al., 2009). In the present work, the prepared implant beds had exactly the same size as the implants. Furthermore, implants were prepared with parallel walls with no threads to monitor natural bone-bonding without the modifying effects of threads and various strengths of thread fixation. During implant placement, hand-free drilling always decreases the accuracy of the process even for experienced surgeons (Payer et al., 2008). Consequently, the application of the surgical guide that we developed and described above significantly increased the accuracy and reproducibility of the drilling position in the centre of the vertebra, perpendicular to the vertebral end-surface. Finally, we developed a post-surgical infection-preventing protocol. All these modifications together yielded a well-defined preclinical model having minimal complications in experiments and very low variability in the data obtained (Blazsek et al., 2009).

Our results showed that the most sensitive and reliable preclinical osseointegration test was the pull-out test. This method has high sensitivity for small and dynamic changes in the implant-bone interface. Data received by the pull-out measurement has a small standard error, which suggests that the biological processes were quite uniform in various animal species (Lutz et al., 2010; Mueller et al., 2011; von Wilmowsky et al., 2014). The disadvantage of the pull-out test is that it is an invasive method (Salmoria et al., 2008), therefore, it is suitable only in preclinical studies. Previous works showed very different outcomes. Experiments with non-threaded implants for pull-out tests, reported in some studies (Nonhoff et al., 2015; Seong et al., 2013; Stubinger et al., 2016), showed that the pull-out test is a very reliable method, yielding a steep increase in extraction force with time. However, since commercially available dental implants are always threaded, the pull-out technique is not suitable for the direct determination of osseointegration, because the values of secondary stability are highly distorted by threads (Brunski et al., 2000; da Cunha et al., 2015; Salmoria et al., 2008). To avoid this problem, simple test bodies (e.g., discs) have been developed (Mathieu et al., 2014; Ronold et al., 2003; Wennerberg et al., 2014). But the validity of these results was limited, since test

bodies were inserted into the cortical bone and fixed with a pre-shaped titanium band, which exerted pressure on the samples and affected healing (Mathieu et al., 2014; Ronold et al., 2003; Wennerberg et al., 2014).

The RFA evaluation has been successfully used in clinical studies as the only non-invasive, functional measurement method. It is regarded as a sufficient tool for evaluating the course of intraosseous implant stability in clinical practice (Diaz-Sanchez et al., 2017; Han et al., 2010; Huwiler et al., 2007; Markovic et al., 2016) and in preclinical settings (Ito et al., 2008; Lee et al., 2016; Mayer et al., 2016; Nagayasu-Tanaka et al., 2017; Sul et al., 2009). We found that ISQ values moderately changed with healing time. Increases in ISQ values showed a significant level at week 16. However, differences fell short of significance at weeks 8 and 12. Other *in vivo* studies involving RFA evaluation is in accordance with our findings (Barewal et al., 2003; Chen et al., 2017). We observed that ISQ values doubled between weeks 4 and 16. A similar magnitude of increase in ISQ values was also previously observed in experiments applying similar timeframe in various species including humans (Huwiler et al., 2007; Lee et al., 2016; Nagayasu-Tanaka et al., 2017; Sul et al., 2009). These results of preclinical studies are contradictory. Some of the studies did not detect any change during the healing from the primary to the secondary stabilities with RFA (Abrahamsson et al., 2009; Manresa et al., 2014). In contrast, other results showed a dynamic increase in ISQ values from the primary stability to the secondary (Huwiler et al., 2007; Ito et al., 2008; Lee et al., 2016; Mayer et al., 2016; Nagayasu-Tanaka et al., 2017; Sul et al., 2009). Taken together, RFA is an appropriate method for determining differences of very early and late stages of osseointegration. But it is not sensitive enough to detect minor changes between relatively close time points during the osseointegration process. Therefore, it is a useful technology but for well-reproducible preclinical screening. Other methods should also be used in parallel such as the pull-out test.

The correlation analysis showed that there was a correlation between ISQ values and pull-out results, both increasing with time but the fitted line is very flat. The pull-out test gives real physical values in Newton, while the RFA test provides only unidimensional relative values. More importantly, we observed a five-fold increase in pull-out values over time with minimal standard errors versus moderate, only a 50 % increase in ISQ mean values accompanied with high standard errors. The simultaneous

application of both methods is essential, because they together provide a reasonable estimation of osseointegration in preclinical research. Additionally, the more sensitive pull-out test cannot be used in clinical situations since it is invasive. Nevertheless, our present results show that the ISQ values provide reasonable functional estimation, although to a lower extent than pull-out values. Therefore, they can be used as a functional test for osseointegration when combined with other, more sensitive methods.

The histomorphometric images showed that the interspace between bone tissue and implants was largely filled with bone debris at week 4, with reduced debris at week 8, and no debris at week 16. Debris can be well-differentiated from real bone implant contact by histomorphometric analysis (Bernhardt et al., 2012), which revealed a more than 140% increase in BIC values. This is in line with multiple preceding studies, and also the related ISO guidelines, suggesting that BIC analysis is the best available non-functional method to evaluate osseointegration (Bissinger et al., 2017; Caroprese et al., 2017; ISO/TS_22911:2016, 2016; Meirelles et al., 2015).

On the contrary, the 2D analysis of micro-CT scans yielded less convincing results. A statistically significant difference in i.S/TS values was observed only between the 8th and 16th weeks. At week 4, the high level of the remaining debris between the implant body and the bony bed masked the relatively low contact between bone and implant. At later time points, the debris-caused background decreased, while real bone-implant intersection areas increased, finally resulting in a much more moderate elevation in i.S/TS values than that in BIC values. This is in line with previous observations indicating that bone debris can overshadow real BIC analysis (Bernhardt et al., 2012; Goelzer et al., 2010; Pandey et al., 2013; Trisi et al., 2011).

As expected, in the 3D evaluation of our work, BV/TV values between weeks 4 and 16 showed no significant differences between the groups in BV/TV results. The ROI for BV/TV detection was done in an 0.46 µm wide cylindrical volume around the titanium implant excluding the 12 pixels dilation range around the implant, that is, in the immediate vicinity of the implant. The macro design of the implants affects the architecture of the bone, which leads to the active bone remodelling process (Schouten et al., 2009). When threads are applied, primary stability is high, but they create high stress in the surrounding bone area leading to highly active resorption and a considerable degree of remodelling (Barone et al., 2016; Misch et al., 2001; Schouten et al., 2009). However,

we used implants without threads and special postoperative care prevented local infections (Renaud et al., 2015) also diminishing the necessary degree of remodelling. Taken together, histomorphometry seems to be superior vs both 2D and 3D micro-CT analyses to monitor osseointegration in our rat tail model.

By using the above described methodology, now we have complex tools for standard comparisons of different implant surfaces during peri-implantitis or during any other generally compromised conditions and their treatment.

5.2 Importance of the newly developed "BD OSSI" and "Gap OSSI" experimental models

For creating transversal bone defects in the rat tail, we had to establish a well-defined drilling protocol. This was successfully developed and tested *ex vivo* in C2-C5 rat tail vertebrae. During drill selections, we aimed to create the largest possible transversal bone defect, which still reproducibly permits the integrity of the remaining bone of the given vertebra. As a result of this procedure, we found that the maximal size of the transversal defect was 2.9x3 mm. By keeping this dimension, the procedure could be standardly reproduced.

The experimental data of the "BD OSSI" and "Gap OSSI" models validate our original assumption that rat caudal vertebrae may serve as a good model for bone reconstruction and regeneration. Consequently, various bone regenerative materials, implant materials, surface treatments and surgical protocols can be studied in the future using the rat tail model. We can evaluate the biocompatibility of implanted biomaterials and self-healing capacity of created defects in physiological conditions by using the "BD OSSI" experimental model.

It is generally accepted that the best animal models should use the minimum number of animals providing reliable results. This is true for the "BD OSSI" and for the "Gap OSSI" models. The possibility of using several vertebrae in the same animal gives a chance to decrease the number of rats using, for example, the same animal as a proper control (Renaud et al., 2015). From a statistical point of view, one vertebra can be used for the control site and the others for different kinds of experiments to compare them on the same rat at the same experimental time. This method also decreases the bias due to

inter-individual variability. The routinely used experimental models for BD creation are in the tibia, femur, calvaria and mandible of laboratory animals (Pearce et al., 2007; Pellegrini et al., 2009; Spicer et al., 2012; Streckbein et al., 2013). The disadvantage of the calvarial defects is the sensitivity of the technique, as a fracture of the cortices may happen during preparation (Li et al., 2015a). Spicer and collaborators defined the 8 mm wide round defect in rat calvaria without healing by itself after a three months' healing period. The bone structure of the tail vertebrae is much more massive and predictably structured. It is also important to note that working with the tail structure during the postoperative care is much easier than with the calvaria of the animal awake. Using the calvaria for BD requires a higher number of animals to meet the statistical requirements.

Because of the difficult accessibility to the mandible and maxilla, different research teams have succeeded in measuring osseointegration mainly in anatomically accessible bone compartments such as the haematopoietic femur (Blazsek et al., 2009; Ysander et al., 2001). From the histological and anatomical points of view, the caudal vertebrae of the rat are similar to human jawbones with abundant cancellous bone delimited with an important cortical bone thickness. The rat caudal vertebrae are also similar to human jaws, with no haematopoiesis, a feature which is different in other bones which are frequently used to create implant beds in animal models (Blazsek et al., 1986). The above fact makes them perfect model sites for evaluating bone regeneration in dental and maxillofacial research in preclinical implant studies. Indeed, following the integration of bone regenerative materials, new bone formation, bone-regenerative material contact or building a kinetic model of healing are possible with this model. However, the disadvantage of the "Gap OSSI" model (Renaud et al., 2015) is that the transversal positioning of the implant into the vertebral body leaves only a minimal amount of bony structure around the hard bed (i.e. a 2 mm thick bone wall), which prevented us from performing biomechanical testing.

The data from "BD OSSI" and "Gap OSSI" descriptive studies show that tail vertebrae may provide ideal tissue support for preclinical implant studies. The stability and longevity of integration of foreign materials into the bone represent a significant problem in tissue engineering. Furthermore, in the "Gap OSSI" model the design of the implant, by narrowing the apical part, allows biomaterial/stem cell/growth factor filling and bone-implant contact experiments in the function of the type of biomaterials

employed.

There are studies describing the distant bone formation around the implants in large mammalians (Choi et al., 2017; Sivolella et al., 2012). It is important to model the conditions of implant-healing when there is a partial gap around the implants. It is because it is necessary to experimentally analyse the influence and the efficiency of different materials on the osseointegration of immediately placed implants. Yet, no small animal model has been established for this clinical demand. The clinical relevance of our pre-clinical screening model is that the data gained using the "Gap OSSI" will help to answer which material has a better effect in such conditions.

Micro-CT analysis may serve to estimate bone density and assess the degree of bone remodelling and bone implant-contact (Boix et al., 2006). Depending on the chosen experimental model, one or even more vertebrae can be used in an animal. Besides, in the future, *in vivo* micro-CT could permit multiple measurements of new bone formation through the calculation of bone density using only a single group of "BD OSSI" and "Gap OSSI" animals.

The clinical relevance of the present work is that it offers a small animal system that is suitable for modelling the osseointegration of various implant materials and surface treatments in an inexpensive, reproducible manner. The rat tail vertebrae have high similarity to the human jaw bone. They consist of massive, cortical and spongious bone compartments, suitable for supporting titanium implants and are devoid of bone marrow parenchyma (Blazsek et al., 2009). Therefore, misbalances in implant integration leading to peri-implantitis and their possible treatment can also be monitored using this novel osseointegration system. In this model, implant osseointegration may also be studied under various adverse conditions such as diabetes (Al-Awar et al., 2016), parathyroid dysfunctions (Jung et al., 2017), osteoporotic conditions (Sophocleous et al., 2014). On the whole, these possibilities can be applied for the development of novel preventive and therapeutic strategies that can then be transferred into clinical practice.

Clearly, the present study has limitations. First of all, the presented animal model could be extrapolated to human clinical situations only with great caution, because of the significant differences between species. Second, in the rat tail model, one of the most important components of the oral osseointegration process, the oral microflora, is missing. Nevertheless, the data provided by our novel model system may yield valuable

preclinical information for the implant osseointegration process, inexpensively and reliably. These results can be applied then to large animal models and also in clinical trials.

5.3 Importance of differences between "non-detaching" and "detaching" techniques for the mylohyoid muscle

Up till now, no comparative, well-controlled studies investigated the amount of soft tissue release that may be achieved by applying different flap-releasing techniques in the posterior mandible. We hypothesized that the novel "non-detaching" technique is less invasive, safer and leads to more flap release without the need of detaching the mylohyoid muscle. Indeed, in our comparative, split-mouth cadaver study, a novel technique for the improvement of the lingual flap in the posterior mandibular sites was found to be more effective than a classic flap management approach.

The mean of the differences between both techniques in terms of flap release was overwhelmingly in favour of the test treatment type (vs control), regardless of the anatomical zone, ranging from 8.273 to 10.273 mm. Although the mean difference of release between groups in Zone I was smaller than that observed in Zones II and III, the actual differences were proportionally far bigger since the flap was released 8.2 times more in Zone I, while in Zones II and III this difference was 2.5 and 5.3, respectively. Unfortunately, it is not possible to contrast our results with others' since we could not identify any other studies involving a similar design and outcome measures, which makes us believe that this is the first study of its kind available in the literature.

It is important to note that the deliberate preservation of the mylohyoid muscle attachment to the body of the mandible in our modified technique is intended to prevent the incidence of serious complications. As aforementioned, classic techniques involve either complete (Pikos, 2005) or partial (Ronda et al., 2011) detachment of the mylohyoid muscle from its mandibular insertion at the mylohyoid line. Complete detachment, however, may lead to the disruption of the diaphragm of the floor of the mouth and may subsequently create a communication between the surgical area and the sublingual and/or submandibular space, which could trigger a severe medical complication in case of a postoperative infection. Partial reflection of the mylohyoid from the internal part of the

flap may result in excessive thinning of the central aspect of the flap when attempting primary closure, as well as possible exposure of the graft to the oral environment in the early stages of healing. Additionally, these techniques primarily advocate for the improvement of the middle portion of the flap, without the inclusion of Zones I and III. This approach is generally not conducive to passive primary closure, particularly in the anterior area (Zone III), because, unless there is a situation of severe ridge atrophy, the mylohyoid muscle insertion tends to be deeper respective to the alveolar ridge crest (Ronda et al., 2011; Wheeler Haines R, 1959).

Our study, of course has some limitations. For example, the examiners were not blinded to what technique was applied on each surgical site. However, we attempted to control the reliability and reproducibility of the measurements by applying the same tensile force to the lingual flap on both control and test sites within the same specimen and the same scaled probe was used for all the flap release assessments. Additionally, measurements were obtained in duplicate in order to minimise the error, and the same experienced surgeon performed all the procedures in order to ensure technical consistency. Another potential limitation is that, although the specimens were carefully selected to include sites that were comparable from side to side, posterior atrophic mandibular ridges rarely present a flat architecture and perfect symmetry. These anatomical variations may have influenced the measurements. However, the primary outcome in this study was the relative difference in flap release from the crest (fiduciary landmark) to the margin of the flap, both at baseline and after complete flap improvement. In order to increase reproducibility, the point of reference on the ridge crest was marked with a surgical pen, so the final measurement could be done from the same reference. For this reason, we believe that the results should not be largely affected by possible anatomical discrepancies between the control and the test sites.

6.CONCLUSIONS

1. In the present work, we **successfully adapted** the method of **resonance frequency analysis** - originally developed for humans - **to the rat tail model**. For that, we **designed** a **special connection** in the implant head, which allowed us to screw in the transductor (SmartPeg) **for resonance frequency analysis**. For the established connection, we also designed a special hook for performing the **pull-out test**.

2. With the newly-established connection, we **developed three implant designs** (full-, half-, non-threaded) which are suitable **for studying implant osseointegration into the rat tail vertebrae** longitudinally. When testing these implant designs, we selected the **non-threaded** one for further applications. This implant shape proved to be the **most sensitive for detecting the density differences** of the hosting tissues in vitro. Thus, we **excluded** the **influence of macro design on** the **bone-bonding strength** to the implant surface caused by the threads. The non-threaded implant design was the **most suitable for** the assessment of **biomechanical implant stability in a vertical direction** by the pull-out test.

3. We **established** a **drilling protocol** of the vertebrae **for positioning the implant bed standardly** in the longitudinal middle of the vertebrae by using a specially-designed surgical guide. Accordingly, we successfully **improved the surgical conditions** and the **postsurgical care** of the rat tail after implantation.

4. We **developed** a **complex biomechanical** evaluation setup **by the combination of resonance frequency analysis and pull-out techniques** for the evaluation of implant stability in rat tail vertebrae. Also, we **were the first** to successfully perform the **non-decalcified tissue-sectioning** of the rat vertebrae **with titanium implants**. In addition, we **designed and optimized a protocol to overcome the X-ray scattering on the metal surface** for micro-CT scanning and reconstruction of rat tail vertebrae with an implant. This was achieved by the removal of threads, minimising the implant's geometrical complexity.

5. Our **methodological developments** resulted in a successful combination of the biomechanical evaluations with structural tests in order to **reliably and multidisciplinarily monitor the osseointegration** process in a caudal vertebra *in vivo*. We called this experimental setup "Direct OSSI" model. This experimental model is

suitable **for** the quantitative **preclinical screening** of the osseointegration of various intraosseous implants after **different surface treatments** under different local and general conditions.

6. We established a **new drilling protocol for** the creation of **multiple bone defects** and **multiple implant placement in** the **rat tail** vertebrae transversally.

7. The **transversally created bone defects** in the rat tail demonstrated **no self-healing** under our experimental conditions unless bone graft material was used. That model is called **"BD OSSI"** experimental model. Moreover, we **successfully modified** the original "OSSI" model and made the rat tail suitable for the placement of **multiple implants** in a perpendicular direction. We named this model **"Gap OSSI"**.

8. We were the first to successfully **determine the effectiveness of two lingual flap preparation techniques** ("non-detaching" and "muscle-detaching") for oral and periodontal surgeries for the extension of lingual flap mobility in a standardized preclinical setup. We found that the **"non-detaching" approach** to lingual flap release in the posterior mandible is superior over the "muscle-detaching" technique. The "non-detaching" technique **significantly increased lingual flap mobility**.

7. SUMMARY

Bone regeneration and functional tooth replacements are applied in the daily practice of modern dentistry. However, well-reproducible, relatively inexpensive experimental models allowing the multiple testing of osseointegration and regeneration of bone defects (BD) are still missing. Accordingly, we aimed to refine the original preclinical *in vivo* rat tail implant model for the quantitative and qualitative monitoring of implant osseointegration by the combination of biomechanical and structural evaluations. We also aimed to develop a novel experimental model for monitoring bone defect regeneration and integration of multiple implants placed simultaneously into the tail. The essential elements for successful bone regeneration include flap design, flap release, flap closure. Different flap management techniques exist for bone augmentation in the posterior mandible. However, some techniques present limitations associated with serious postoperative complications and have limited evidence. Hence, we attempted to determine the effectiveness of two different flap designs for oral and periodontal surgeries for the extension of lingual flap mobility.

The experimental setup for osseointegration and bone regeneration was based on previous rat vertebrae studies. Here a unique implant was developed allowing structural, biomechanical analysis to provide a highly reliable, reproducible outcome. Contact type osteogenesis was analysed by longitudinally placed implants into the vertebrae ("Direct OSSI"). For distant osteogenesis analysis ("Gap OSSI"), multiple implant placements were done transversely to the longitudinal axes of the vertebrae, with a space between the implant body and the bone. For bone regeneration analysis in the rat tail, multiple transversal BDs were left empty or filled with bone-grafting material ("BD OSSI"). The progress of healing in our rat tail models was evaluated biomechanically by resonance frequency analysis (RFA) and pull-out tests and - structurally - by micro-CT and histomorphometry. For the evaluation of different flap impovement techniques a split-mouth cadaver study was conducted to compare the mylohyoid muscle "non-detaching" and muscle "detaching" techniques for the enhancement of lingual flap mobility in the posterior mandible.

Our complex biomechanical and structural analysis quantitatively revealed the time-dependent progress of the osseointegration of the titanium implant using the "Direct OSSI" model. The "BD OSSI" model, demonstrated no self-healing under our experimental conditions. The "Gap OSSI" showed distant osteogenesis around multiply-placed implants. Furthermore, we successfully determined the effectiveness of two lingual flap designs for oral, periodontal surgeries. In conclusion, our results provide evidence that the caudal vertebra is a useful standard for the preclinical evaluation of bone tissue regeneration and is appropriate for assessing osseointegration by structural, biomechanical analysis. The "non-detaching" technique is superior over the "detaching" technique to improve lingual flap mobility. Altogether, the results may widen our knowledge about bone regeneration and osseointegration, supporting future clinical developments.

8.ÖSSZEFOGLALÓ

A csontregeneráció és a hiányzó fogak funkcionális pótlása általánosan alkalmazott módszerek a modern fogászat mindennapi gyakorlatában. Ennek ellenére, még nem állnak rendelkezésünkre jól reprodukálható és viszonylagosan olcsó kísérleti állatmodellek az osszeointegráció és csontdefektusok regenerációjának többirányú tesztelésére. Ennek megfelelően célkitűzésünk volt, az eredeti preklinikai patkány farok implantációs modellt továbbfejleszteni, az implantátumok osszeointegrációjának kvantitatív és kvalitatív monitorozása céljából, biomechanikai és strukturális értékelési módok kombinációjával. Továbbá célunk volt, egy új kísérleti modell kidolgozása a csontdefektus-regeneráció megfigyelésére és egyszerre több, a farokcsigolyákba merőlegesen elhelyezett implantátum integrációjának nyomon követésére. A sikeres csontregeneráció lényeges elemei közé tartozik a lebeny képzése, preparálása és zárása. A mandibula hátulsó régiója csontdefektusainak vertikális augmentációjára különböző lebeny képzési technikák léteznek. Egyes technikák alkalmazhatóságát azonban korlátozzák a súlyos posztoperatív szövődmények. Ennél fogva megpróbáltunk két különböző lebeny preparálási technikának - amelyek a linguális lebeny mobilitását növelik szájsebészeti és parodontális műtétek esetén -, meghatározni a hatékonyságát. Egyedi implantátumokat fejlesztettünk ki olyan módon, hogy mind a strukturális, mind a biomechanikai elemzéseket lehetővé tették, a megbízható és reprodukálható értékeléseket. A kontakt oszteogenezis elemzéséhez a csigolyákban hosszirányba helyeztük el az implantátumokat ("Direct OSSI"). A távoli oszteogenezis elemzéséhez egyszerre több implantátum került behelyezésre (tér hagyással az implantátum teste és a csont között) a csigolyák hossztengelyeire merőlegesen ("Gap OSSI"). A csontregeneráció vizsgálatához többszörös, transzverzális csontdefektust ki a patkány farokban ("BD OSSI"). A különböző lebeny preparálási technikák értékeléséhez humán cadaver-vizsgálatot végeztünk a m. mylohyoideust "leválasztó" és "nem-leválasztó" módszereinek összehasonlítására a linguális lebeny mobilitásának javítására.

A "Direct OSSI" modell kvantitatívan feltárta a titán implantátum osszeointegrációjának időbeli változásait.. A "BD OSSI" modellben a csontdefektusok a kísérleti körülmények között nem mutattak öngyógyulást abban az esetben. A "Gap OSSI" távolsági oszteogenezist mutatott a patkányfarkokban elhelyezett implantátumok körül. Továbbá sikeresen megállapítottuk két lingualis lebeny képzés hatékonyságát. Eredményeink azt mutatják, hogy a patkány farok csigolya hasznos modellként szolgálhat a csontszövet regeneráció preklinikai értékeléséhez, és alkalmas az osszeointegráció strukturális és biomechanikai elemzésekkel történő értékelésére. A m. mylohyoideus estében a "nem-leválasztó" technika jobb a "leválasztó" technikánál a lingualis lebeny mobilitásának javítására a posterior mandibulában. Összességében az eredmények bővíthetik tudásunkat a csontregenerációról és az osszeointegrációról, előmozdíthatják és támogathatják a jövőbeli klinikai fejlesztéseket.

9. BIBLIOGRAPHY

Abduljabbar, T., Kellesarian, S. V., Vohra, F., Akram, Z., Kotsakis, G. A., Yunker, M., Romanos, G. E., & Javed, F. (2017). Effect of Growth Hormone Supplementation on Osseointegration: A Systematic Review and Meta-analyses. *Implant Dent, 26*(4), 613-620. doi:10.1097/ID.0000000000000616

Abrahamsson, I., Linder, E., & Lang, N. P. (2009). Implant stability in relation to osseointegration: an experimental study in the Labrador dog. *Clin Oral Implants Res, 20*(3), 313-318.

Acil, Y., Sievers, J., Gulses, A., Ayna, M., Wiltfang, J., & Terheyden, H. (2017). Correlation between resonance frequency, insertion torque and bone-implant contact in self-cutting threaded implants. *Odontology, 105*(3), 347-353. doi:10.1007/s10266-016-0265-2

Agarwal, R., & Garcia, A. J. (2015). Biomaterial strategies for engineering implants for enhanced osseointegration and bone repair. *Adv Drug Deliv Rev, 94*, 53-62. doi:10.1016/j.addr.2015.03.013

Al-Awar, A., Kupai, K., Veszelka, M., Szucs, G., Attieh, Z., Murlasits, Z., Torok, S., Posa, A., & Varga, C. (2016). Experimental Diabetes Mellitus in Different Animal Models. *J Diabetes Res, 2016*, 9051426. doi:10.1155/2016/9051426

Al-Sawai, A. A., & Labib, H. (2016). Success of immediate loading implants compared to conventionally-loaded implants: a literature review. *J Investig Clin Dent, 7*(3), 217-224. doi:10.1111/jicd.12152

Albandar, J. M. (2014). Aggressive and acute periodontal diseases. *Periodontol 2000, 65*(1), 7-12. doi:10.1111/prd.12013

Alsaadi, G., Quirynen, M., Michiels, K., Jacobs, R., & van Steenberghe, D. (2007). A biomechanical assessment of the relation between the oral implant stability at insertion and subjective bone quality assessment. *J Clin Periodontol, 34*(4), 359-366. doi:10.1111/j.1600-051X.2007.01047.x

Anderson, P. J., Yong, R., Surman, T. L., Rajion, Z. A., & Ranjitkar, S. (2014). Application of three-dimensional computed tomography in craniofacial clinical practice and research. *Aust Dent J, 59 Suppl 1*, 174-185. doi:10.1111/adj.12154

Anitua, E., Alkhraisat, M. H., Pinas, L., & Orive, G. (2015). Efficacy of biologically guided implant site preparation to obtain adequate primary implant stability. *Ann Anat, 199*, 9-15. doi:10.1016/j.aanat.2014.02.005

Anwandter, A., Bohmann, S., Nally, M., Castro, A. B., Quirynen, M., & Pinto, N. (2016). Dimensional changes of the post extraction alveolar ridge, preserved with Leukocyte- and Platelet Rich Fibrin: A clinical pilot study. *J Dent, 52*, 23-29. doi:10.1016/j.jdent.2016.06.005

ASTM, A. S. f. T. a. M.-. (2016). ASTM F1839-08(2016), Standard Specification for Rigid Polyurethane Foam for Use as a Standard Material for Testing Orthopaedic Devices and Instruments, . In. United States: ASTM International, West Conshohocken, PA,.

ASTM, A. S. f. T. a. M.-. (2017). ASTM F543-17, Standard Specification and Test Methods for Metallic Medical Bone Screws. In. West Conshohocken, PA, 2017,: ASTM International,.

Atsumi, M., Park, S. H., & Wang, H. L. (2007). Methods used to assess implant stability: current status. *Int J Oral Maxillofac Implants, 22*(5), 743-754.

Back, D. A., Pauly, S., Rommel, L., Haas, N. P., Schmidmaier, G., Wildemann, B., & Greiner, S. H. (2012). Effect of local zoledronate on implant osseointegration in a rat model. *BMC Musculoskelet Disord, 13*, 42. doi:10.1186/1471-2474-13-42

Baig, M. R., & Rajan, M. (2007). Effects of smoking on the outcome of implant treatment: a literature review. *Indian J Dent Res, 18*(4), 190-195.

Banse, X., Delloye, C., Cornu, O., & Bourgois, R. (1996). Comparative left-right mechanical testing of cancellous bone from normal femoral heads. *J Biomech, 29*(10), 1247-1253.

Barewal, R. M., Oates, T. W., Meredith, N., & Cochran, D. L. (2003). Resonance frequency measurement of implant stability in vivo on implants with a sandblasted and acid-etched surface. *Int J Oral Maxillofac Implants, 18*(5), 641-651.

Barikani, H., Rashtak, S., Akbari, S., Badri, S., Daneshparvar, N., & Rokn, A. (2013). The effect of implant length and diameter on the primary stability in different bone types. *J Dent (Tehran), 10*(5), 449-455.

Barone, A., Alfonsi, F., Derchi, G., Tonelli, P., Toti, P., Marchionni, S., & Covani, U. (2016). The Effect of Insertion Torque on the Clinical Outcome of Single Implants:

A Randomized Clinical Trial. *Clin Implant Dent Relat Res, 18*(3), 588-600. doi:10.1111/cid.12337

Batista, M. J., Lawrence, H. P., & de Sousa Mda, L. (2014). Impact of tooth loss related to number and position on oral health quality of life among adults. *Health Qual Life Outcomes, 12*, 165. doi:10.1186/s12955-014-0165-5

Bayarchimeg, D., Namgoong, H., Kim, B. K., Kim, M. D., Kim, S., Kim, T. I., Seol, Y. J., Lee, Y. M., Ku, Y., Rhyu, I. C., Lee, E. H., & Koo, K. T. (2013). Evaluation of the correlation between insertion torque and primary stability of dental implants using a block bone test. *J Periodontal Implant Sci, 43*(1), 30-36. doi:10.5051/jpis.2013.43.1.30

Bell, S., Ajami, E., & Davies, J. E. (2014). An improved mechanical testing method to assess bone-implant anchorage. *J Vis Exp*(84), e51221. doi:10.3791/51221

Berglundh, T., Abrahamsson, I., Lang, N. P., & Lindhe, J. (2003). De novo alveolar bone formation adjacent to endosseous implants. *Clin Oral Implants Res, 14*(3), 251-262.

Bernhardt, R., Kuhlisch, E., Schulz, M. C., Eckelt, U., & Stadlinger, B. (2012). Comparison of bone-implant contact and bone-implant volume between 2D-histological sections and 3D-SRmicroCT slices. *Eur Cell Mater, 23*, 237-247; discussion 247-238.

Bhardwaj A, B. S. (2012). Contribution of Animal Models in Periodontal Research. *Int. J. Agro Vet. Med. Sci., 6,*(3), 150-157.

Bielemann, A. M., Marcello-Machado, R. M., Del Bel Cury, A. A., & Faot, F. (2018). Systematic review of wound healing biomarkers in peri-implant crevicular fluid during osseointegration. *Arch Oral Biol, 89*, 107-128. doi:10.1016/j.archoralbio.2018.02.013

Biguetti, C. C., Cavalla, F., Silveira, E. M., Fonseca, A. C., Vieira, A. E., Tabanez, A. P., Rodrigues, D. C., Trombone, A. P. F., & Garlet, G. P. (2018). Oral implant osseointegration model in C57Bl/6 mice: microtomographic, histological, histomorphometric and molecular characterization. *J Appl Oral Sci, 26*, e20170601. doi:10.1590/1678-7757-2017-0601

Bissinger, O., Probst, F. A., Wolff, K. D., Jeschke, A., Weitz, J., Deppe, H., & Kolk, A. (2017). Comparative 3D micro-CT and 2D histomorphometry analysis of dental

implant osseointegration in the maxilla of minipigs. *J Clin Periodontol, 44*(4), 418-427. doi:10.1111/jcpe.12693

Blazsek, D. J. (2008). *A szöveti regeneráció experimentális vizsgálataa szájnyálkahártya,- és csontszövet-regeneráció vizsgálata állat modell rendszerekben.* (PhD), Semmelweis University,

Blazsek, I., Goldschmidt, E., Machover, D., Misset, J. L., Benavides, M., Comisso, M., Ceresi, E., Canon, C., Labat, M. L., & Mathe, G. (1986). Excess of lympho-reticular cell complexes in the bone marrow linked to T cell mediated dysmyelopoiesis. *Biomed Pharmacother, 40*(1), 28-32.

Blazsek, J., Dobo Nagy, C., Blazsek, I., Varga, R., Vecsei, B., Fejerdy, P., & Varga, G. (2009). Aminobisphosphonate stimulates bone regeneration and enforces consolidation of titanium implant into a new rat caudal vertebrae model. *Pathol Oncol Res, 15*(4), 567-577. doi:10.1007/s12253-009-9156-y

Boix, D., Weiss, P., Gauthier, O., Guicheux, J., Bouler, J. M., Pilet, P., Daculsi, G., & Grimandi, G. (2006). Injectable bone substitute to preserve alveolar ridge resorption after tooth extraction: a study in dog. *J Mater Sci Mater Med, 17*(11), 1145-1152. doi:10.1007/s10856-006-0542-7

Bosch, C., Melsen, B., & Vargervik, K. (1998). Importance of the critical-size bone defect in testing bone-regenerating materials. *J Craniofac Surg, 9*(4), 310-316.

Bosshardt, D. D., Salvi, G. E., Huynh-Ba, G., Ivanovski, S., Donos, N., & Lang, N. P. (2011). The role of bone debris in early healing adjacent to hydrophilic and hydrophobic implant surfaces in man. *Clin Oral Implants Res, 22*(4), 357-364. doi:10.1111/j.1600-0501.2010.02107.x

Branemark, P. I. (1983). Osseointegration and its experimental background. *J Prosthet Dent, 50*(3), 399-410.

Branemark, P. I., Adell, R., Breine, U., Hansson, B. O., Lindstrom, J., & Ohlsson, A. (1969). Intra-osseous anchorage of dental prostheses. I. Experimental studies. *Scand J Plast Reconstr Surg, 3*(2), 81-100.

Branemark, R., Ohrnell, L. O., Skalak, R., Carlsson, L., & Branemark, P. I. (1998). Biomechanical characterization of osseointegration: an experimental in vivo investigation in the beagle dog. *J Orthop Res, 16*(1), 61-69. doi:10.1002/jor.1100160111

Brunski, J. B. (1999). In vivo bone response to biomechanical loading at the bone/dental-implant interface. *Adv Dent Res, 13*, 99-119. doi:10.1177/08959374990130012301

Brunski, J. B., Puleo, D. A., & Nanci, A. (2000). Biomaterials and biomechanics of oral and maxillofacial implants: current status and future developments. *Int J Oral Maxillofac Implants, 15*(1), 15-46.

Calvo-Guirado, J. L., Satorres-Nieto, M., Aguilar-Salvatierra, A., Delgado-Ruiz, R. A., Mate-Sanchez de Val, J. E., Gargallo-Albiol, J., Gomez-Moreno, G., & Romanos, G. E. (2015). Influence of surface treatment on osseointegration of dental implants: histological, histomorphometric and radiological analysis in vivo. *Clin Oral Investig, 19*(2), 509-517. doi:10.1007/s00784-014-1241-2

Campana, V., Milano, G., Pagano, E., Barba, M., Cicione, C., Salonna, G., Lattanzi, W., & Logroscino, G. (2014). Bone substitutes in orthopaedic surgery: from basic science to clinical practice. *J Mater Sci Mater Med, 25*(10), 2445-2461. doi:10.1007/s10856-014-5240-2

Candel-Marti, M. E., Ata-Ali, J., Penarrocha-Oltra, D., Penarrocha-Diago, M., & Bagan, J. V. (2011). Dental implants in patients with oral mucosal alterations: An update. *Med Oral Patol Oral Cir Bucal, 16*(6), e787-793.

Caplan, A. I. (1987). Bone development and repair. *Bioessays, 6*(4), 171-175. doi:10.1002/bies.950060406

Carano, R. A., & Filvaroff, E. H. (2003). Angiogenesis and bone repair. *Drug Discov Today, 8*(21), 980-989.

Caroprese, M., Lang, N. P., Rossi, F., Ricci, S., Favero, R., & Botticelli, D. (2017). Morphometric evaluation of the early stages of healing at cortical and marrow compartments at titanium implants: an experimental study in the dog. *Clin Oral Implants Res, 28*(9), 1030-1037. doi:10.1111/clr.12913

Carvalho, C. M., Carvalho, L. F., Costa, L. J., Sa, M. J., Figueiredo, C. R., & Azevedo, A. S. (2010). Titanium implants: a removal torque study in osteopenic rabbits. *Indian J Dent Res, 21*(3), 349-352. doi:10.4103/0970-9290.70798

Cesar-Neto, J. B., Benatti, B. B., Sallum, E. A., Sallum, A. W., & Nociti, F. H., Jr. (2005). Bone filling around titanium implants may benefit from smoking cessation: a

histologic study in rats. *J Periodontol, 76*(9), 1476-1481. doi:10.1902/jop.2005.76.9.1476

Cha, J. Y., Lim, J. K., Song, J. W., Sato, D., Kenmotsu, M., Inoue, T., & Park, Y. C. (2009). Influence of the length of the loading period after placement of orthodontic mini-implants on changes in bone histomorphology: microcomputed tomographic and histologic analysis. *Int J Oral Maxillofac Implants, 24*(5), 842-849.

Chambrone, L., Pannuti, C. M., Guglielmetti, M. R., & Chambrone, L. A. (2011). Evidence grade associating periodontitis with preterm birth and/or low birth weight: II: a systematic review of randomized trials evaluating the effects of periodontal treatment. *J Clin Periodontol, 38*(10), 902-914. doi:10.1111/j.1600-051X.2011.01761.x

Chang, P. C., Lang, N. P., & Giannobile, W. V. (2010). Evaluation of functional dynamics during osseointegration and regeneration associated with oral implants. *Clin Oral Implants Res, 21*(1), 1-12. doi:10.1111/j.1600-0501.2009.01826.x

Chang, P. C., Seol, Y. J., Goldstein, S. A., & Giannobile, W. V. (2013). Determination of the Dynamics of Healing at the Tissue-Implant Interface by Means of Microcomputed Tomography and Functional Apparent Moduli. *International Journal of Oral & Maxillofacial Implants, 28*(1), 68-76. doi:10.11607/jomi.2614

Chatvaratthana, K., Thaworanunta, S., Seriwatanachai, D., & Wongsirichat, N. (2017). Correlation between the thickness of the crestal and buccolingual cortical bone at varying depths and implant stability quotients. *PLoS One, 12*(12), e0190293. doi:10.1371/journal.pone.0190293

Chen, H. H., Lai, W. Y., Chee, T. J., Chan, Y. H., & Feng, S. W. (2017). Monitoring the Changes of Material Properties at Bone-Implant Interface during the Healing Process In Vivo: A Viscoelastic Investigation. *Biomed Res Int, 2017*, 1945607. doi:10.1155/2017/1945607

Cheng, Y. C., Lin, D. H., & Jiang, C. P. (2015). Application of uniform design to improve dental implant system. *Biomed Mater Eng, 26 Suppl 1*, S533-539. doi:10.3233/BME-151343

Choi, J. Y., Sim, J. H., & Yeo, I. L. (2017). Characteristics of contact and distance osteogenesis around modified implant surfaces in rabbit tibiae. *J Periodontal Implant Sci, 47*(3), 182-192. doi:10.5051/jpis.2017.47.3.182

Chrcanovic, B. R., Martins, M. D., & Wennerberg, A. (2015). Immediate placement of implants into infected sites: a systematic review. *Clin Implant Dent Relat Res, 17 Suppl 1*, e1-e16. doi:10.1111/cid.12098

Chugh, T., Jain, A. K., Jaiswal, R. K., Mehrotra, P., & Mehrotra, R. (2013). Bone density and its importance in orthodontics. *J Oral Biol Craniofac Res, 3*(2), 92-97. doi:10.1016/j.jobcr.2013.01.001

Claes, L. E., Heigele, C. A., Neidlinger-Wilke, C., Kaspar, D., Seidl, W., Margevicius, K. J., & Augat, P. (1998). Effects of mechanical factors on the fracture healing process. *Clin Orthop Relat Res*(355 Suppl), S132-147.

Cochran, D. L., Schenk, R. K., Lussi, A., Higginbottom, F. L., & Buser, D. (1998). Bone response to unloaded and loaded titanium implants with a sandblasted and acid-etched surface: a histometric study in the canine mandible. *J Biomed Mater Res, 40*(1), 1-11.

Cohen, D. (2012). How a fake hip showed up failings in European device regulation. *BMJ, 345*, e7090. doi:10.1136/bmj.e7090

Colnot, C., Romero, D. M., Huang, S., Rahman, J., Currey, J. A., Nanci, A., Brunski, J. B., & Helms, J. A. (2007). Molecular analysis of healing at a bone-implant interface. *J Dent Res, 86*(9), 862-867. doi:10.1177/154405910708600911

Cortes, A. R., Eimar, H., Barbosa Jde, S., Costa, C., Arita, E. S., & Tamimi, F. (2015). Sensitivity and specificity of radiographic methods for predicting insertion torque of dental implants. *J Periodontol, 86*(5), 646-655. doi:10.1902/jop.2015.140584

Cranin, A. N., DeGrado, J., Kaufman, M., Baraoidan, M., DiGregorio, R., Batgitis, G., & Lee, Z. (1998). Evaluation of the Periotest as a diagnostic tool for dental implants. *J Oral Implantol, 24*(3), 139-146. doi:10.1563/1548-1336(1998)024<0139:EOTPAA>2.3.CO;2

da Cunha, A. C., Marquezan, M., Lima, I., Lopes, R. T., Nojima, L. I., & Sant'Anna, E. F. (2015). Influence of bone architecture on the primary stability of different mini-implant designs. *Am J Orthod Dentofacial Orthop, 147*(1), 45-51. doi:10.1016/j.ajodo.2014.09.011

Davies, J. E. (2003). Understanding peri-implant endosseous healing. *J Dent Educ, 67*(8), 932-949.

Davies, J. E. (2007). Bone bonding at natural and biomaterial surfaces. *Biomaterials, 28*(34), 5058-5067. doi:10.1016/j.biomaterials.2007.07.049

De Angelis, F., Papi, P., Mencio, F., Rosella, D., Di Carlo, S., & Pompa, G. (2017). Implant survival and success rates in patients with risk factors: results from a long-term retrospective study with a 10 to 18 years follow-up. *Eur Rev Med Pharmacol Sci, 21*(3), 433-437.

Demmer, R. T., Desvarieux, M., Holtfreter, B., Jacobs, D. R., Jr., Wallaschofski, H., Nauck, M., Volzke, H., & Kocher, T. (2010). Periodontal status and A1C change: longitudinal results from the study of health in Pomerania (SHIP). *Diabetes Care, 33*(5), 1037-1043. doi:10.2337/dc09-1778

Di Stefano, D. A., Arosio, P., Piattelli, A., Perrotti, V., & Iezzi, G. (2015). A torque-measuring micromotor provides operator independent measurements marking four different density areas in maxillae. *J Adv Prosthodont, 7*(1), 51-55. doi:10.4047/jap.2015.7.1.51

Diaz-Sanchez, R. M., Delgado-Munoz, J. M., Hita-Iglesias, P., Pullen, K. T., Serrera-Figallo, M. A., & Torres-Lagares, D. (2017). Improvement in the Initial Implant Stability Quotient Through Use of a Modified Surgical Technique. *J Oral Implantol, 43*(3), 186-193. doi:10.1563/aaid-joi-D-16-00159

Dorogoy, A., Rittel, D., Shemtov-Yona, K., & Korabi, R. (2017). Modeling dental implant insertion. *J Mech Behav Biomed Mater, 68*, 42-50. doi:10.1016/j.jmbbm.2017.01.021

Dos Santos, M. V., Elias, C. N., & Cavalcanti Lima, J. H. (2011). The effects of superficial roughness and design on the primary stability of dental implants. *Clin Implant Dent Relat Res, 13*(3), 215-223. doi:10.1111/j.1708-8208.2009.00202.x

Ebina, H., Hatakeyama, J., Onodera, M., Honma, T., Kamakura, S., Shimauchi, H., & Sasano, Y. (2009). Micro-CT analysis of alveolar bone healing using a rat experimental model of critical-size defects. *Oral Dis, 15*(4), 273-280. doi:10.1111/j.1601-0825.2009.01522.x

Einhorn, T. A., & Gerstenfeld, L. C. (2015). Fracture healing: mechanisms and interventions. *Nat Rev Rheumatol, 11*(1), 45-54. doi:10.1038/nrrheum.2014.164

Eke, P. I., Dye, B. A., Wei, L., Slade, G. D., Thornton-Evans, G. O., Borgnakke, W. S., Taylor, G. W., Page, R. C., Beck, J. D., & Genco, R. J. (2015). Update on Prevalence of Periodontitis in Adults in the United States: NHANES 2009 to 2012. *J Periodontol, 86*(5), 611-622. doi:10.1902/jop.2015.140520

Ekfeldt, A., Christiansson, U., Eriksson, T., Linden, U., Lundqvist, S., Rundcrantz, T., Johansson, L. A., Nilner, K., & Billstrom, C. (2001). A retrospective analysis of factors associated with multiple implant failures in maxillae. *Clin Oral Implants Res, 12*(5), 462-467.

Elgali, I., Omar, O., Dahlin, C., & Thomsen, P. (2017). Guided bone regeneration: materials and biological mechanisms revisited. *Eur J Oral Sci, 125*(5), 315-337. doi:10.1111/eos.12364

Ernstberger, T., Heidrich, G., & Buchhorn, G. (2007). Postimplantation MRI with cylindric and cubic intervertebral test implants: evaluation of implant shape, material, and volume in MRI artifacting--an in vitro study. *Spine J, 7*(3), 353-359. doi:10.1016/j.spinee.2006.03.016

Espitalier, F., Vinatier, C., Lerouxel, E., Guicheux, J., Pilet, P., Moreau, F., Daculsi, G., Weiss, P., & Malard, O. (2009). A comparison between bone reconstruction following the use of mesenchymal stem cells and total bone marrow in association with calcium phosphate scaffold in irradiated bone. *Biomaterials, 30*(5), 763-769. doi:10.1016/j.biomaterials.2008.10.051

EuropeanParliament. (1993). *Council Directive 93/42/EEC of 14 June 1993 concerning medical devices OJ L 169 of 12 July 1993*. Retrieved from http://ec.europa.eu/growth/single-market/european-standards/harmonised-standards/medical-devices/

EuropeanParliament. (2017). Regulation (EU) 2017/745 of the European Parliament and of the council of 5 April 2017 on medical devices, amending Directive 2001/83/EC, Regulation (EC) No 178/2002 and Regulation (EC) No 1223/2009 and repealing Council Directives 90/385/EEC and 93/42/EEC *Official Journal of the European Union, L 117/1*

Fan, X., Alekseyenko, A. V., Wu, J., Peters, B. A., Jacobs, E. J., Gapstur, S. M., Purdue, M. P., Abnet, C. C., Stolzenberg-Solomon, R., Miller, G., Ravel, J., Hayes, R. B., & Ahn, J. (2016). Human oral microbiome and prospective risk for pancreatic

cancer: a population-based nested case-control study. *Gut*. doi:10.1136/gutjnl-2016-312580

Farkasdi, S., Pammer, D., Racz, R., Hriczo-Koperdak, G., Szabo, B. T., Dobo-Nagy, C., Keremi, B., Blazsek, J., Cuisinier, F., Wu, G., & Varga, G. (2018). Development of a quantitative preclinical screening model for implant osseointegration in rat tail vertebra. *Clin Oral Investig*. doi:10.1007/s00784-018-2661-1

Fernandez, T., Olave, G., Valencia, C. H., Arce, S., Quinn, J. M., Thouas, G. A., & Chen, Q. Z. (2014). Effects of calcium phosphate/chitosan composite on bone healing in rats: calcium phosphate induces osteon formation. *Tissue Eng Part A, 20*(13-14), 1948-1960. doi:10.1089/ten.TEA.2013.0696

French-Mowat, E., & Burnett, J. (2012). How are medical devices regulated in the European Union? *J R Soc Med, 105 Suppl 1*, S22-28. doi:10.1258/jrsm.2012.120036

Friberg, B., Sennerby, L., Linden, B., Grondahl, K., & Lekholm, U. (1999). Stability measurements of one-stage Branemark implants during healing in mandibles. A clinical resonance frequency analysis study. *International journal of oral and maxillofacial surgery, 28*, 266-272.

Friberg, B., Sennerby, L., Roos, J., Johansson, P., Strid, C. G., & Lekholm, U. (1995). Evaluation of bone density using cutting resistance measurements and microradiography: an in vitro study in pig ribs. *Clin Oral Implants Res, 6*(3), 164-171.

Frost, H. M. (1989a). The biology of fracture healing. An overview for clinicians. Part I. *Clin Orthop Relat Res*(248), 283-293.

Frost, H. M. (1989b). The biology of fracture healing. An overview for clinicians. Part II. *Clin Orthop Relat Res*(248), 294-309.

Gallucci, G. O., Benic, G. I., Eckert, S. E., Papaspyridakos, P., Schimmel, M., Schrott, A., & Weber, H. P. (2014). Consensus statements and clinical recommendations for implant loading protocols. *Int J Oral Maxillofac Implants, 29 Suppl*, 287-290. doi:10.11607/jomi.2013.g4

Gehrke, S. A., da Silva, U. T., & Del Fabbro, M. (2015). Does Implant Design Affect Implant Primary Stability? A Resonance Frequency Analysis-Based Randomized

Split-Mouth Clinical Trial. *J Oral Implantol, 41*(6), e281-286. doi:10.1563/aaid-joi-D-13-00294

Gelazius, R., Poskevicius, L., Sakavicius, D., Grimuta, V., & Juodzbalys, G. (2018). Dental Implant Placement in Patients on Bisphosphonate Therapy: a Systematic Review. *J Oral Maxillofac Res, 9*(3), e2. doi:10.5037/jomr.2018.9302

Gerritsen, A. E., Allen, P. F., Witter, D. J., Bronkhorst, E. M., & Creugers, N. H. (2010). Tooth loss and oral health-related quality of life: a systematic review and meta-analysis. *Health Qual Life Outcomes, 8*, 126. doi:10.1186/1477-7525-8-126

Ghiasi, M. S., Chen, J., Vaziri, A., Rodriguez, E. K., & Nazarian, A. (2017). Bone fracture healing in mechanobiological modeling: A review of principles and methods. *Bone Rep, 6*, 87-100. doi:10.1016/j.bonr.2017.03.002

Goelzer, J. G., Avelar, R. L., de Oliveira, R. B., Hubler, R., Silveira, R. L., & Machado, R. A. (2010). Self-drilling and self-tapping screws: an ultrastructural study. *J Craniofac Surg, 21*(2), 513-515. doi:10.1097/SCS.0b013e3181d023bd

Gomez-de Diego, R., Mang-de la Rosa Mdel, R., Romero-Perez, M. J., Cutando-Soriano, A., & Lopez-Valverde-Centeno, A. (2014). Indications and contraindications of dental implants in medically compromised patients: update. *Med Oral Patol Oral Cir Bucal, 19*(5), e483-489.

Greco, C. (2015). The Poly Implant Prothese breast prostheses scandal: Embodied risk and social suffering. *Soc Sci Med, 147*, 150-157. doi:10.1016/j.socscimed.2015.10.068

Greenberg, A. M. (2015). Digital technologies for dental implant treatment planning and guided surgery. *Oral Maxillofac Surg Clin North Am, 27*(2), 319-340. doi:10.1016/j.coms.2015.01.010

Greenstein, G., Cavallaro, J., Romanos, G., & Tarnow, D. (2008). Clinical recommendations for avoiding and managing surgical complications associated with implant dentistry: a review. *J Periodontol, 79*(8), 1317-1329. doi:10.1902/jop.2008.070067

Haga, M., Fujii, N., Nozawa-Inoue, K., Nomura, S., Oda, K., Uoshima, K., & Maeda, T. (2009). Detailed process of bone remodeling after achievement of osseointegration in a rat implantation model. *Anat Rec (Hoboken), 292*(1), 38-47. doi:10.1002/ar.20748

Han, J., Lulic, M., & Lang, N. P. (2010). Factors influencing resonance frequency analysis assessed by Osstell mentor during implant tissue integration: II. Implant surface modifications and implant diameter. *Clin Oral Implants Res, 21*(6), 605-611. doi:10.1111/j.1600-0501.2009.01909.x

Harris, J. S., Bemenderfer, T. B., Wessel, A. R., & Kacena, M. A. (2013). A review of mouse critical size defect models in weight bearing bones. *Bone, 55*(1), 241-247. doi:10.1016/j.bone.2013.02.002

Hartung, T. (2010). Comparative analysis of the revised Directive 2010/63/EU for the protection of laboratory animals with its predecessor 86/609/EEC - a t4 report. *ALTEX, 27*(4), 285-303.

Heneghan, C. (2012). The saga of Poly Implant Prosthese breast implants. *BMJ, 344*, e306. doi:10.1136/bmj.e306

Heneghan, C., Langton, D., & Thompson, M. (2012). Ongoing problems with metal-on-metal hip implants. *BMJ, 344*, e1349. doi:10.1136/bmj.e1349

Hof, M., Tepper, G., Semo, B., Arnhart, C., Watzek, G., & Pommer, B. (2014). Patients' perspectives on dental implant and bone graft surgery: questionnaire-based interview survey. *Clin Oral Implants Res, 25*(1), 42-45. doi:10.1111/clr.12061

Howard, J. J. (2016). Balancing innovation and medical device regulation: the case of modern metal-on-metal hip replacements. *Med Devices (Auckl), 9*, 267-275. doi:10.2147/MDER.S113067

Huang, H., Wismeijer, D., Shao, X., & Wu, G. (2016). Mathematical evaluation of the influence of multiple factors on implant stability quotient values in clinical practice: a retrospective study. *Ther Clin Risk Manag, 12*, 1525-1532. doi:10.2147/TCRM.S113764

Humphrey, L. L., Fu, R., Buckley, D. I., Freeman, M., & Helfand, M. (2008). Periodontal disease and coronary heart disease incidence: a systematic review and meta-analysis. *J Gen Intern Med, 23*(12), 2079-2086. doi:10.1007/s11606-008-0787-6

Huwiler, M. A., Pjetursson, B. E., Bosshardt, D. D., Salvi, G. E., & Lang, N. P. (2007). Resonance frequency analysis in relation to jawbone characteristics and during early healing of implant installation. *Clin Oral Implants Res, 18*(3), 275-280. doi:10.1111/j.1600-0501.2007.01336.x

Hwang, D., & Wang, H. L. (2006). Medical contraindications to implant therapy: part I: absolute contraindications. *Implant Dent, 15*(4), 353-360. doi:10.1097/01.id.0000247855.75691.03

Hwang, D., & Wang, H. L. (2007). Medical contraindications to implant therapy: Part II: Relative contraindications. *Implant Dent, 16*(1), 13-23. doi:10.1097/ID.0b013e31803276c8

Iezzi, G., Scarano, A., Di Stefano, D. A., Arosio, P., Doi, K., Ricci, L., Piattelli, A., & Perrotti, V. (2015). Correlation between the bone density recorded by a computerized implant motor and by a histomorphometric analysis: a preliminary in vitro study on bovine ribs. *Clin Implant Dent Relat Res, 17 Suppl 1*, e35-44. doi:10.1111/cid.12121

Iniesta, M., Herrera, D., Montero, E., Zurbriggen, M., Matos, A. R., Marin, M. J., Sanchez-Beltran, M. C., Llama-Palacio, A., & Sanz, M. (2012). Probiotic effects of orally administered Lactobacillus reuteri-containing tablets on the subgingival and salivary microbiota in patients with gingivitis. A randomized clinical trial. *J Clin Periodontol, 39*(8), 736-744. doi:10.1111/j.1600-051X.2012.01914.x

ISO/TS_22911:2016. (2016). Dentistry - Preclinical evaluation of dental implant systems - Animal test methods. *https://www.iso.org/obp/ui/#iso:std:iso:ts:22911:ed-2:v1:en*.

Ito, Y., Sato, D., Yoneda, S., Ito, D., Kondo, H., & Kasugai, S. (2008). Relevance of resonance frequency analysis to evaluate dental implant stability: simulation and histomorphometrical animal experiments. *Clin Oral Implants Res, 19*(1), 9-14. doi:10.1111/j.1600-0501.2007.01419.x

Jariwala, S. H., Wee, H., Roush, E. P., Whitcomb, T. L., Murter, C., Kozlansky, G., Lakhtakia, A., Kunselman, A. R., Donahue, H. J., Armstrong, A. D., & Lewis, G. S. (2017). Time course of peri-implant bone regeneration around loaded and unloaded implants in a rat model. *J Orthop Res, 35*(5), 997-1006. doi:10.1002/jor.23360

Javed, F., Ahmed, H. B., Crespi, R., & Romanos, G. E. (2013). Role of primary stability for successful osseointegration of dental implants: Factors of influence and evaluation. *Interv Med Appl Sci, 5*(4), 162-167. doi:10.1556/IMAS.5.2013.4.3

Javed, F., Al-Hezaimi, K., Al-Rasheed, A., Almas, K., & Romanos, G. E. (2010). Implant survival rate after oral cancer therapy: a review. *Oral Oncol, 46*(12), 854-859. doi:10.1016/j.oraloncology.2010.10.004

Jerome, C. P., & Peterson, P. E. (2001). Nonhuman primate models in skeletal research. *Bone, 29*(1), 1-6.

Jimbo, R., & Albrektsson, T. (2015). Long-term clinical success of minimally and moderately rough oral implants: a review of 71 studies with 5 years or more of follow-up. *Implant Dent, 24*(1), 62-69. doi:10.1097/ID.0000000000000205

Jung, K. Y., Hong, A. R., Lee, D. H., Kim, J. H., Kim, K. M., Shin, C. S., Kim, S. Y., & Kim, S. W. (2017). The natural history and hip geometric changes of primary hyperparathyroidism without parathyroid surgery. *J Bone Miner Metab, 35*(3), 278-288. doi:10.1007/s00774-016-0751-1

Kang, S. W., Lee, W. J., Choi, S. C., Lee, S. S., Heo, M. S., Huh, K. H., Kim, T. I., & Yi, W. J. (2015). Volumetric quantification of bone-implant contact using micro-computed tomography analysis based on region-based segmentation. *Imaging Sci Dent, 45*(1), 7-13. doi:10.5624/isd.2015.45.1.7

Karami, D., Alborzinia, H. R., Amid, R., Kadkhodazadeh, M., Yousefi, N., & Badakhshan, S. (2017). In-Office Guided Implant Placement for Prosthetically Driven Implant Surgery. *Craniomaxillofac Trauma Reconstr, 10*(3), 246-254. doi:10.1055/s-0036-1584891

Kassebaum, N. J., Smith, A. G. C., Bernabe, E., Fleming, T. D., Reynolds, A. E., Vos, T., Murray, C. J. L., Marcenes, W., & Collaborators, G. B. D. O. H. (2017). Global, Regional, and National Prevalence, Incidence, and Disability-Adjusted Life Years for Oral Conditions for 195 Countries, 1990-2015: A Systematic Analysis for the Global Burden of Diseases, Injuries, and Risk Factors. *J Dent Res, 96*(4), 380-387. doi:10.1177/0022034517693566

Kataoka, M. L., Hochman, M. G., Rodriguez, E. K., Lin, P. J., Kubo, S., & Raptopolous, V. D. (2010). A review of factors that affect artifact from metallic hardware on multi-row detector computed tomography. *Curr Probl Diagn Radiol, 39*(4), 125-136. doi:10.1067/j.cpradiol.2009.05.002

Katsoulis, J., Pazera, P., & Mericske-Stern, R. (2009). Prosthetically driven, computer-guided implant planning for the edentulous maxilla: a model study. *Clin Implant Dent Relat Res, 11*(3), 238-245. doi:10.1111/j.1708-8208.2008.00110.x

Khojasteh, A., Kheiri, L., Motamedian, S. R., & Khoshkam, V. (2017). Guided Bone Regeneration for the Reconstruction of Alveolar Bone Defects. *Ann Maxillofac Surg, 7*(2), 263-277. doi:10.4103/ams.ams_76_17

Kinane, D. F., & Marshall, G. J. (2001). Periodontal manifestations of systemic disease. *Aust Dent J, 46*(1), 2-12.

Kinane, D. F., Stathopoulou, P. G., & Papapanou, P. N. (2017). Periodontal diseases. *Nat Rev Dis Primers, 3*, 17038. doi:10.1038/nrdp.2017.38

Korfage, A., Raghoebar, G. M., Meijer, H. J. A., & Vissink, A. (2018). Patients' expectations of oral implants: a systematic review. *Eur J Oral Implantol, 11 Suppl 1*, S65-S76.

Kuchler, U., Chappuis, V., Bornstein, M. M., Siewczyk, M., Gruber, R., Maestre, L., & Buser, D. (2016). Development of Implant Stability Quotient values of implants placed with simultaneous sinus floor elevation - results of a prospective study with 109 implants. *Clin Oral Implants Res*. doi:10.1111/clr.12768

Kumar, P., Vinitha, B., & Fathima, G. (2013). Bone grafts in dentistry. *J Pharm Bioallied Sci, 5*(Suppl 1), S125-127. doi:10.4103/0975-7406.113312

Kummari, S. R., Davis, A. J., Vega, L. A., Ahn, N., Cassinelli, E. H., & Hernandez, C. J. (2009). Trabecular microfracture precedes cortical shell failure in the rat caudal vertebra under cyclic overloading. *Calcif Tissue Int, 85*(2), 127-133. doi:10.1007/s00223-009-9257-3

Kuzyk, P. R., & Schemitsch, E. H. (2011). The basic science of peri-implant bone healing. *Indian J Orthop, 45*(2), 108-115. doi:10.4103/0019-5413.77129

Kwon, T., & Levin, L. (2014). Cause-related therapy: a review and suggested guidelines. *Quintessence Int, 45*(7), 585-591. doi:10.3290/j.qi.a31808

Larsen, T., & Fiehn, N. E. (2017). Dental biofilm infections - an update. *APMIS, 125*(4), 376-384. doi:10.1111/apm.12688

Laudenbach, J. M., & Simon, Z. (2014). Common dental and periodontal diseases: evaluation and management. *Med Clin North Am, 98*(6), 1239-1260. doi:10.1016/j.mcna.2014.08.002

Le Guehennec, L., Soueidan, A., Layrolle, P., & Amouriq, Y. (2007). Surface treatments of titanium dental implants for rapid osseointegration. *Dent Mater, 23*(7), 844-854. doi:10.1016/j.dental.2006.06.025

Ledermann, P. D., Schenk, R. K., & Buser, D. (1998). Long-lasting osseointegration of immediately loaded, bar-connected TPS screws after 12 years of function: a histologic case report of a 95-year-old patient. *Int J Periodontics Restorative Dent, 18*(6), 552-563.

Lee, J., Lee, E. N., Yoon, J., Chung, S. M., Prasad, H., Susin, C., & Wikesjo, U. M. (2013). Comparative study of Chinese hamster ovary cell versus Escherichia coli-derived bone morphogenetic protein-2 using the critical-size supraalveolar peri-implant defect model. *J Periodontol, 84*(3), 415-422. doi:10.1902/jop.2012.110369

Lee, J. H., Oh, J. Y., Choi, J. K., Kim, Y. T., Park, Y. S., Jeong, S. N., & Choi, S. H. (2017). Trends in the incidence of tooth extraction due to periodontal disease: results of a 12-year longitudinal cohort study in South Korea. *J Periodontal Implant Sci, 47*(5), 264-272. doi:10.5051/jpis.2017.47.5.264

Lee, J. T., & Cho, S. A. (2016). Biomechanical evaluation of laser-etched Ti implant surfaces vs. chemically modified SLA Ti implant surfaces: Removal torque and resonance frequency analysis in rabbit tibias. *J Mech Behav Biomed Mater, 61*, 299-307. doi:10.1016/j.jmbbm.2016.03.034

Lekholm U, Z. G. (1985). In: Patient selection and preparation. Tissue integrated prostheses: osseointegration in clinical dentistry. Branemark PI, Zarb GA, Albrektsson T, editor. *Chicago: Quintessence Publishing Company;*, p. 199–209.

Li, J., Yin, X., Huang, L., Mouraret, S., Brunski, J. B., Cordova, L., Salmon, B., & Helms, J. A. (2017). Relationships among Bone Quality, Implant Osseointegration, and Wnt Signaling. *J Dent Res, 96*(7), 822-831. doi:10.1177/0022034517700131

Li, Y., Chen, S. K., Li, L., Qin, L., Wang, X. L., & Lai, Y. X. (2015a). Bone defect animal models for testing efficacy of bone substitute biomaterials. *J Orthop Translat, 3*(3), 95-104. doi:10.1016/j.jot.2015.05.002

Li, Z., Kuhn, G., von Salis-Soglio, M., Cooke, S. J., Schirmer, M., Muller, R., & Ruffoni, D. (2015b). In vivo monitoring of bone architecture and remodeling after implant insertion: The different responses of cortical and trabecular bone. *Bone, 81*, 468-477. doi:10.1016/j.bone.2015.08.017

Liu, J., & Kerns, D. G. (2014). Mechanisms of guided bone regeneration: a review. *Open Dent J, 8*, 56-65. doi:10.2174/1874210601408010056

Liu, Y., Huse, R. O., de Groot, K., Buser, D., & Hunziker, E. B. (2007). Delivery mode and efficacy of BMP-2 in association with implants. *Journal of Dental Research, 86*(1), 84-89. doi:Doi 10.1177/154405910708600114

Lockhart, P. B., Bolger, A. F., Papapanou, P. N., Osinbowale, O., Trevisan, M., Levison, M. E., Taubert, K. A., Newburger, J. W., Gornik, H. L., Gewitz, M. H., Wilson, W. R., Smith, S. C., Jr., Baddour, L. M., American Heart Association Rheumatic Fever, E., Kawasaki Disease Committee of the Council on Cardiovascular Disease in the Young, C. o. E., Prevention, C. o. P. V. D., & Council on Clinical, C. (2012). Periodontal disease and atherosclerotic vascular disease: does the evidence support an independent association?: a scientific statement from the American Heart Association. *Circulation, 125*(20), 2520-2544. doi:10.1161/CIR.0b013e31825719f3

Lozano-Carrascal, N., Salomo-Coll, O., Gilabert-Cerda, M., Farre-Pages, N., Gargallo-Albiol, J., & Hernandez-Alfaro, F. (2016). Effect of implant macro-design on primary stability: A prospective clinical study. *Med Oral Patol Oral Cir Bucal, 21*(2), e214-221.

Lutz, R., Srour, S., Nonhoff, J., Weisel, T., Damien, C. J., & Schlegel, K. A. (2010). Biofunctionalization of titanium implants with a biomimetic active peptide (P-15) promotes early osseointegration. *Clin Oral Implants Res, 21*(7), 726-734. doi:10.1111/j.1600-0501.2009.01904.x

Machtei, E. E. (2001). The effect of membrane exposure on the outcome of regenerative procedures in humans: a meta-analysis. *J Periodontol, 72*(4), 512-516. doi:10.1902/jop.2001.72.4.512

Majzoub, Z., Berengo, M., Giardino, R., Aldini, N. N., & Cordioli, G. (1999). Role of intramarrow penetration in osseous repair: a pilot study in the rabbit calvaria. *J Periodontol, 70*(12), 1501-1510. doi:10.1902/jop.1999.70.12.1501

Makihara, T., Sakane, M., Noguchi, H., Tsukanishi, T., Suetsugu, Y., & Yamazaki, M. (2018). Formation of osteon-like structures in unidirectional porous hydroxyapatite substitute. *J Biomed Mater Res B Appl Biomater*. doi:10.1002/jbm.b.34083

Mamalis, A. A., & Cochran, D. L. (2013). The role of hypoxia in the regulation of osteogenesis and angiogenesis coupling in intraoral regenerative procedures: a review of the literature. *Int J Periodontics Restorative Dent, 33*(4), 519-524. doi:10.11607/prd.0868

Manresa, C., Bosch, M., & Echeverria, J. J. (2014). The comparison between implant stability quotient and bone-implant contact revisited: an experiment in Beagle dog. *Clin Oral Implants Res, 25*(11), 1213-1221. doi:10.1111/clr.12256

Marcello-Machado, R. M., Faot, F., Schuster, A. J., Nascimento, G. G., & Del Bel Cury, A. A. (2018). Mini-implants and narrow diameter implants as mandibular overdenture retainers: A systematic review and meta-analysis of clinical and radiographic outcomes. *J Oral Rehabil, 45*(2), 161-183. doi:10.1111/joor.12585

Markovic, A., Dinic, A., Calvo Guirado, J. L., Tahmaseb, A., Scepanovic, M., & Janjic, B. (2016). Randomized clinical study of the peri-implant healing to hydrophilic and hydrophobic implant surfaces in patients receiving anticoagulants. *Clin Oral Implants Res*. doi:10.1111/clr.12948

Marsell, R., & Einhorn, T. A. (2010). Emerging bone healing therapies. *J Orthop Trauma, 24 Suppl 1*, S4-8. doi:10.1097/BOT.0b013e3181ca3fab

Marsell, R., & Einhorn, T. A. (2011). The biology of fracture healing. *Injury, 42*(6), 551-555. doi:10.1016/j.injury.2011.03.031

Martiniakova, M., Grosskopf, B., Omelka, R., Vondrakova, M., & Bauerova, M. (2006). Differences among species in compact bone tissue microstructure of mammalian skeleton: use of a discriminant function analysis for species identification. *J Forensic Sci, 51*(6), 1235-1239. doi:10.1111/j.1556-4029.2006.00260.x

Marzona, L., & Pavolini, B. (2009). Play and players in bone fracture healing match. *Clin Cases Miner Bone Metab, 6*(2), 159-162.

Mathieu, V., Anagnostou, F., Soffer, E., & Haiat, G. (2011a). Numerical simulation of ultrasonic wave propagation for the evaluation of dental implant biomechanical stability. *J Acoust Soc Am, 129*(6), 4062-4072. doi:10.1121/1.3586788

Mathieu, V., Anagnostou, F., Soffer, E., & Haiat, G. (2011b). Ultrasonic evaluation of dental implant biomechanical stability: an in vitro study. *Ultrasound Med Biol, 37*(2), 262-270. doi:10.1016/j.ultrasmedbio.2010.10.008

Mathieu, V., Vayron, R., Richard, G., Lambert, G., Naili, S., Meningaud, J. P., & Haiat, G. (2014). Biomechanical determinants of the stability of dental implants: influence of the bone-implant interface properties. *J Biomech, 47*(1), 3-13. doi:10.1016/j.jbiomech.2013.09.021

Mavrogenis, A. F., Dimitriou, R., Parvizi, J., & Babis, G. C. (2009). Biology of implant osseointegration. *J Musculoskelet Neuronal Interact, 9*(2), 61-71.

Mayer, L., Gomes, F. V., de Oliveira, M. G., de Moraes, J. F., & Carlsson, L. (2016). Peri-implant osseointegration after low-level laser therapy: micro-computed tomography and resonance frequency analysis in an animal model. *Lasers Med Sci, 31*(9), 1789-1795. doi:10.1007/s10103-016-2051-3

Mazzo, C. R., Reis, A. C., Shimano, A. C., & Valente, M. L. (2012). In vitro analysis of the influence of surface treatment of dental implants on primary stability. *Braz Oral Res, 26*(4), 313-317.

McKibbin, B. (1978). The biology of fracture healing in long bones. *J Bone Joint Surg Br, 60-B*(2), 150-162.

Meirelles, L., Branemark, P. I., Albrektsson, T., Feng, C., & Johansson, C. (2015). Histological evaluation of bone formation adjacent to dental implants with a novel apical chamber design: preliminary data in the rabbit model. *Clin Implant Dent Relat Res, 17*(3), 453-460. doi:10.1111/cid.12139

Meredith, N. (1998). Assessment of implant stability as a prognostic determinant. *Int J Prosthodont, 11*(5), 491-501.

Merheb, J., Temmerman, A., Rasmusson, L., Kubler, A., Thor, A., & Quirynen, M. (2016). Influence of Skeletal and Local Bone Density on Dental Implant Stability in Patients with Osteoporosis. *Clin Implant Dent Relat Res, 18*(2), 253-260. doi:10.1111/cid.12290

Meyer, R. A., Jr., Tsahakis, P. J., Martin, D. F., Banks, D. M., Harrow, M. E., & Kiebzak, G. M. (2001). Age and ovariectomy impair both the normalization of mechanical properties and the accretion of mineral by the fracture callus in rats. *J Orthop Res, 19*(3), 428-435. doi:10.1016/S0736-0266(00)90034-2

Michaud, D. S., Izard, J., Wilhelm-Benartzi, C. S., You, D. H., Grote, V. A., Tjonneland, A., Dahm, C. C., Overvad, K., Jenab, M., Fedirko, V., Boutron-Ruault, M. C., Clavel-Chapelon, F., Racine, A., Kaaks, R., Boeing, H., Foerster, J., Trichopoulou,

A., Lagiou, P., Trichopoulos, D., Sacerdote, C., Sieri, S., Palli, D., Tumino, R., Panico, S., Siersema, P. D., Peeters, P. H., Lund, E., Barricarte, A., Huerta, J. M., Molina-Montes, E., Dorronsoro, M., Quiros, J. R., Duell, E. J., Ye, W., Sund, M., Lindkvist, B., Johansen, D., Khaw, K. T., Wareham, N., Travis, R. C., Vineis, P., Bueno-de-Mesquita, H. B., & Riboli, E. (2013). Plasma antibodies to oral bacteria and risk of pancreatic cancer in a large European prospective cohort study. *Gut, 62*(12), 1764-1770. doi:10.1136/gutjnl-2012-303006

Michaud, D. S., Joshipura, K., Giovannucci, E., & Fuchs, C. S. (2007). A prospective study of periodontal disease and pancreatic cancer in US male health professionals. *J Natl Cancer Inst, 99*(2), 171-175. doi:10.1093/jnci/djk021

Michaud, D. S., Kelsey, K. T., Papathanasiou, E., Genco, C. A., & Giovannucci, E. (2016). Periodontal disease and risk of all cancers among male never smokers: an updated analysis of the Health Professionals Follow-up Study. *Ann Oncol, 27*(5), 941-947. doi:10.1093/annonc/mdw028

Michaud, D. S., Liu, Y., Meyer, M., Giovannucci, E., & Joshipura, K. (2008). Periodontal disease, tooth loss, and cancer risk in male health professionals: a prospective cohort study. *Lancet Oncol, 9*(6), 550-558. doi:10.1016/S1470-2045(08)70106-2

Misch, C. E. (1989). Bone classification, training keys to implant success. *Dent Today, 8*(4), 39-44.

Misch, C. E. (1990). Density of bone: effect on treatment plans, surgical approach, healing, and progressive boen loading. *Int J Oral Implantol, 6*(2), 23-31.

Misch, C. E., Bidez, M. W., & Sharawy, M. (2001). A bioengineered implant for a predetermined bone cellular response to loading forces. A literature review and case report. *J Periodontol, 72*(9), 1276-1286. doi:10.1902/jop.2000.72.9.1276

Monje, A., Ortega-Oller, I., Galindo-Moreno, P., Catena, A., Monje, F., O'Valle, F., Suarez, F., & Wang, H. L. (2014). Sensitivity of resonance frequency analysis for detecting early implant failure: a case-control study. *Int J Oral Maxillofac Implants, 29*(2), 456-461. doi:10.11607/jomi.3357

Morad, G., Kheiri, L., & Khojasteh, A. (2013). Dental pulp stem cells for in vivo bone regeneration: a systematic review of literature. *Arch Oral Biol, 58*(12), 1818-1827. doi:10.1016/j.archoralbio.2013.08.011

Moraschini, V., Poubel, L. A., Ferreira, V. F., & Barboza Edos, S. (2015). Evaluation of survival and success rates of dental implants reported in longitudinal studies with a follow-up period of at least 10 years: a systematic review. *Int J Oral Maxillofac Surg, 44*(3), 377-388. doi:10.1016/j.ijom.2014.10.023

Mueller, C. K., Thorwarth, M., Schmidt, M., Schlegel, K. A., & Schultze-Mosgau, S. (2011). Comparative analysis of osseointegration of titanium implants with acid-etched surfaces and different biomolecular coatings. *Oral Surg Oral Med Oral Pathol Oral Radiol Endod, 112*(6), 726-736. doi:10.1016/j.tripleo.2011.01.004

Nagayasu-Tanaka, T., Nozaki, T., Miki, K., Sawada, K., Kitamura, M., & Murakami, S. (2017). FGF-2 promotes initial osseointegration and enhances stability of implants with low primary stability. *Clin Oral Implants Res, 28*(3), 291-297. doi:10.1111/clr.12797

Nedir, R., Bischof, M., Szmukler-Moncler, S., Bernard, J. P., & Samson, J. (2004). Predicting osseointegration by means of implant primary stability. *Clin Oral Implants Res, 15*(5), 520-528. doi:10.1111/j.1600-0501.2004.01059.x

Nienkemper, M., Wilmes, B., Panayotidis, A., Pauls, A., Golubovic, V., Schwarz, F., & Drescher, D. (2013). Measurement of mini-implant stability using resonance frequency analysis. *Angle Orthod, 83*(2), 230-238. doi:10.2319/043012-354.1

Nonhoff, J., Moest, T., Schmitt, C. M., Weisel, T., Bauer, S., & Schlegel, K. A. (2015). Establishment of a new pull-out strength testing method to quantify early osseointegration-An experimental pilot study. *J Craniomaxillofac Surg, 43*(10), 1966-1973. doi:10.1016/j.jcms.2015.10.005

Ogrendik, M. (2017). Periodontal Pathogens in the Etiology of Pancreatic Cancer. *Gastrointest Tumors, 3*(3-4), 125-127. doi:10.1159/000452708

Okazaki, Y., & Gotoh, E. (2005). Comparison of metal release from various metallic biomaterials in vitro. *Biomaterials, 26*(1), 11-21. doi:10.1016/j.biomaterials.2004.02.005

Ono, T., & Takayanagi, H. (2017). Osteoimmunology in Bone Fracture Healing. *Curr Osteoporos Rep, 15*(4), 367-375. doi:10.1007/s11914-017-0381-0

OsstellAB. Measurement procedure Taking a measurement with Osstell IDx. Retrieved from https://www.osstell.com/wp-content/uploads/2015/03/25077-01-Taking-a-measurement-with-Osstell-IDx.pdf

Pal, U. S., Dhiman, N. K., Singh, G., Singh, R. K., Mohammad, S., & Malkunje, L. R. (2011). Evaluation of implants placed immediately or delayed into extraction sites. *Natl J Maxillofac Surg, 2*(1), 54-62. doi:10.4103/0975-5950.85855

Palmer, R. M., Floyd, P. D., Palmer, P. J., Smith, B. J., Johansson, C. B., & Albrektsson, T. (1994). Healing of implant dehiscence defects with and without expanded polytetrafluoroethylene membranes: a controlled clinical and histological study. *Clin Oral Implants Res, 5*(2), 98-104.

Pandey, R. K., & Panda, S. S. (2013). Drilling of bone: A comprehensive review. *J Clin Orthop Trauma, 4*(1), 15-30. doi:10.1016/j.jcot.2013.01.002

Pasupuleti, M. K., Molahally, S. S., & Salwaji, S. (2016). Ethical guidelines, animal profile, various animal models used in periodontal research with alternatives and future perspectives. *J Indian Soc Periodontol, 20*(4), 360-368. doi:10.4103/0972-124X.186931

Payer, M., Kirmeier, R., Jakse, N., Pertl, C., Wegscheider, W., & Lorenzoni, M. (2008). Surgical factors influencing mesiodistal implant angulation. *Clin Oral Implants Res, 19*(3), 265-270. doi:10.1111/j.1600-0501.2007.01464.x

Pearce, A. I., Richards, R. G., Milz, S., Schneider, E., & Pearce, S. G. (2007). Animal models for implant biomaterial research in bone: a review. *Eur Cell Mater, 13*, 1-10.

Pellegrini, G., Seol, Y. J., Gruber, R., & Giannobile, W. V. (2009). Pre-clinical models for oral and periodontal reconstructive therapies. *J Dent Res, 88*(12), 1065-1076. doi:10.1177/0022034509349748

Pikos, M. A. (2005). Atrophic posterior maxilla and mandible: alveolar ridge reconstruction with mandibular block autografts. *Alpha Omegan, 98*(3), 34-45.

Pjetursson, B. E., Tan, W. C., Zwahlen, M., & Lang, N. P. (2008). A systematic review of the success of sinus floor elevation and survival of implants inserted in combination with sinus floor elevation. *J Clin Periodontol, 35*(8 Suppl), 216-240. doi:10.1111/j.1600-051X.2008.01272.x

Potier, E., Ferreira, E., Andriamanalijaona, R., Pujol, J. P., Oudina, K., Logeart-Avramoglou, D., & Petite, H. (2007). Hypoxia affects mesenchymal stromal cell osteogenic differentiation and angiogenic factor expression. *Bone, 40*(4), 1078-1087. doi:10.1016/j.bone.2006.11.024

Renaud, M., Farkasdi, S., Pons, C., Panayotov, I., Collart-Dutilleul, P. Y., Taillades, H., Desoutter, A., Bousquet, P., Varga, G., Cuisinier, F., & Yachouh, J. (2015). A New Rat Model for Translational Research in Bone Regeneration. *Tissue Eng Part C Methods*. doi:10.1089/ten.TEC.2015.0187

Ritter, L., Elger, M. C., Rothamel, D., Fienitz, T., Zinser, M., Schwarz, F., & Zoller, J. E. (2014). Accuracy of peri-implant bone evaluation using cone beam CT, digital intra-oral radiographs and histology. *Dentomaxillofac Radiol, 43*(6), 20130088. doi:10.1259/dmfr.20130088

Rodrigo, D., Aracil, L., Martin, C., & Sanz, M. (2010). Diagnosis of implant stability and its impact on implant survival: a prospective case series study. *Clin Oral Implants Res, 21*(3), 255-261. doi:10.1111/j.1600-0501.2009.01820.x

Ronda, M., & Stacchi, C. (2011). Management of a coronally advanced lingual flap in regenerative osseous surgery: a case series introducing a novel technique. *Int J Periodontics Restorative Dent, 31*(5), 505-513.

Ronold, H. J., Ellingsen, J. E., & Lyngstadaas, S. P. (2003). Tensile force testing of optimized coin-shaped titanium implant attachment kinetics in the rabbit tibiae. *J Mater Sci Mater Med, 14*(10), 843-849.

Runyan, C. M., & Gabrick, K. S. (2017). Biology of Bone Formation, Fracture Healing, and Distraction Osteogenesis. *J Craniofac Surg, 28*(5), 1380-1389. doi:10.1097/SCS.0000000000003625

S. Titsinides, G. A., T. Karatzas,. (2018). Bone grafting materials in dentoalveolar reconstruction: A comprehensive review. *Japanese Dental Science Review*.

Sadeghi, R., Rokn, A. R., & Miremadi, A. (2015). Comparison of Implant Stability Using Resonance Frequency Analysis: Osteotome Versus Conventional Drilling. *J Dent (Tehran), 12*(9), 647-654.

Sakka, S., Baroudi, K., & Nassani, M. Z. (2012). Factors associated with early and late failure of dental implants. *J Investig Clin Dent, 3*(4), 258-261. doi:10.1111/j.2041-1626.2012.00162.x

Saldanha, J. B., Pimentel, S. P., Casati, M. Z., Sallum, E. A., Barbieri, D., Moreno, H. J., & Nociti, F. H. (2004). Guided bone regeneration may be negatively influenced by nicotine administration: a histologic study in dogs. *J Periodontol, 75*(4), 565-571. doi:10.1902/jop.2004.75.4.565

Salimov, F., Tatli, U., Kurkcu, M., Akoglan, M., Oztunc, H., & Kurtoglu, C. (2014). Evaluation of relationship between preoperative bone density values derived from cone beam computed tomography and implant stability parameters: a clinical study. *Clin Oral Implants Res, 25*(9), 1016-1021. doi:10.1111/clr.12219

Salmoria, K. K., Tanaka, O. M., Guariza-Filho, O., Camargo, E. S., de Souza, L. T., & Maruo, H. (2008). Insertional torque and axial pull-out strength of mini-implants in mandibles of dogs. *Am J Orthod Dentofacial Orthop, 133*(6), 790 e715-722. doi:10.1016/j.ajodo.2007.12.020

Scarano, A., Degidi, M., Iezzi, G., Petrone, G., & Piattelli, A. (2006). Correlation between implant stability quotient and bone-implant contact: a retrospective histological and histomorphometrical study of seven titanium implants retrieved from humans. *Clin Implant Dent Relat Res, 8*(4), 218-222. doi:10.1111/j.1708-8208.2006.00022.x

Schell, H., Duda, G. N., Peters, A., Tsitsilonis, S., Johnson, K. A., & Schmidt-Bleek, K. (2017). The haematoma and its role in bone healing. *J Exp Orthop, 4*(1), 5. doi:10.1186/s40634-017-0079-3

Schenk RK, O. A., Herrmann W. (1984). Preparation of calcified tissues for light microscopy. In: GR D, editor. *Methods of Calcified Tissue Preparation. Amsterdam: Elsevier Science Publishers B.V.;*, 1-56.

Schmitz, J. P., & Hollinger, J. O. (1986). The critical size defect as an experimental model for craniomandibulofacial nonunions. *Clin Orthop Relat Res*(205), 299-308.

Schouten, C., Meijer, G. J., van den Beucken, J. J., Spauwen, P. H., & Jansen, J. A. (2009). The quantitative assessment of peri-implant bone responses using histomorphometry and micro-computed tomography. *Biomaterials, 30*(27), 4539-4549. doi:10.1016/j.biomaterials.2009.05.017

Schreiber, J. J., Anderson, P. A., Rosas, H. G., Buchholz, A. L., & Au, A. G. (2011). Hounsfield units for assessing bone mineral density and strength: a tool for osteoporosis management. *J Bone Joint Surg Am, 93*(11), 1057-1063. doi:10.2106/JBJS.J.00160

Schwarz, F., Ferrari, D., Herten, M., Mihatovic, I., Wieland, M., Sager, M., & Becker, J. (2007). Effects of surface hydrophilicity and microtopography on early stages of soft and hard tissue integration at non-submerged titanium implants: an

immunohistochemical study in dogs. *J Periodontol, 78*(11), 2171-2184. doi:10.1902/jop.2007.070157

Schwarz, M. L., Kowarsch, M., Rose, S., Becker, K., Lenz, T., & Jani, L. (2009). Effect of surface roughness, porosity, and a resorbable calcium phosphate coating on osseointegration of titanium in a minipig model. *J Biomed Mater Res A, 89*(3), 667-678. doi:10.1002/jbm.a.32000

Sennerby, L., & Meredith, N. (1998). Resonance frequency analysis: measuring implant stability and osseointegration. *Compend Contin Educ Dent, 19*(5), 493-498, 500, 502; quiz 504.

Seong, W. J., Grami, S., Jeong, S. C., Conrad, H. J., & Hodges, J. S. (2013). Comparison of push-in versus pull-out tests on bone-implant interfaces of rabbit tibia dental implant healing model. *Clin Implant Dent Relat Res, 15*(3), 460-469. doi:10.1111/j.1708-8208.2011.00357.x

Sfeir C, H. L., Doll BA, Azari K, Hollinger JO. . (2005). Fracture repair. In F. G. Lieberman JR (Ed.), *Bone Regeneration and Repair:Biology and Clinical Applications* (pp. 21–44). Totowa, NJ: Humana Press Inc.

Shah, F. A., Thomsen, P., & Palmquist, A. (2019). Osseointegration and current interpretations of the bone-implant interface. *Acta Biomater, 84*, 1-15. doi:10.1016/j.actbio.2018.11.018

Shanbhag, S., Shanbhag, V., & Stavropoulos, A. (2015). Genomic analyses of early peri-implant bone healing in humans: a systematic review. *Int J Implant Dent, 1*(1), 5. doi:10.1186/s40729-015-0006-2

Shapiro, F. (2008). Bone development and its relation to fracture repair. The role of mesenchymal osteoblasts and surface osteoblasts. *Eur Cell Mater, 15*, 53-76.

Shapurian, T., Damoulis, P. D., Reiser, G. M., Griffin, T. J., & Rand, W. M. (2006). Quantitative evaluation of bone density using the Hounsfield index. *Int J Oral Maxillofac Implants, 21*(2), 290-297.

Shui, W., Zhou, M., Chen, S., Pan, Z., Deng, Q., Yao, Y., Pan, H., He, T., & Wang, X. (2017). The production of digital and printed resources from multiple modalities using visualization and three-dimensional printing techniques. *Int J Comput Assist Radiol Surg, 12*(1), 13-23. doi:10.1007/s11548-016-1461-9

Shukla, D., Fitzsimmons, J., An, K. N., & O'Driscoll, S. (2014). Prosthetic radial head stem pull-out as a mode of failure: a biomechanical study. *Int Orthop, 38*(1), 89-93. doi:10.1007/s00264-013-2074-3

Silk, H. (2014). Diseases of the mouth. *Prim Care, 41*(1), 75-90. doi:10.1016/j.pop.2013.10.011

Simeone, S. G., Rios, M., & Simonpietri, J. (2016). "Reverse torque of 30 Ncm applied to dental implants as test for osseointegration"-a human observational study. *Int J Implant Dent, 2*(1), 26. doi:10.1186/s40729-016-0060-4

Simion, M., Baldoni, M., Rossi, P., & Zaffe, D. (1994a). A comparative study of the effectiveness of e-PTFE membranes with and without early exposure during the healing period. *Int J Periodontics Restorative Dent, 14*(2), 166-180.

Simion, M., Dahlin, C., Trisi, P., & Piattelli, A. (1994b). Qualitative and quantitative comparative study on different filling materials used in bone tissue regeneration: a controlled clinical study. *Int J Periodontics Restorative Dent, 14*(3), 198-215.

Simion, M., Fontana, F., Rasperini, G., & Maiorana, C. (2007). Vertical ridge augmentation by expanded-polytetrafluoroethylene membrane and a combination of intraoral autogenous bone graft and deproteinized anorganic bovine bone (Bio Oss). *Clin Oral Implants Res, 18*(5), 620-629. doi:10.1111/j.1600-0501.2007.01389.x

Simion, M., Trisi, P., & Piattelli, A. (1994c). Vertical ridge augmentation using a membrane technique associated with osseointegrated implants. *Int J Periodontics Restorative Dent, 14*(6), 496-511.

Sivolella, S., Bressan, E., Salata, L. A., Urrutia, Z. A., Lang, N. P., & Botticelli, D. (2012). Osteogenesis at implants without primary bone contact - an experimental study in dogs. *Clin Oral Implants Res, 23*(5), 542-549. doi:10.1111/j.1600-0501.2012.02423.x

Sivolella, S., Brunello, G., Ferroni, L., Berengo, M., Meneghello, R., Savio, G., Piattelli, A., Gardin, C., & Zavan, B. (2015). A Novel In Vitro Technique for Assessing Dental Implant Osseointegration. *Tissue Eng Part C Methods*. doi:10.1089/ten.TEC.2015.0158

Song, J. W., Cha, J. Y., Bechtold, T. E., & Park, Y. C. (2013). Influence of peri-implant artifacts on bone morphometric analysis with micro-computed tomography. *Int J Oral Maxillofac Implants, 28*(2), 519-525. doi:10.11607/jomi.1632

Sophocleous, A., & Idris, A. I. (2014). Rodent models of osteoporosis. *Bonekey Rep, 3*, 614. doi:10.1038/bonekey.2014.109

Spicer, P. P., Kretlow, J. D., Young, S., Jansen, J. A., Kasper, F. K., & Mikos, A. G. (2012). Evaluation of bone regeneration using the rat critical size calvarial defect. *Nat Protoc, 7*(10), 1918-1929. doi:10.1038/nprot.2012.113

Stanley, M., Braga, F. C., & Jordao, B. M. (2017). Immediate Loading of Single Implants in the Anterior Maxilla: A 1-Year Prospective Clinical Study on 34 Patients. *Int J Dent, 2017*, 8346496. doi:10.1155/2017/8346496

Stavropoulos, A., Sculean, A., Bosshardt, D. D., Buser, D., & Klinge, B. (2015). Pre-clinical in vivo models for the screening of bone biomaterials for oral/craniofacial indications: focus on small-animal models. *Periodontol 2000, 68*(1), 55-65. doi:10.1111/prd.12065

Streckbein, P., Jackel, S., Malik, C. Y., Obert, M., Kahling, C., Wilbrand, J. F., Zahner, D., Heidinger, K., Kampschulte, M., Pons-Kuhnemann, J., Kohler, K., Sauer, H., Kramer, M., & Howaldt, H. P. (2013). Reconstruction of critical-size mandibular defects in immunoincompetent rats with human adipose-derived stromal cells. *J Craniomaxillofac Surg, 41*(6), 496-503. doi:10.1016/j.jcms.2013.04.002

Stricker, A., Fleiner, J., Dard, M., Voss, P., Sauerbier, S., & Bosshardt, D. D. (2014). Evaluation of a new experimental model to study bone healing after ridge expansion with simultaneous implant placement--a pilot study in minipigs. *Clin Oral Implants Res, 25*(11), 1265-1272. doi:10.1111/clr.12265

Stubinger, S., Drechsler, A., Burki, A., Klein, K., Kronen, P., & von Rechenberg, B. (2016). Titanium and hydroxyapatite coating of polyetheretherketone and carbon fiber-reinforced polyetheretherketone: A pilot study in sheep. *J Biomed Mater Res B Appl Biomater, 104*(6), 1182-1191. doi:10.1002/jbm.b.33471

Sul, Y. T., Jonsson, J., Yoon, G. S., & Johansson, C. (2009). Resonance frequency measurements in vivo and related surface properties of magnesium-incorporated, micropatterned and magnesium-incorporated TiUnite, Osseotite, SLA and

TiOblast implants. *Clin Oral Implants Res, 20*(10), 1146-1155. doi:10.1111/j.1600-0501.2009.01767.x

Swami, V., Vijayaraghavan, V., & Swami, V. (2016). Current trends to measure implant stability. *J Indian Prosthodont Soc, 16*(2), 124-130. doi:10.4103/0972-4052.176539

Szmukler-Moncler, S., Salama, H., Reingewirtz, Y., & Dubruille, J. H. (1998). Timing of loading and effect of micromotion on bone-dental implant interface: review of experimental literature. *J Biomed Mater Res, 43*(2), 192-203.

Tan, W. C., Lang, N. P., Zwahlen, M., & Pjetursson, B. E. (2008). A systematic review of the success of sinus floor elevation and survival of implants inserted in combination with sinus floor elevation. Part II: transalveolar technique. *J Clin Periodontol, 35*(8 Suppl), 241-254. doi:10.1111/j.1600-051X.2008.01273.x

Tengvall, P., & Lundstrom, I. (1992). Physico-chemical considerations of titanium as a biomaterial. *Clin Mater, 9*(2), 115-134.

Thrivikraman, G., Athirasala, A., Twohig, C., Boda, S. K., & Bertassoni, L. E. (2017). Biomaterials for Craniofacial Bone Regeneration. *Dent Clin North Am, 61*(4), 835-856. doi:10.1016/j.cden.2017.06.003

Tinti, C., & Parma-Benfenati, S. (1998). Vertical ridge augmentation: surgical protocol and retrospective evaluation of 48 consecutively inserted implants. *Int J Periodontics Restorative Dent, 18*(5), 434-443.

Trisi, P., De Benedittis, S., Perfetti, G., & Berardi, D. (2011). Primary stability, insertion torque and bone density of cylindric implant ad modum Branemark: is there a relationship? An in vitro study. *Clin Oral Implants Res, 22*(5), 567-570. doi:10.1111/j.1600-0501.2010.02036.x

Trisi, P., Perfetti, G., Baldoni, E., Berardi, D., Colagiovanni, M., & Scogna, G. (2009). Implant micromotion is related to peak insertion torque and bone density. *Clin Oral Implants Res, 20*(5), 467-471. doi:10.1111/j.1600-0501.2008.01679.x

Tsiridis, E., Upadhyay, N., & Giannoudis, P. (2007). Molecular aspects of fracture healing: which are the important molecules? *Injury, 38 Suppl 1*, S11-25. doi:10.1016/j.injury.2007.02.006

Turkyilmaz, I., & Company, A. M. (2011). Sensitivity of resonance frequency analysis method to assess implant stability. *N Y State Dent J, 77*(5), 44-49.

Turkyilmaz, I., Ozan, O., Yilmaz, B., & Ersoy, A. E. (2008). Determination of bone quality of 372 implant recipient sites using Hounsfield unit from computerized tomography: a clinical study. *Clin Implant Dent Relat Res, 10*(4), 238-244. doi:10.1111/j.1708-8208.2008.00085.x

Urban, I. A., Lozada, J. L., Jovanovic, S. A., Nagursky, H., & Nagy, K. (2014). Vertical ridge augmentation with titanium-reinforced, dense-PTFE membranes and a combination of particulated autogenous bone and anorganic bovine bone-derived mineral: a prospective case series in 19 patients. *Int J Oral Maxillofac Implants, 29*(1), 185-193. doi:10.11607/jomi.3346

Urban, I. A., Lozada, J. L., Wessing, B., Suarez-Lopez del Amo, F., & Wang, H. L. (2016). Vertical Bone Grafting and Periosteal Vertical Mattress Suture for the Fixation of Resorbable Membranes and Stabilization of Particulate Grafts in Horizontal Guided Bone Regeneration to Achieve More Predictable Results: A Technical Report. *Int J Periodontics Restorative Dent, 36*(2), 153-159. doi:10.11607/prd.2627

Urban, I. A., Monje, A., Lozada, J. L., & Wang, H. L. (2017). Long-term Evaluation of Peri-implant Bone Level after Reconstruction of Severely Atrophic Edentulous Maxilla via Vertical and Horizontal Guided Bone Regeneration in Combination with Sinus Augmentation: A Case Series with 1 to 15 Years of Loading. *Clin Implant Dent Relat Res, 19*(1), 46-55. doi:10.1111/cid.12431

Valente, M. L., de Castro, D. T., Shimano, A. C., Lepri, C. P., & dos Reis, A. C. (2016). Analyzing the Influence of a New Dental Implant Design on Primary Stability. *Clin Implant Dent Relat Res, 18*(1), 168-173. doi:10.1111/cid.12324

van Arkel, R. J., Ghouse, S., Milner, P. E., & Jeffers, J. R. T. (2018). Additive manufactured push-fit implant fixation with screw-strength pull out. *J Orthop Res, 36*(5), 1508-1518. doi:10.1002/jor.23771

van Griensven, M. (2015). Preclinical testing of drug delivery systems to bone. *Adv Drug Deliv Rev, 94*, 151-164. doi:10.1016/j.addr.2015.07.006

Vanden Bogaerde, L. (2004). A proposal for the classification of bony defects adjacent to dental implants. *Int J Periodontics Restorative Dent, 24*(3), 264-271.

Vieira, A. E., Repeke, C. E., Ferreira Junior Sde, B., Colavite, P. M., Biguetti, C. C., Oliveira, R. C., Assis, G. F., Taga, R., Trombone, A. P., & Garlet, G. P. (2015).

Intramembranous bone healing process subsequent to tooth extraction in mice: micro-computed tomography, histomorphometric and molecular characterization. *PLoS One, 10*(5), e0128021. doi:10.1371/journal.pone.0128021

von Wilmowsky, C., Moest, T., Nkenke, E., Stelzle, F., & Schlegel, K. A. (2014). Implants in bone: part II. Research on implant osseointegration: material testing, mechanical testing, imaging and histoanalytical methods. *Oral Maxillofac Surg, 18*(4), 355-372. doi:10.1007/s10006-013-0397-2

Vortkamp, A., Pathi, S., Peretti, G. M., Caruso, E. M., Zaleske, D. J., & Tabin, C. J. (1998). Recapitulation of signals regulating embryonic bone formation during postnatal growth and in fracture repair. *Mech Dev, 71*(1-2), 65-76.

Wada, M., Suganami, T., Sogo, M., & Maeda, Y. (2016). Can we predict the insertion torque using the bone density around the implant? *Int J Oral Maxillofac Surg, 45*(2), 221-225. doi:10.1016/j.ijom.2015.09.013

Wada, M., Tsuiki, Y., Suganami, T., Ikebe, K., Sogo, M., Okuno, I., & Maeda, Y. (2015). The relationship between the bone characters obtained by CBCT and primary stability of the implants. *Int J Implant Dent, 1*(1), 3. doi:10.1186/s40729-014-0003-x

Walker, L. R., Morris, G. A., & Novotny, P. J. (2011). Implant insertional torque values predict outcomes. *J Oral Maxillofac Surg, 69*(5), 1344-1349. doi:10.1016/j.joms.2010.11.008

Wancket, L. M. (2015). Animal Models for Evaluation of Bone Implants and Devices: Comparative Bone Structure and Common Model Uses. *Vet Pathol, 52*(5), 842-850. doi:10.1177/0300985815593124

Wang, G., Li, J., Lv, K., Zhang, W., Ding, X., Yang, G., Liu, X., & Jiang, X. (2016). Surface thermal oxidation on titanium implants to enhance osteogenic activity and in vivo osseointegration. *Sci Rep, 6*, 31769. doi:10.1038/srep31769

Wang, L., Wu, Y., Perez, K. C., Hyman, S., Brunski, J. B., Tulu, U., Bao, C., Salmon, B., & Helms, J. A. (2017). Effects of Condensation on Peri-implant Bone Density and Remodeling. *J Dent Res, 96*(4), 413-420. doi:10.1177/0022034516683932

Wennerberg, A., Jimbo, R., Stubinger, S., Obrecht, M., Dard, M., & Berner, S. (2014). Nanostructures and hydrophilicity influence osseointegration: a biomechanical

study in the rabbit tibia. *Clin Oral Implants Res, 25*(9), 1041-1050. doi:10.1111/clr.12213

Wheeler Haines R, B. S. (1959). The structure of the mouth in the mandibular molar region. *J Prosthet Dent, 9*, 962–974. doi:https://doi.org/10.1016/0022-3913(59)90156-8

Windisch, P., Martin, A., Shahbazi, A., & Molnar, B. (2017). Reconstruction of horizontovertical alveolar defects. Presentation of a novel split-thickness flap design for guided bone regeneration: A case report with 5-year follow-up. *Quintessence Int, 48*(7), 535-547. doi:10.3290/j.qi.a38354

Yakir, M. Y., A. (n.d.). OSSEOsource: Dental Implant Manufacturers. Retrieved from http://osseosource.com/dental-implants/allmanufacturers.php

Yashwant, A. V., Dilip, S., Krishnaraj, R., & Ravi, K. (2017). Does Change in Thread Shape Influence the Pull Out Strength of Mini Implants? An In vitro Study. *J Clin Diagn Res, 11*(5), ZC17-ZC20. doi:10.7860/JCDR/2017/25774.9808

Yin, X., Li, J., Chen, T., Mouraret, S., Dhamdhere, G., Brunski, J. B., Zou, S., & Helms, J. A. (2016). Rescuing failed oral implants via Wnt activation. *J Clin Periodontol, 43*(2), 180-192. doi:10.1111/jcpe.12503

Ysander, M., Branemark, R., Olmarker, K., & Myers, R. R. (2001). Intramedullary osseointegration: development of a rodent model and study of histology and neuropeptide changes around titanium implants. *J Rehabil Res Dev, 38*(2), 183-190.

Zanetti, E. M., Pascoletti, G., Cali, M., Bignardi, C., & Franceschini, G. (2018). Clinical Assessment of Dental Implant Stability During Follow-Up: What Is Actually Measured, and Perspectives. *Biosensors (Basel), 8*(3). doi:10.3390/bios8030068

Zarb, G. A., & Zarb, F. L. (1985). Tissue integrated dental prostheses. *Quintessence Int, 16*(1), 39-42.

Zitzmann, N. U., Naef, R., & Scharer, P. (1997). Resorbable versus nonresorbable membranes in combination with Bio-Oss for guided bone regeneration. *Int J Oral Maxillofac Implants, 12*(6), 844-852.

Zix, J., Hug, S., Kessler-Liechti, G., & Mericske-Stern, R. (2008). Measurement of dental implant stability by resonance frequency analysis and damping capacity

assessment: comparison of both techniques in a clinical trial. *Int J Oral Maxillofac Implants, 23*(3), 525-530.

Zoetis, T., Tassinari, M. S., Bagi, C., Walthall, K., & Hurtt, M. E. (2003). Species comparison of postnatal bone growth and development. *Birth Defects Res B Dev Reprod Toxicol, 68*(2), 86-110. doi:10.1002/bdrb.10012

10. LIST OF OWN PUBLICATIONS

The publications related to the PhD thesis:

1) **Farkasdi S**, Pammer D, Rácz R, Hriczó-Koperdák G, Szabó BT, Dobó-Nagy Cs, Kerémi B, Blazsek J, Cuisinier F, Wu G, Varga G *„Development of a quantitative preclinical screening model for implant osseointegration in rat tail vertebra"*, Clin Oral Investig. 2018 Oct 29. doi: 10.1007/s00784-018-2661-1. [Epub ahead of print] PubMed PMID: 30374828.

2) Urban I, Traxler H, Romero-Bustillos M, **Farkasdi S**, Bartee B, Baksa G, Avila-Ortiz G. *„Effectiveness of Two Different Lingual Flap Advancing Techniques for Vertical Bone Augmentation in the Posterior Mandible: A Comparative, Split-Mouth Cadaver Study."* Int J Periodontics Restorative Dent. 2018 Jan/Feb;38(1):35-40. doi: 10.11607/prd.3227. PubMed PMID: 29240202.

3) Renaud M, **Farkasdi S**, Pons C, Panayotov I, Collart-Dutilleul PY, Taillades H, Desoutter A, Bousquet P, Varga G, Cuisinier F, Yachouh J. *"New Rat Model for Translational Research in Bone Regeneration."* Tissue Eng Part C Methods. 2015 Dec 31. [Epub ahead of print] PubMed PMID: 26472155.

The publications non-related PhD thesis:

1) Liu J, Pathak JL, Hu X, Jin Y, Wu Z, Al-Baadani MA, Wu S, Zhang H, **Farkasdi S**, Liu Y, Ma J, Wu G. "*Sustained Release of Zoledronic Acid from Mesoporous TiO_2-Layered Implant Enhances Implant Osseointegration in Osteoporotic Condition.*" J Biomed Nanotechnol. 2018 Nov 1;14(11):1965-1978. doi: 10.1166/jbn.2018.2635. PubMed PMID: 30165932.

2) Perczel-Kovách K E; **Farkasdi S**; Kálló K; Hegedűs O; Kerémi B; Cuisner F; Blazsek J; Varga, G *„Effect of stem cells of dental pulp origin on osseointegration of titanium implant in a novel rat vertebra model"* FOGORVOSI SZEMLE vol.:110, issue.:1, p.:7-14. January 2017, ISSN: 0015-5314

3) Matthieu, Renaud, **Farkasdi Sandor**, Desoutter Alban, Varga Gabor, Cuisinier Frédéric, and Bousquet Philippe. 2016. *"A Rat Tail Model for Osseointegration Studies and New*

Bone Formation Follow-Up." Journal of cell science & therapy 7 (3). doi:10.4172/2157-7013.1000244.

4) A.S.Grigoryan, E.V.Kiseleva, M.P. Filonov, D.V. Shtanskij, T.K. Khamraev, A.K.Toporkova, A.B. Gastiev, **Sh. Farkashdi**: *„A novel type of a polytetrafluorethylene-based tissue-engineered construction with nanopattered muitifunctional biocompatible nonresorbed coating."* Cellular Transplantation and Tissue Engineering. 2010; V(3):71-76.

11. ACKNOWLEDGEMENTS